



Cover pictures; Business Wire [1], Paint [2] and EL-PRO-CUS [3].

# Designing Efficient Renewable Energy Portfolios: A Dutch Case Study Including Dynamic Tidal Power

# A Novel Application of the Modern Portfolio Theory

Master thesis submitted to Delft University of Technology in partial fulfilment of the requirements for the degree of

#### MASTER OF SCIENCE

#### in Management of Technology

Faculty of Technology, Policy and Management

by

#### M.P. Tönis

Student number: 4748220

To be defended in public on the  $5^{\rm th}$  of March, 2021

#### Graduation committee

Chairperson : Dr. Ir. R.M. Stikkelman, Section Engineering, Systems and Services First Supervisor: Dr. Ir. R.M. Stikkelman, Section Engineering, Systems and Services Second Supervisor: Dr. E. Schröder, Section Economics of Technology and Innovation External Supervisor: Dr. Ir. S.N. Jonkman, Section Hydraulic Structures and Flood Risk





## Abstract

By signing the Paris Climate Agreement, The Netherlands has committed itself to curtail its CO<sub>2</sub>-emissions in order to keep global warming well below 2°C above pre-industrial levels. Pivotal to achieve these targets is the phase-out of CO<sub>2</sub>-intensive electricity generation technologies and investments in renewables. Current investments aiming to decarbonise the electricity system are predominantly allocated to solar PV and off- and onshore wind energy. However, this trajectory might change as the development of Dynamic Tidal power (DTP) might soon enable The Netherlands to harvest the North Sea's currently unutilised tidal currents to generate clean electricity. DTP uses a 30-70 kilometre long dam perpendicular to the coast to capture the North Sea's tidal currents. The alternating currents that proceed parallel to the coast create a hydraulic head over the dam, which turbines in the dam convert into electricity.

However, the variable availability of solar irradiation, wind, and tidal currents makes it increasingly complex and costly to match electricity supply and demand as their shares in the electricity mix increase. To ensure electricity security, freely dispatchable energy generators (e.g. natural gas, biomass or coal turbines) are deployed to cover the electricity load that could not be met by the variable renewable energy (VRE) generators. However, due to the fuel used to generate electricity, dispatchable energy sources tend to emit CO<sub>2</sub> and bear higher marginal energy generation costs than VRES.

To address this problem, the portfolio shares of solar PV, offshore wind, onshore wind and DTP that minimise the need for dispatchable backup capacity and the energy generation costs were computed in this study. Due to its novelty, special attention was paid to the effect of DTP on a VRE system's ability to efficiently match supply and demand.

In order to achieve these objectives a novel application of the Modern Portfolio Theory (MPT) was used. The MPT originates from the stock market but is often used to comprise VRE portfolios that maximise the electricity output. However, as the aim was to minimise the residual load, demand-variability was introduced into the MPT. Existing literature had not covered this topic. Hence, by assessing to what extent including demand-variability in the MPT affects the selection of efficient VRE portfolios, this study filled a gap in the literature and serves as a starting point for future research into the application of the MPT.

In total, three different electricity demand scenarios were optimised; the contemporary load profile (1), increased peak loads due to an extreme penetration of electric vehicles (EV) and electric heat pumps (HP) (2), and a flat load profile due to an extreme penetration of demand-responsive measures (3). The most efficient portfolio shares for each demand scenario were found by computing how 35GW should be distributed among solar PV, offshore wind, onshore wind and DTP in order to minimise the need backup capacity and the energy generation costs.

The results of this study indicate that regardless of the demand profile, The Netherlands' VRE system would be most costs-efficient in meeting demand when comprised of approximately 75% DTP and 25% offshore wind. However, only under the condition that the DTP-dams are geographically dispersed. Geographically dispersed DTP-dams, for example, located in Zeeland (south of The Netherlands) and off the coast of Texel (north of The Netherlands), cancels out the volatility in the electricity output caused by high and low tide. This reduces a VRE system's volatility in electricity output and stabilises the electricity output from the dispatchable backup system, which minimises the system's electricity generation costs.

However, in terms of the amount of backup capacity required, it was found that a system comprised entirely of DTP with an integrated battery storage system would be even more efficient. The battery storage system eliminates all variability in the electricity output from DTP, which minimises the need for dispatchable backup capacity. However, as battery storage costs are significant (approx. 100,000 €/MWh), it is unlikely that a DTP-dam with a storage system large enough to flatten its electricity output is economically viable under the current market circumstances. This might change when DTP is combined with other storage systems or if battery storage costs reduce due to learning-effect, economies of scale or technical innovations.



As DTP is still in its initial development phase, it is not certain DTP will successfully penetrate the power generation market. If DTP fails to enter the market, the current VRE system (61% solar PV, 8% offshore wind and 31% onshore wind) is fairly cost-efficient. However, if the aim is to reduce the amount of dispatchable backup capacity required to ensure energy security, future investments should be allocated to offshore wind.

The overarching conclusion is that there is no unequivocal VRE portfolio that is most efficient to meet demand as it depends on the perspective taken (required backup capacity versus electricity generation costs). However, this study shows that the current VRE system benefits from the inclusion of DTP, both in terms of the required amount of backup capacity and the system's energy generation costs. Only if DTP is combined with a large battery storge system to flatten its electricity output do the system's energy generation costs surpass the costs of the current VRE system.

In regards to the effect of including demand-variability in the MPT, it was found that demand-variability has a limited effect on the selection of efficient VRE portfolio shares. Only in a scenario (2) with increased peak loads did the share of offshore wind slightly increase. This is due to the fact that the peaks in electricity supply from offshore wind coincide with the peaks in demand from electric HP (winter).



# List of acronyms and symbols

CCGT Combined Cycle Gas Turbine

CF Capacity factor
CI Confidence interval
DTP Dynamic Tidal Power
ETS Emission Trading System

EV Electric vehicle(s) HP Heat Pump(s)

LCOE Levelized Costs of Energy
MPT Modern Portfolio Theory

NPV Net present value

NRMSE Normalised Root mean square error

O&M Operations & maintenance

PV Photovoltaics

RES Renewable energy sources

RL Residual load

RMSE Root mean square error RQ Research question STD Standard deviation

TSO Transmission System Operator VRE Variable renewable energy

VRES Variable renewable energy sources

 $\sigma$  Standard deviation (STD)

Cov Covariance

 $\rho$  Correlation coefficient

 $\mu$  Mean



# Table of contents

$\mathbf{Abstract}$ 4					
Li	ist of ac	ronyms and symbols	6		
1.	Intr	oduction	10		
	1.1	Background	10		
	1.2	Problem definition	11		
	1.2.1				
	1.2.2	Academic problem definition	12		
	1.3	Research outline	12		
2	Lite	rature review	15		
	2.1	The Modern Portfolio Theory	15		
	2.1.1				
	2.1.2	1			
	2.1.3	The efficient frontier	17		
	2.2	The Modern Portfolio theory applied to the electricity market	18		
	2.3	Limitations of the Modern Portfolio Theory	19		
3.	Metl	10dology	20		
	3.1	Comprising efficient VRE portfolios	20		
	3.1.1				
	3.1.2	Normalising electricity supply	21		
	3.1.3	1 0 0			
	3.1.4				
	3.1.5				
	3.1.6				
	3.2	Dispatchable backup capacity	25		
	3.3	Energy generation costs	27		
4	Case	study: The Netherlands	29		
	4.1	Electricity supply solar PV and wind	29		
	4.1.1	Data collection			
	4.1.2	Electricity output solar PV and wind	31		
	4.2	Electricity supply Dynamic Tidal Energy	32		
	4.2.1				
	4.2.2	v 1			
	4.2.3				
	4.2.4	Electricity output single DTP-dam with an integrated storage system	36		
	4.3	Electricity demand			
	4.3.1				
	4.3.2	±			
	4.3.3	1			
	4.4	Electricity generation costs			
	4.4.1	±			
	4.4.2				
	4.5	Overview demand scenarios and technical configurations	44		



5	$\mathbf{Resu}$	llts	45	
	5.1	Minimum-variance frontiers		
	5.1.1 $5.1.2$	Demand scenario 1: contemporary load profile		
	5.1.2 $5.1.3$	<u> •</u>		
	5.2	Most efficient portfolios: dispatchable backup capacity		
	5.3	Most efficient portfolios: electricity generation costs		
	5.4	Sensitivity analysis	58	
	5.4.1	System size		
	5.4.2	1 1 0		
	5.4.3	CO <sub>2</sub> price	62	
6	Disc	ussion	65	
	6.1	Reflection on the methodology	65	
	6.1.1	v v		
	6.1.2	Methodological limitations	66	
	6.2	Interpretation of the main findings	69	
	6.3	Market entry strategy Dynamic Tidal Power	72	
7	Conclusion and recommendations			
	7.1	Conclusion	74	
	7.2	Recommendations and suggestions for future research	75	
8	Pers	onal reflection and acknowledgements	77	
		es		
A	ppendix	x A: Battery system DTP	83	
A	ppendi	x B: LCOE calculation	86	
	Append	ix B1: Solar PV	86	
	Append	ix B2: Offshore wind	87	
	Append	ix B3: Onshore wind	88	
	Append	ix B4: DTP	89	
	Append	ix B5: DTP incl. storage system	91	
	Append	ix B6: Flexible CCGT	93	
$\mathbf{A}$	ppendi	x C: Efficient portfolio shares and backup capacity	94	
	 Append	ix C1: Demand scenario 1 – contemporary load profile	94	
	Append	ix C2: Demand scenario 2 - increased peak loads	95	
	Append	ix C3: Demand scenario 3 - flat load profile	96	
A	ppendi	x D: Efficient portfolio shares, backup capacity and system's LCOE	98	
		ix D1: Demand scenario 1 – contemporary load profile		
		ix D2: Demand scenario 2 - increased peak loads		
		ix D3: Demand scenario 3 - flat load profile		



Appendix E: Sensitivity analysis - system size	
Appendix E1: Efficient portfolio shares and backup capacity - $25GW\ VRE$	103
$Appendix\ E2:\ Efficient\ portfolio\ shares\ and\ backup\ capacity\ -\ 45GW\ VRE\$	104
Appendix F: Sensitivity analysis - increased confidence interval	106
Appendix G: Sensitivity analysis - increased CO2 price	108
Appendix H: Distribution residual loads	110



## 1. Introduction

This chapter first provides some indispensable background information. Subsequentially, section 1.2 discusses the practical and academic problem this study addressed. Section 1.3. elaborates on the main objectives of this research and the research questions that were formulated to achieve these objectives. The last section also briefly elaborates on the fundamental assumptions undelaying this research, and the structure of the remaining of this report.

### 1.1 Background

In 2015, the growing recognition that global warming is unequivocal had led The Netherlands and 186 other nations to sign the Paris Climate Agreement, to keep "global average temperature rise to well below 2°C above pre-industrial level, and to pursue efforts to limit warming to 1.5°C" [4]. As a result of the scientific consensus that climatic change is aggravated by the emission of greenhouse gasses, particularly carbon dioxide [5], The Netherlands has committed itself to reduce its CO<sub>2</sub>-emissions. To curtail CO<sub>2</sub>-emissions, a transformation of the electricity sector is pivotal. Not only because the power generation market is responsible for 23% of the Netherlands' CO<sub>2</sub>-emissions [6], but also because the transformation of numerous other CO<sub>2</sub>-intensive sectors depends on a sustainable electricity system. To accelerate the decarbonisation of its electricity system, The Netherlands has set the target to generate almost 100% of its electricity CO<sub>2</sub>-neutral by 2050 [7].

In The Netherlands' current (2020) electricity mix, clean, renewable energy sources, in particular; wind (51%), solar PV (23%) and biomass (25%), account for 18.5% of the electricity generated [8]. Apart from 3% nuclear energy, the remaining is produced burning CO<sub>2</sub>-intensive fossil fuels, especially natural gas (77%) [8]. Hence, large investments in renewable energy technologies are needed to achieve 2050's sustainability target.

Most of the current investments aiming to decarbonise The Netherlands' electricity system are allocated to solar PV and wind, with offshore wind gaining significant momentum over the past years [9]. However, due to the development of a novel energy technology, The Netherlands might soon be able to generate clean electricity by harnessing the North Sea's tidal currents. Tidal currents are alternating horizontal movements of water driven by the regular rise and fall of the astronomic tides [10]. Hence, tidal currents are more predictable than solar irradiation and wind speeds [11]. As most conventional tidal power generators require flow speeds that are rarely met in the Dutch part of the North Sea [12] [13], tidal currents are currently unutilised. However, due to its size, Dynamic Tidal Power (DTP), a technology still in its initial phase of development, is theoretically capable of generating electricity at low water velocities. DTP uses a 30-70 kilometre long dam perpendicular to the coast to capture the North Sea's tidal currents that proceed parallel to the coastline (fig. 1). The alternating currents create a water level difference on both sides of the DTP-dam (fig. 2), which turbines in the dam can convert into electricity (fig. 3). Theoretically, DTP can cover 55% of The Netherlands' electricity load, a CE Delft study states [14].



Figure 1: impression of a DTP-dam perpendicular to the cost [99].

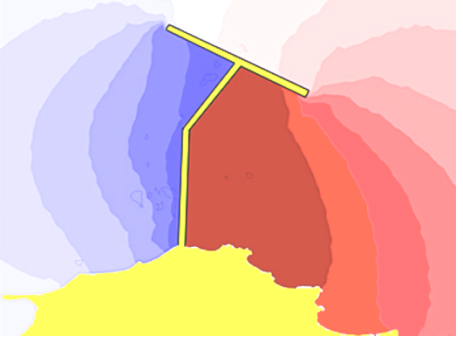


Figure 2: visualisation of the difference in water level over an exemplary DTPdam as a result of the tidal current [101].



Figure 3: impression of the turbines in a DTP-dam [100].



#### 1.2 Problem definition

The problem this research address is characterised by a practical and academic aspect. Both are discussed in this section.

#### 1.2.1 Practical problem definition

Investments in solar PV, on-/offshore wind energy and DTP will significantly accelerate the abatement of carbon emissions but also hampers the electricity system's ability to match supply and demand [11]. To explain this problem, a simplified representation of The Netherlands' electricity system is visualised in figure 4.

Solar PV, wind energy and DTP are variable renewable energy (VRE) technologies, which, unlike dispatchable energy technologies (e.g. coal or natural gas power plants), cannot be deployed on request as they only generate electricity when the conditions are right. The electricity output from solar PV and wind energy depends on the weather, making their electricity output volatile and highly unpredictable. Although tidal currents are weather-independent and thus perfectly predictable, DTP's electricity output remains variable due to the alternating tides. As a result of the fluctuating electricity output from VRE generators, it becomes increasingly difficult to match supply and demand as their shares in the electricity mix increase [15].

To ensure electricity security during periods of little VRE output, The Netherlands deploys (fossil fuel-intensive) dispatchable backup generators to cover the residual load [15]. The residual load is "the difference between actual power demand and the feed-in of non-dispatchable and inflexible generators" [16]. However, due to the fuel used to generate electricity (e.g. coal or natural gas), dispatchable energy sources tend to emit CO<sub>2</sub> and bear higher marginal energy generation costs than VRE technologies. To minimise the need for backup capacity and the system's energy generation costs, this study aimed to find the mix of solar PV, wind and DTP that minimises the residual load and the variance of the residual load. Because of its novelty, special attention was paid to whether DTP improves the current VRE system's ability to match supply and demand.

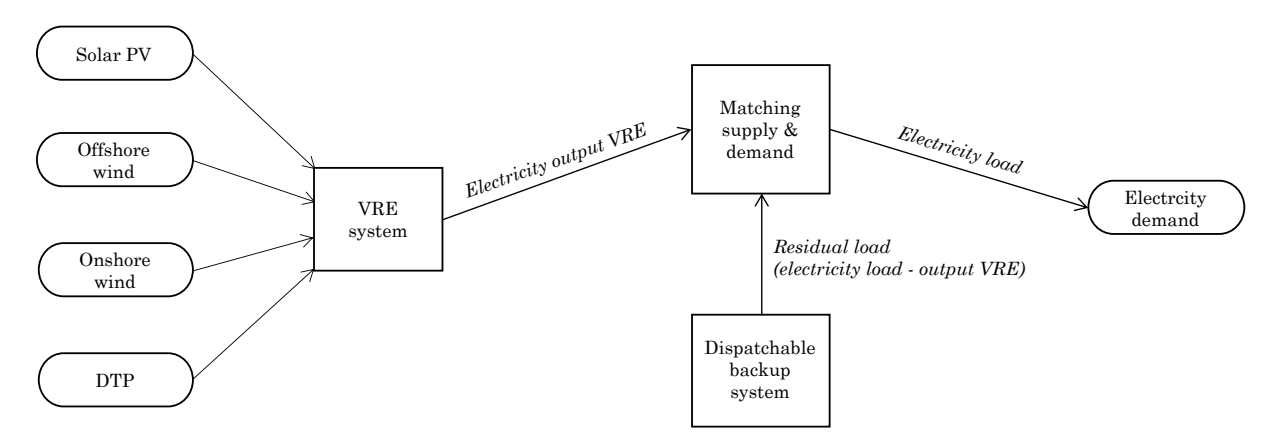


Figure 4: simplified representation of The Netherlands' electricity system.



#### 1.2.2 Academic problem definition

A dominant method to comprise efficient VRE portfolios is the Modern Portfolio Theory (MPT) [17]. The MPT originates from the stock market but is often used as a tool to compute energy-generating portfolios. The MPT is unique compared to traditional energy planning tools, as it includes the correlation between the electricity outputs from individual energy-generating technologies [18]. By comprising VRE portfolios that draw from negatively correlating energy sources, the variance in electricity output from the system as a whole can be lower than the variance in electricity output from each independent VRE technology compromising the portfolio [18]. Traditionally, when the MPT is applied to the electricity market, the aim is to maximise a portfolio's average electricity output and minimise its variance in supply [17]. This relation is characterised by a trade-off; a portfolio's average electricity output increases proportionally with its variance [19]. However, rather than maximising the electricity output, this study aimed to find the VRE portfolios that minimise the residual load and the volatility of the residual load. This is different as electricity demand is not necessarily consistent, quite the contrary. Therefore, solely aiming for a consistent electricity output might still result in the need for dispatchable backup capacity.

There is one study [20] that uses the residual load to gauge the efficiency of portfolios, but it fails to optimise the system by minimising the residual load. Cunha et al. [18] ratify that this objective is understudied by stating that 'future work addressing RES portfolios should also consider the demand variability and its relationship to RES power output aiming to minimise not only the variability of the portfolio output (standard deviation) but also to minimise the deviation between the demand and the RES production in each moment" [18]. To bridge this gap in the literature, this present study has developed a modified version of the MPT that minimises the mean residual load and its variance. This modified version of the MPT was applied to the case study of The Netherlands in order to find the portfolios of solar PV, wind and DTP that most efficiently meet demand.

#### 1.3 Research outline

This section discusses the overarching objectives of this research and the research questions that were formulated to achieve these objectives. Subsequentially, this section briefly elaborates on; how these research questions were answered, the fundamental assumptions underlaying this research and how the rest of this report is structured.

The objective of this research was three-folded. Firstly, this study aimed to find the portfolios of wind energy, solar PV and DTP that minimise the need for back-up capacity and energy generation costs. This information helps governmental energy planners to develop a roadmap towards the efficient integration of VRES.

Secondly, this research aimed to provide insights into the extent to which incorporating tidal energy improves The Netherlands' contemporary VRE system's (wind and solar PV) ability to meet demand. This information is not only valuable for the DTP Foundation in The Netherlands but might also be of interest to other countries with a potential for tidal current energy.

Third and last, this research intended to contribute to the further development of the MPT. Unlike existing studies that apply the MPT to the electricity market, this study included demand-variability to find the VRE portfolios that minimise the residual load. As such, this study provides fundamental new insights into the role of electricity demand in the selection of efficient VRE portfolios. Hence, this study contributes to the academic discussion regarding the MPT and serves as a starting point for future research into the application of the MPT.

To achieve the main objective of this research and find the most efficient VRE portfolios, the following research question was formulated;

What are the efficient portfolios of onshore wind, offshore wind, solar PV and Dynamic Tidal Power to meet demand?



Research questions (RQ) 1-3 were formulated to obtain all the necessary input data in order to answer the main research question. To achieve the other two objectives of this research, and assess the effects of DTP on a VRE system's ability to meet demand and to what extent including demand variability in the MPT affects the selection of efficient VRE portfolios, research questions 4 and 5 were formulated. Hence, apart from the main research question, research questions 4 and 5 are also answered in the conclusion (chapter 7).

- RQ1. What are the hourly electricity generation profiles of onshore wind, offshore wind, solar PV and DTP?
- RQ2. What is The Netherlands' hourly electricity demand profile?
- RQ3. What are the energy generation costs of onshore wind, offshore wind, PV, DTP and a dispatchable backup system?
- RQ4 What are the effects of DTP on The Netherlands' current VRE system's ability to meet demand?
- RQ4. To what extent does including demand-variability in the MPT affect the selection of efficient VRE portfolios?

To answer research questions 1-3, a literature study was conducted, and electricity output and demand data was derived from various sources. To answer research questions 4, 5 and the main research question, this study investigated how 35GW of installed capacity should be distributed among solar PV, offshore wind, onshore wind and DTP to efficiently meet demand. 35GW was initially optimised because it is similar to the current (2020) installed capacity in The Netherlands (33353 MW) [21]. However, in the sensitivity analysis, the system's size was changed to 25 and 45GW in order to assess whether a system's size affects which portfolio shares are most efficient.

A VRE portfolio's efficiency is measured using two performance indicators; the amount of dispatchable backup capacity required to ensure energy security (I) and the system's total energy generation costs (II). The latter thus includes the costs of the VRE system and the costs of the dispatchable backup system required to ensure energy security. The VRE portfolio that requires the least backup capacity and the system that bears the lowest energy generation costs are considered to be most efficient in meeting demand. These are not necessarily the same VRE portfolios. Hence, different portfolios can be most efficient depending on the performance indicator that is considered.

It is important to stress that the 35GW electricity system that was optimised to find the most efficient VRE portfolios is a simplified representation of real-life. As a result, this study's scope was geographically demarcated, solely focusing on The Netherlands. Hence, it is assumed that The Netherland's electricity system is a closed energy system. In real-life, electricity surplus or deficiencies can be partly offset by selling electricity to or purchasing electricity from neighbouring countries. However, for simplification reasons, international electricity trading was not included in this study, and electricity surplus and deficiencies were treated as equally inefficient.

Secondly, The Netherland's current electricity generation infrastructure was not taken into account in this study. Hence, when the electricity system was optimised, no constraints were set to the amount of capacity installed of specific energy technologies. This study thus optimised The Netherlands' electricity system from scratch.

A third assumption concerns the sequence in which energy generators are deployed to cover demand. This study assumed that VRE technologies are deployed first and that any residual load left is then covered by the dispatchable backup system. This assumption is derived from the real-life electricity market, in which the energy technologies' marginal costs determine the deployment sequence. As VRE technologies use no fuel and thus have marginal costs close to zero, they are deployed before dispatchable energy technologies that burn fuel to generate electricity.



The remaining of this report is structured as follows. The following chapter first elaborates on the relevant literature, aiming to explain the fundamentals of the MPT and how the existing literature applied the MPT to the electricity market. Chapter 3 explains the novel methodology that was developed to find the most efficient VRE portfolios. In chapter 4, the case study of The Netherlands and the input data for the optimisation model is discussed. Hence, this chapter answers research question 1-3. Chapter 5 presents the results and the VRE portfolios that are most efficient in meeting demand based on the two performance indicators. Chapter 6 reflects on the results presented in chapter 5 and the novel methodology that was used to derive these results. Especially the latter is reflected on in great detail as this study's application of the MPT is entirely novel. In the seventh and concluding chapter, the answers to research questions 4, 5 and the main research question are provided.



### 2 Literature review

In this chapter, the relevant literature regarding the Modern Portfolio Theory (MPT) is discussed. The MPT, initially proposed by Markowitz [22] in 1952, originates from the stock market and only later (1976) became an energy planning tool [23]. To acquire a thorough understanding of the MPT, section 2.1 first explains its original application to the financial markets. Subsequently, section 2.2 explains how the MPT is used as an energy planning tool. Section 2.2 also reviews the existing literature applying the MPT to the electricity market in order to identify potential knowledge gaps. In section 2.3, the main limitations of the MPT, as described in the literature, are discussed.

### 2.1 The Modern Portfolio Theory

This section firsts provides some context and background theory about the trade-offs risk-averse investors make before investing in a financial asset. Subsequently, the fundamentals of the MPT are explained and how investors use the MPT as a tool to maximise the expected return on their investments while minimising the risk.

Risk-averse investors prefer a safe income over a risky income of the same average amount [24]. Hence, before investing, investors will always evaluate the expected return and risk of a financial asset (e.g. stock). The expected return ( $E(R_i)$ ) of a stock can be estimated by evaluating it historical returns. E.g. based on historical data from 2010-2015, the average percentage increase in value per euro invested is 2%. Comparing these average historical returns tells the investor how much she can expect to earn on a certain stock, and which stock is expected to yield the highest returns [25].

However, on average, a stock might yield high returns, if its returns are highly volatile, the investor might as well earn nothing. The volatility of a stock's returns (eq. 2.1) is referred to as its risk and commonly measures by the standard deviation. The standard deviation is the root of the sum of the squared deviation from the mean  $((R_i - \bar{R})^2)$  divided by the number of observations minus 1 (n-1) [25];

$$\sigma = \sqrt{\frac{\sum_{i=1}^{i=n} (R_i - \overline{R}_i)^2}{n-1}}$$
 (Eq. 2.1)

A standard deviation (STD) of zero indicates that a stock's returns are perfectly consistent and that the stock is risk-free [25]. When investing in a stock with a STD equal to zero, one can be certain to receive the expected return. The higher the STD, the more spread out a stock's returns are and the riskier a stock becomes. If a stock's volatility increases, investors expect a higher risk premium in order to compensate for the relatively higher risk they are taking [24]. As a result, a stock's expected return increases proportionally with its risk and the investor is thus faced with a trade-off [19].

Deviations in a stock's return are usually the result of some sort of news. There are two types of news that might affect a stock's return; firm-specific news and market news. Firm-specific news is news about a single company and only affects the return on their stock (e.g. earnings announcements). Volatility caused by firm-specific news is uncorrelated among stocks and therefore also referred to as independent risk. On the other hand, market-wide news is news about the whole economy and affects all stocks simultaneously (e.g. increasing interest rates). This type of risk is also called common risk [25].



#### 2.1.1 Portfolio diversification

The notion that stocks carry different types of risk is the foundation for the Modern Portfolio Theory (MPT). The fundamental idea behind the MPT is that investment diversification reduces the independent risk. By combining multiple stocks in a large portfolio rather than investing in a single stock, each stock's independent risk averages out. Certain news might be good for some stocks, while bad for others, but the overall amount of good and bad news is relatively consistent. Diversification only averages out the independent risk. Hence, if a portfolio of multiple stocks carries both types of risk, the volatility declines until only the common risk remains. Due to this diversification, a portfolio's risk can be less than the risk of each stock comprising the portfolio [25].

An investment portfolio is described by its portfolio weights, which indicate how the invested money is distributed among different individual stocks. E.g. if the invested resources are evenly distributed over two stocks, the portfolio weights are 0.5. The portfolio weights always add up to 1 and cannot be negative. To find the portfolio weights that maximise the diversification effects and the expected return, one needs to calculate the return and risk for different portfolio weights, and generate an efficient frontier [19].

### 2.1.2 Portfolio's expected return and risk

The return of a portfolio  $(E(R_p))$  with n stocks is simply the sum of the portfolio weights  $(X_i)$  times the expected return on each stock  $(E(R_i))$  [19];

$$E(R_p) = \sum_{i=1}^{i=n} X_i * E(R_i)$$
 (Eq. 2.2)

Unlike the return of a portfolio, a portfolio's risk cannot be computed by simply multiplying the portfolio weights with the risk on the individual stocks. To account for the diversification effects, one also has to include the degree to which the stocks in the portfolio carry common risks, and their returns move together. The co-movement between the returns on different stocks is measured by the covariance and the correlation. The covariance is the product of the deviation of two returns  $(R_{i/j})$  from their means  $(\bar{R}_{i/j})$ , divided by the number of observations (n) [19];

$$Cov(R_i, R_j) = \frac{\sum_{i=1}^{i=n} (R_i - \overline{R}_i) * (R_j - \overline{R}_j)}{n}$$
 (Eq. 2.3)

If the two stocks' returns tend to be above or below its average return at the same time, the two stocks move together, and their covariance is positive. The covariance is negative when the two stocks' returns move in opposite directions; the return of one stock is above its average while the other is below its average. The sign of the covariance is easy to interpret, its magnitude on the other is not. Therefore, the correlation is often used to gauge the strength of the relationship between stock's returns. The correlation is the covariance between two returns (eq. 2.3) divided by the standard deviation of the two individual stock's returns  $(\sigma(R_{i/j}))$  [19];

$$\rho(R_i, R_j) = \frac{Cov(R_i, R_j)}{\sigma(R_i) * \sigma(R_j)}$$
 (Eq. 2.4)

Dividing the covariance by the standard deviations ensures that the correlation is always between -1 and +1, enabling the easy gauging of the strength of the relationship between the two stock's returns. The closer the correlation is to +1, the more common risk the two stocks carry and the more their returns tend to move together. The closer the correlation is to -1, the more the returns tend to move in opposite directions. If the correlation equals zero, the two stocks' returns move neither together nor in the opposite direction and their returns are uncorrelated. When a portfolio consists of more than two stocks, the correlations (eq. 2.4) between all the different stocks have to be determined [19].



Now that the risk on the individual stocks (eq. 2.1) and the correlation between each stock's returns (eq. 2.4) are known, we can calculate the risk (volatility) for portfolios with different weights. For a two stock portfolio this looks as following [19];

$$\sigma(R_p) = \sqrt{X_i^2 * \sigma(R_i)^2 + X_j^2 * \sigma(R_j)^2 + 2 * X_i^2 * X_j^2 * \rho(R_i, R_j) * \sigma(R_i) * \sigma(R_j)}$$
 (Eq. 2.5)

Knowing that investors care about a portfolio's expected return and the volatility, we must consider both simultaneously. By adjusting the portfolio weights  $(X_i)$ , the expected return on a portfolio (eq. 2.2) and the associated risk (eq. 2.5) can be calculated for different portfolios. Doing so, results in a list of different portfolios shares, who's weights always add up to 1, followed by their expected return and risk. However, how does one find the most efficient portfolio in this long list of possible portfolio combinations?

#### 2.1.3 The efficient frontier

The most efficient portfolios can be found by plotting the calculated returns and risks of all the portfolios in a scatter plot. Figure 5 illustrates a simplified example of such a scatter plot. The horizontal axis indicates a portfolios expected return, and the vertical axis a portfolio's risk (STD). The large dots in the scatter plot are portfolios comprised of assets from a single company, for example, five Shell stocks. The small dots represent weighted portfolios that include assets from multiple firms, for instance; three Shell stocks and two Ørsted stocks. Note that when the investment portfolio is diversified among multiple stocks, the independent risk averages out and the portfolios volatility (risk) decreases. The minimum-variance frontier (blue line) marks all the portfolios with the lowest possible risk level for each expected return. The portfolio that eliminates all the independent risk, so that only the common risk remains, can be found at the uttermost left point on the minimum-variance frontier [19].

Although all portfolios on the minimum-variance frontier curtail risk to the minimum, they are not equally efficient. The dashed line marks the tipping point between efficient and inefficient portfolios. The portfolios located on the lower part of the minimum-variance frontier (under the dashed line) are inefficient as other portfolios yield a higher return for the same risk. The efficient portfolios are located on the upper part of the minimum-variance since no other portfolios offer a higher expected return with lower volatility. This part of the minimum-variance frontier is referred to as the efficient frontier and represents all portfolios that maximise the expected return for a given level of risk [18]. However, while it is easy to eliminate the inefficient portfolios, the efficient ones cannot easily be ranked. Investors will have to choose among them based on their own preferences for return versus risk.

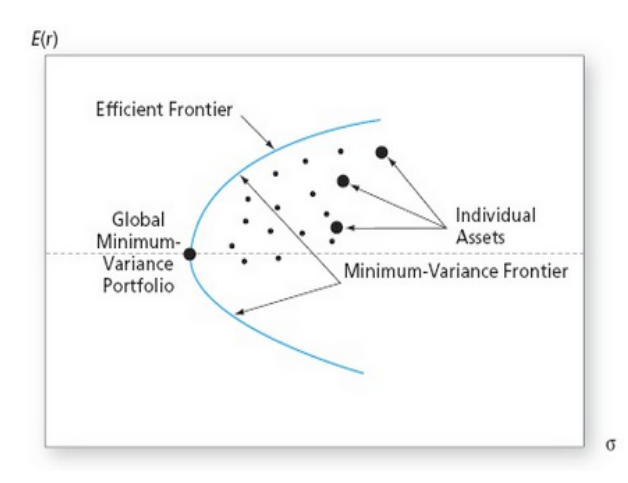


Figure 5: exemplary minimum-variance frontier [92].

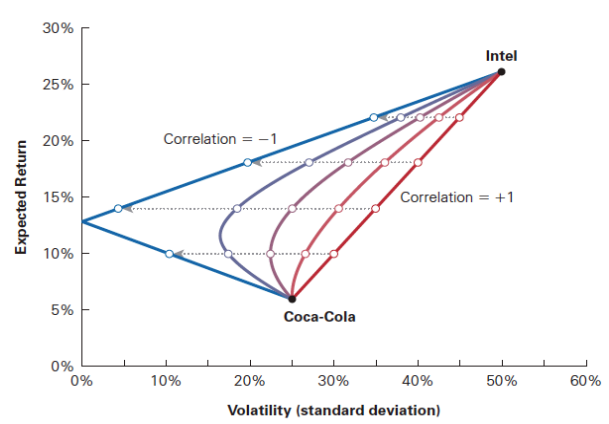


Figure 6: the effect of correlation on a portfolio's volatility. Correlations of -1, -0.5, 0, 0,5 and 1 [19].



The pivotal role of the correlation among stock's returns in the MPT cannot be stressed enough and becomes evident in figure 6. When stocks bear a high level of common risk, and their returns are positively correlated, diversification results in little risk reduction. But as stocks carry more independent risk and their correlation decreases, the reduction in risk due to diversification increases. To such an extent, that when two stocks are perfectly negatively correlated (-1), it is possible to hold a portfolio that carries absolutely no risk. Stocks in the same industry face common risks, and their returns tend to move together (positive correlation). Therefore, it is most efficient to diversify among stocks whose returns are not affected by similar economic events [19].

### 2.2 The Modern Portfolio theory applied to the electricity market

In energy planning, the least-cost approach has always been the favoured and most commonly used planning tool to select power generation assets [17]. The least-cost approach evaluates each electricity-generating technology according to its levelized cost of electricity (LCOE), expressed in €/MWh produced [23] [26]. By comparing the LCOE of each electricity generation technology, the technology with the lowest LCOE can be identified, which is assumed to be the best investment [26]. However, as energy planning has become tremendously complex due to factors, such as; the introduction of VRES, storage systems and demand-side flexibility, numerous authors (e.g. [17] [23]) argue that generation technologies cannot be selected solely based on the lowest LCOE anymore. The intermittency associated with certain electricity generation technologies and the complementary effects between technologies should also be included in the decision-making process [18] [23].

As a result of this increased complexity, numerous researchers (e.g. [27] [28] [29] [30] [31] [32]) started applying the Modern Portfolio Theory (MPT) to the electricity market as a more comprehensive alternative to the least-cost method. The fundamental idea behind the MPT, as described in section 2.1, remains the same when applied to a VRE system. The main difference is that the variance of returns on electricity generation technologies is not caused by firm-specific or market news, but by the availability or costs of the energy source used to generate electricity. For example, the electricity produced (return) by one MW of installed wind energy declines as wind speeds decrease. Hence, as VRES are not always available, the electricity output from VRE technologies tend to have a higher variance than the output from dispatchable energy sources. Similar to financial assets portfolios, composing energy generation portfolios that draw from negatively correlating energy sources reduces the variance in output of the whole portfolio [18].

Ever since Bar-Lev and Katz [28] applied the MPT to the electricity market in 1976 to analyse the relation between fossil resources and the power generation industry, the MPT has become a well-established energy generation planning tool [23]. Based on what researches define as the return on an energy generation portfolio, the vast body of literature applying the MPT can be divided into two literature approaches, research focusing on; economic criteria and on power production criteria [23].

Research focusing on economic criteria (e.g. [33] [34] [35]) delineate the most efficient electricity portfolios by maximising revenue (or minimising costs) for a given level of risk. By defining the expected return as the revenue generated from the sale of the electricity produced by the weighted portfolio and risk as the variance of the revenue, cost-risk efficient frontiers are generated [23]. The second literature stream consists of studies (e.g. [36] [37] [18]) that generate an efficient frontier by optimising the electricity output, measured in physical units of production, rather than monetary units [23]. Hence, the return on an energy portfolio is expressed as the number of electricity units generated per unit installed, which is known as the capacity factor (CF). The risk on a portfolio is the variance of the portfolio's capacity factor.

As this thesis aims to minimise the residual and its variance, measured in physical units of production, it can best be placed in the second literature stream.



As most researches focus on the monetary units of analysis, the literature stream using the MPT to optimise a system's physical units is small. Cunha et al. [18] applied the MPT to Portugal's historic wind, solar PV and reservoir hydro data to find the portfolios that maximise the electricity output and minimise the variance in supply. The authors found that reservoir hydropower's electricity output positively correlates with wind power, and that PV negatively correlates with both hydro and wind power [18]. The authors also concluded that future research should consider the load variability, aiming to minimise not only the variability of the portfolio's output but also the deviation between production and demand [18].

A recently published study [20], which aimed to compute the most efficient portfolios of geographically dispersed wind farms in South-Africa, including demand-variability. However, the authors first computed the portfolios that maximise the electricity output and subtract their output from the national demand profile to find the residual load. Van Vuren et al. [20] thus failed to optimise the system by minimising the residual load. The authors solely used the residual load as a means to gauge the efficiency of the portfolios. Hence, the existing literature has never optimised an electricity system by including demand-variability in MPT. The effect of demand-variability on the selection of efficient VRE portfolios is thus unknown, a knowledge gap this study aims to fill.

Just as Vuren et al. [20] and Cunha et al. [18], most researches, aiming to analyse the effects of energy diversification, apply the MPT to well-established VRE technologies, such as; wind (e.g. [38] [29] [36] [39]), PV (e.g. [38] [29] [36] [39]), reservoir hydropower (e.g. [38] [29] [36]) and biomass (e.g. [29] [36] [39]). Though little has been documented about the diversification effects of tidal energy, one study [29] suggest that tidal technologies might reduce a portfolio's risk when included in the energy mix. Allan et al. [29], optimised different scenarios for the Scottish 2020 generation mix and incorporated tidal energy in their analysis. Despite only including a maximum share of 5% tidal energy in their initial analysis, the authors doubled the share of tidal power in the sensitivity analysis. They found that the efficient frontier moved to the left, indicating the risk-mitigating effect of tidal energy [29]. However, there is no literature indicating that this positive effect preserves when tidal power covers more than 10% of the energy mix, which is the case with DTP.

### 2.3 Limitations of the Modern Portfolio Theory

The first, but most fundamental limitation of Markowitz's MPT, is that the MPT derives future returns and risks on assets from historical data, assuming future representativeness [23]. In reality, there are many factors, such as; climate conditions, political factors, social factors or economic factors affecting the future return and risk on asset portfolios [30]. Therefore, A. Stirling [40] [41] claims that using only historical data to support the portfolio model might lead to erroneous results [23]. Some scientists just accept this limitation and state that the effect of unexpected events is already included in the historical data [29], while other authors try to mitigate this limitation by combining historical data with forecasts [31].

Another limitation that materialises when Markowitz's MPT is applied to the electricity market lies in the different nature of the assets [23]. Unlike financial assets, for which the MPT was originally designed, real assets such as energy-generating technologies, are indivisible into small shares, making them highly illiquid and difficult to trade [23]. Additionally, the length required to recover from an investment is much longer for real assets than financial assets. Hence, changing over from an inefficient to an efficient real asset portfolio involves very high costs, for which the MPT does not account [23].

A third limitation of the MPT occurs when renewable energy technologies are included in the optimisation model [23]. Just as conventional fossil energy sources, renewables are included in the MPT optimisation model based on their costs and risks. However, renewables are characterised by certain positive externalities, such as; the lack of CO<sub>2</sub>-emissions. But the MPT does not account for these externalities [34]. To overcome this limitation, numerous authors (e.g. [29] [33] [42]) include the CO<sub>2</sub>-emission costs into the technology's costs structure in order to reduce the cost distance between polluting technologies and renewables.



# 3. Methodology

The methodology used to achieve the objectives described in section 1.3 was, although based on the traditional MPT, entirely new. The methodology is characterised by three steps, which are visualised in figure 7. First, the VRE portfolio shares that minimise the mean residual load and the standard deviation (STD) of the residual load were computed. Second, for each VRE portfolio, the dispatchable backup capacity required to cover the residual load and ensure electricity security was determined. The required dispatchable backup capacity is the first performance indicator used to gauge how efficient a VRE portfolio is in meeting demand. And third, the computed backup capacity was added to the VRE system, and the entire system's energy generation costs were determined. The energy generation costs were used as the second performance indicator to gauge a VRE portfolio's efficiency.

Section 3.1, 3.2 and 3.3 elaborate in detail on these three steps. Throughout this chapter examples are used to demonstrate the methodology.

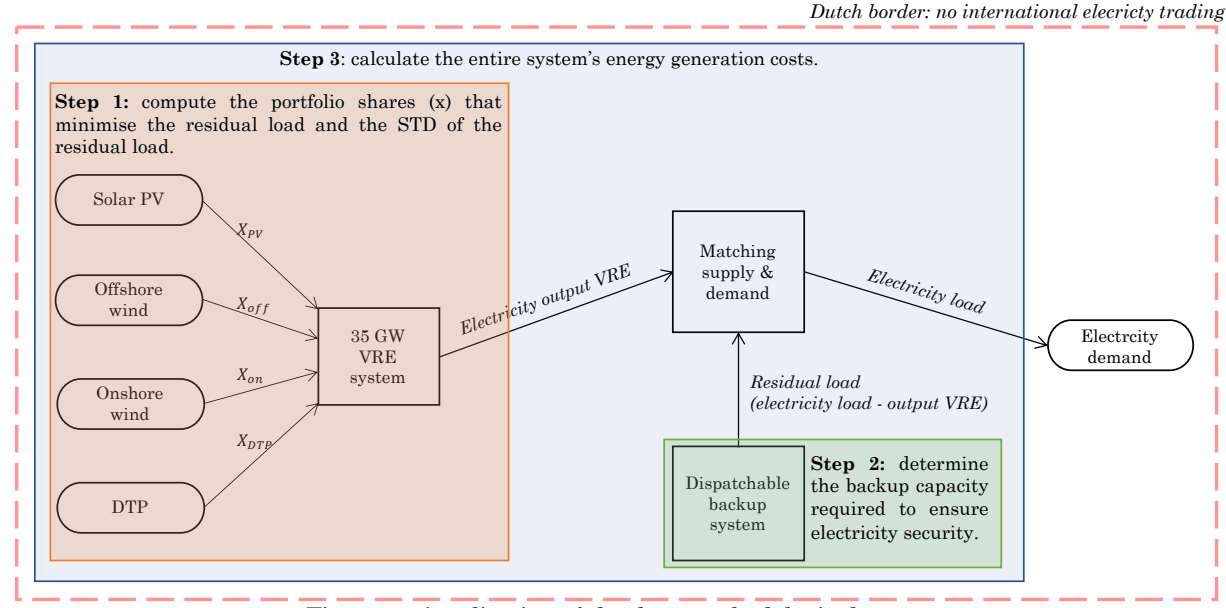


Figure 7: visualisation of the three methodological steps.

#### 3.1 Comprising efficient VRE portfolios

In this section, the methodology used to find the VRE portfolios that minimise the mean residual load and the STD of the residual load is discussed. In section 3.1.1, the data collection method is elaborated. Section 3.1.2, 3.1.3 and 3.1.4 discuss how the data was prepared and how the proxy variables for the MPT optimisation were derived. How a portfolios' mean residual load and the STD of its residual load was determined is outlined in section 3.1.5. Section 3.1.6 explains how the minimum-variance frontiers were generated by solving the optimisation problem.

#### 3.1.1 Data collection method

Applying the MPT optimisation to the electricity market requires electricity output data from all electricity generation technologies included in the optimisation. As stressed before, this study included; solar PV, wind and Dynamic Tidal Power (DTP). The wind and solar PV output data was drawn from the publicly accessible ENTSO-E Transparency Platform. The ENTSO-E Transparency Platform collects the historical data each National Transmission System Operator (TSO) is obliged to provide since 2013 under the 543 EU regulation, which aims to make the electricity market more transparent [21].



However, unlike wind turbines and solar PV cells, there is no DTP-dam from which historical electricity output data could be drawn. Therefore, DTP's electricity output was mathematically calculated by the DTP foundation using MATHLAB.

Unlike other studies that have applied the MPT to the electricity market, this study also included demand-variability. Therefore, electricity demand data was obtained. Similar to the output data, the demand data was collected from the ENTSO-E Transparency Platform. In order to minimise random annual differences in electricity supply or demand, all the historical data was collected over three years (2017-2019) and converted into time intervals of an hour.

#### 3.1.2 Normalising electricity supply

The electricity output on the ENTSO-E Transparency Platform are absolute values and thus depend on the amount of installed capacity. To allow for comparability among the energy generation technologies, their hourly electricity outputs were normalised by the respective installed capacity for each year (eq. 3.1). This was done for each hour in the period that was analysed (2017-2019), and resulted in 26,280 capacity factors for each energy-generating technology. The hourly capacity factor indicates how much electricity each unit of installed capacity produces at a specific moment in time and is often expressed in percentages.

Normalised electricity output = capacity factor 
$$[\%] = \frac{Units\ produced\ [e.g.\ MW]}{Units\ installed\ [e.g.\ MW]}$$
 (Eq. 3.1)

Subsequentially, the hourly capacity factors were multiplied with the size of the VRE system that is being optimised (eq. 3.2). As elaborated in section 1.3, this study initially optimised a 35GW VRE system. In the sensitivity analysis the system size was changed to 25 and 45GW in order to assess whether the system's size affects the outcome. For each energy generation technology and each hour in period that was analyse (2017-2019), the capacity factors were multiplied with 35GW.

Hourly electricty output  $[MW] = capacity \ factor \ [\%] * VRE \ system's \ size \ [35,000MW] \ (Eq. 3.2)$ 

#### 3.1.3 Computing the hourly residual load

Existing studies have used the normalised electricity output to maximise a VRE system's mean electricity output and minimise the STD of its output. However, this study aimed to find the VRE portfolio shares that minimise the mean residual load and the STD of the residual load. The hourly residual load is what is left after the output from VRE is subtracted from the actual electricity demand (eq. 3.3).

Hourly residual load  $[MW] = hourly \ electricity \ deman[MW] - hourly \ electricity \ output[MW] \ (Eq. 3.3)$ 

To clarify the principle of the residual load, it is visualised in an example (fig. 8). The blue line illustrates the amount of electricity demanded from the system and the orange line illustrated how much electricity is supplied by 35GW of solar PV. For example, at 5 o'clock, the 35GW solar PV system's electricity output is 13GW and demand is 16 GW, so the residual load is 3GW. A negative residual load indicates that the 35GW system produces more electricity than is demanded. In this study, electricity surplus and deficiencies were treated as equally inefficient. The residual load was determined for each energy-generating technology and hour in period that was analysed (2017-2019).



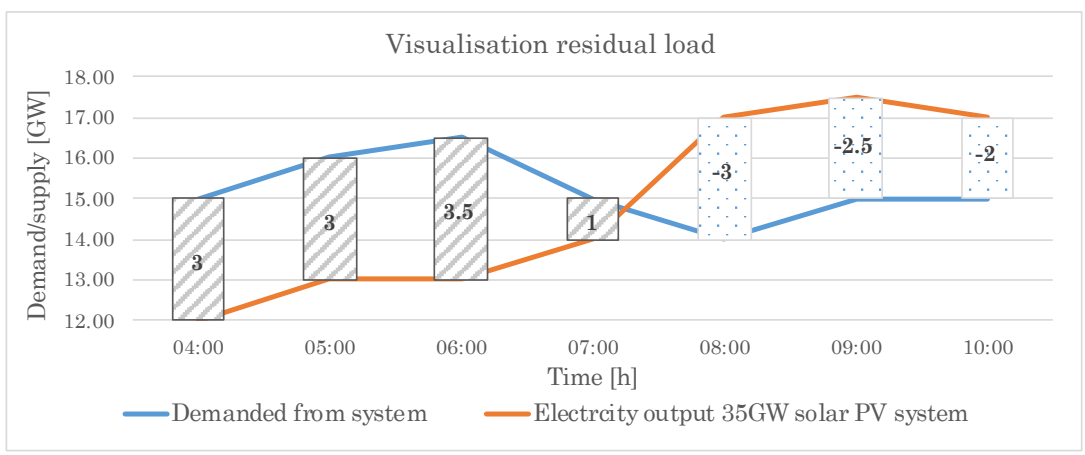


Figure 8: visualisation residual load.

#### 3.1.4 Deriving the proxy variables

After the hourly residual loads were determined for each energy generation technology, the proxy variables were derived. The proxy variables are not in itself directly relevant but serve as input parameters for the MPT optimisation. Three different proxy variables are needed; the energy technologies' mean residual loads (I), the standard deviation (STD) of a technologies' residual loads (II) and the correlation coefficients among all technologies' residual loads (III).

#### Proxy variable I: mean residual load

A technology's mean residual load is the average of all the hourly residual loads (eq. 3.4). A technology's mean residual load indicates how much of the electricity demand, on average, could not be covered, if 35GW of that specific technology were to be deployed to cover demand.

$$RL_i = \frac{RL_{i,1} + RL_{i,2} ... + RL_{i,n}}{n}$$
 (Eq. 3.4)

#### Proxy variable II: standard deviation

The STD of a technology's residual load ( $\sigma(RL_i)$ ) is the root of the sum of the squared deviations from its mean residual load ( $(R_i - \bar{R})^2$ ) divided by the number of observations minus 1 (n-1) (eq. 3.5). The STD of a technology's residual load indicates how volatile the residual loud is, if 35GW of that specific technology were to be deployed to cover demand

$$\sigma\left(RL_{i}\right) = \sqrt{\frac{\sum_{i=1}^{i=n} (RL_{i} - \overline{RL})^{2}}{n-1}}$$
 (Eq. 3.5)

#### Proxy variable III: correlation coefficient

The correlation (eq. 3.6) between the residual loads of two energy-generated technologies  $(\rho(RL_i,RL_j))$  is the covariance  $(Cov(RL_i,RL_j))$  divided by the standard deviation of the two individual residual loads  $(\sigma(RL_i))$ . The covariance (eq. 3.7) is characterised as the product of the deviation of two residual loads from its mean residual loads  $((RL_i - \overline{RL_i}))$  divided by the number of observations (n). The correlation coefficient varies between -1 to 1 and measures to what degree the two technologies' residual loads move together. If two technologies' residual loads tend to be above or below its mean residual load at the same time, the two stocks move together and their correlation is positive. The correlation is negative when the technologies' residuals loads move in opposite direction and zero if there is no correlation. The corelation coefficient has to be calculated for all possible combinations of two energy-generating technologies.



$$\rho(RL_i, RL_j) = \frac{Cov(RL_i, RL_j)}{\sigma(RL_i) * \sigma(RL_i)}$$
 (Eq. 3.6)

$$Cov(RL_i, RL_j) = \frac{\sum_{i=1}^{i=n} (RL_i - \overline{RL_i}) * (RL_j - \overline{RL_j})}{n}$$
 (Eq. 3.7)

#### 3.1.5 VRE portfolio's mean residual load and standard deviation

At this stage, we could determine the mean residual load and its standard deviation for a 35GW VRE portfolio that is comprised of a single energy technology. However, the goal is to combine multiple technologies in a portfolio. Hence, we are interested in a portfolio's mean residual load (I) and the STD of a portfolio's residual load (II). These can be computed using the technologies' proxy variables.

#### I portfolio's mean residual load

A VRE portfolio's mean residual load  $(E(RL_p))$  is the sum of all the portfolio weights  $(X_i)$  times the expected mean residual load of each technology  $(E(RL_i))$  (eq. 3.8). Note that there are two constraints to the portfolio weights; portfolio weights always have to add up to a 100% and portfolio weights cannot be negative. A VRE portfolio's mean residual indicates how much of the electricity load, on average, could not be covered by the portfolio, if 35GW were to be installed according to the portfolios shares that that are plugged into the equation.

$$\sum_{i=1}^{n} X_{i} = 1$$

$$E(RL_{p}) = \sum_{i=1}^{i=n} X_{i} * E(RL_{i})$$
 (Eq. 3.8)

#### II portfolio's standard deviation

Unlike the VRE portfolio's mean residual load, its STD is not just the weighted average of each technology's residual load, but also includes the correlation coefficient between technologies' residual loads. The variance of a portfolio, is a multiplication of the portfolio weights, the variance of each individual technology's residual load and the mutual correlation between the residual loads (eq. 3.9). The STD of a VRE portfolio's residual indicates how volatile the residual load is, if 35GW were to be installed according to the weights that are plugged into the equation.

$$\sigma(RL_p) = \sqrt{X_i^2 * \sigma(RL_i)^2 + X_j^2 * \sigma(RL_j)^2 + 2 * X_i^2 * X_j^2 * \rho(RL_i, RL_j) * \sigma(RL_i) * \sigma(RL_j)}$$
 (Eq. 3.9)

#### 3.1.6 Solving the optimisation problem: the minimum-variance frontier

At this point, one can plug in any portfolio shares, as long as they accumulate to 100%, and derive the portfolio's mean residual load and the STD of its residual load. However, the goal is the find all the VRE portfolios that minimise both the mean residual load and the STD of the residual load. These portfolios are best in meeting demand. This optimisation problem could be solved by plugging different portfolio weights in the equations (3.8 & 3.9) and compute the mean residual load and the variance of the residual load. This would, however, be very time-consuming. Therefore, Excel Solver was used to solve this optimisation problem.



Solver is a Microsoft Excel add-in program, which can be used to find optimum values. To find these optimum values, one has to define the objective function, the degrees of freedom, and the constraints. The objective function is an equation that is either minimised or maximised. The degrees of freedom are the variables that are adjusted in order to minimise or maximise the objective function. Constraints are certain conditions that need to be satisfied while finding the optimum value.

To find the most efficient portfolios, the objective was to find the VRE portfolios that minimise the residual load and the volatility of the residual load. However, Solver cannot optimise two values simultaneously. Therefore, either the mean residual load or STD of the residual load had to be fixed. For this optimisation, the mean residual load was fixed and set as a constrain. Hence, the STD of a VRE portfolio's residual load was the objective function. A portfolio's STD changes as the portfolio weights are adjusted. Therefore, the energy technologies' portfolio weights were the degrees freedom in this optimisation. However, the weights cannot be negative and must add up to 100%, which were the second and third constraints.

To find all the efficient VRE portfolio shares, the model was run as following. First, the mean residual load was fixed at a value that lies within the range of the individual technologies' mean residual loads. The model was run and the STD and the corresponding portfolio shares were obtained. Hence, these are the portfolio shares that correspond with the first efficient VRE portfolio. Subsequentially, the mean residual load was increased with 500MW and the STD, and corresponding portfolio shares were obtained. This is the second efficient VRE portfolio. This process was repeated until the whole range of possible mean residual loads was covered. When all the mean residual loads and STDs are plotted in a scatter plot, the minimum-variance frontier is generated. Hence, the minimum-variance frontier is the outcome of the optimisation problem.

Figure 9 illustrates an exemplary minimum-variance frontier. The vertical axis represents a portfolios mean residual load and the horizontal axis its STD. As explained in detail in section 2.1.3, not all the portfolios on the minimum-variance frontier are equally efficient. Although all portfolios on the minimum-variance frontier minimise the STD of the residual load, only the portfolios on efficient frontier minimise both the STD and the mean residual load. In figure 9, the inefficient part of the minimum-variance frontier is coloured red, the efficient frontier is marked green. As a result, all the VRE portfolios on the minimum-variance frontier's inefficient part (red) can be eliminated, leaving only the portfolios on the efficient frontier (green).

Figure 10 illustrates an example of the portfolio composition of the VRE portfolios located on the efficient frontier (green line fig. 9). The vertical axis indicates the portfolio shares and the horizontal axis a portfolios mean residual load and STD. Hence, the latter corresponds with the vertical and horizontal axis of figure 9 and thus indicates where on the efficient frontier (green line in fig. 9) a portfolio is located. This study's final results are similarly visualised.

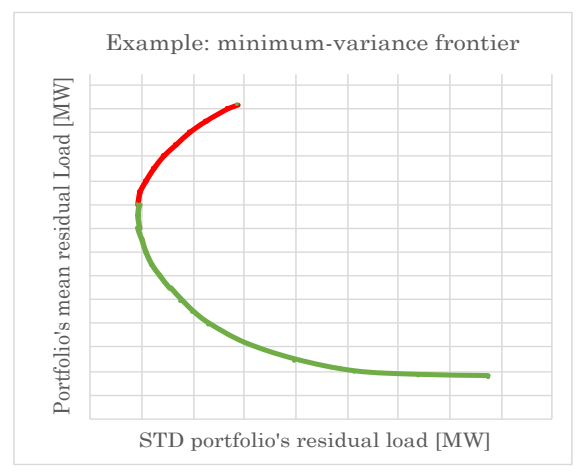


Figure 9: exemplary minimum-variance frontier. Red marks the inefficient part of the minimumvariance frontier and green the efficient frontier.

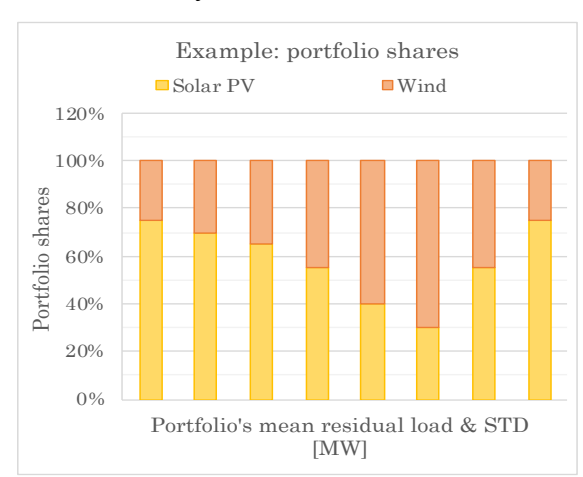


Figure 10: exemplary overview portfolio shares.



### 3.2 Dispatchable backup capacity

Although the MPT allows for the elimination of some VRE portfolios, there are still multiple portfolios located on the efficient frontier. As these are considered equally efficient, it is impossible to determine which VRE portfolio is best in meeting demand and should be perused by energy planners. While other studies [18] leave this decision to the energy planner's preferences, this study aimed to find an unambiguous answer to the question; which VRE portfolios are most efficient in meeting demand. Therefore, this study has gauged and compared the portfolios on the efficient frontier by mean of two performance indicators; the amount of dispatchable backup capacity that is required to cover a VRE portfolio's residual load (1) and a system's total energy generation costs (2). This section elaborates on the methodology that was used to determine the size of the required backup system. Section 3.3 explains how the system's energy generation costs were determined.

The size of a VRE portfolio's backup system was derived from the characteristics of a VRE portfolio – its mean residual load and STD – and the assumption that the residual load data is normally distributed. Normally distributed data should be more or less shaped as a bell curve, which is visualised in figure 11. The horizontal axis is the value in question – the residual load in this instance – and the vertical axis is the number of data points for each value. To verify whether the residual load data lies within the margins to be considered normally distributed George et al. [43] boundaries for skewness<sup>1</sup> and kurtosis<sup>2</sup> (+2 / -2) were followed, the results can be found in appendix H.

When data is normally distributed the STD, which indicates how tightly data is clustered around its mean, can be used to demarcate the confidence interval (CI). The CI is the probability that a number (i.e. an hourly residual load) falls between two specific values. Figure 11 visualises this concept; it is 68.3% certain that an hourly residual load data point lies within one standard deviation away from the mean residual load. More explicitly, if 100 random residual loads were to be drawn from the data set, 68 of them would lie one standard deviation away from the mean residual load. The other 32 values are either higher or lower than the value one standard deviation away from the mean, and are thus located at either end of the bell curve. When the number of standard deviations from the mean is increased, more data lies within this range, and the confidence interval inflates. The number of STD that corresponds with a certain confidence interval is called the z-score.

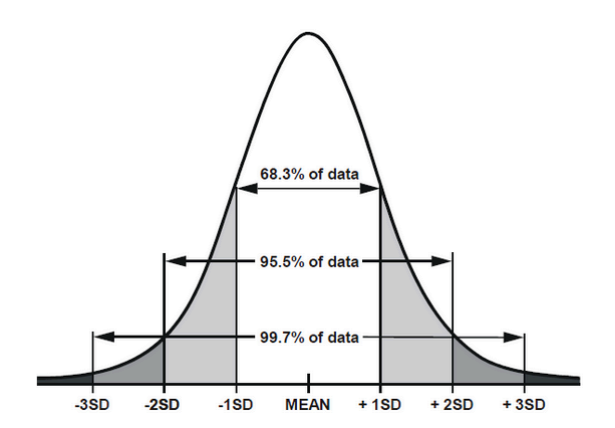


Figure 11: visualisation normally distributed data set with a two-tailed confidence level. SD is standard deviations [85].

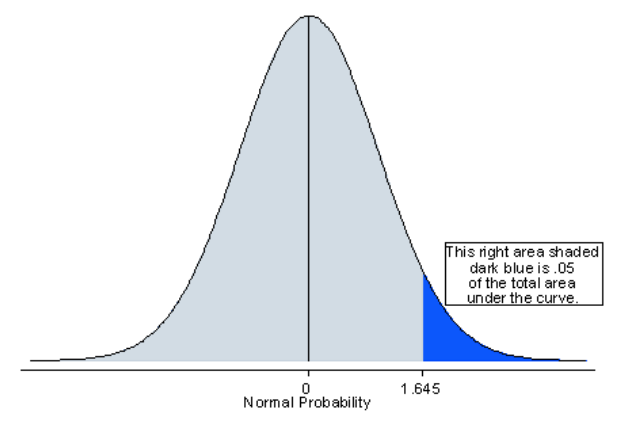


Figure 12: visualisation normally distributed data set with a 95% one-tailed confidence level [84].

<sup>&</sup>lt;sup>1</sup> "Skewness is a measure of the asymmetry of the distribution of a variable" [93].

<sup>&</sup>lt;sup>2</sup> "Kurtosis measures the tailedness of the distribution" [93].



This property of normally distributed data and the fact that the portfolios' mean residual loads and standard deviations are known, were used to determine the backup capacity. However, a backup system does not draw random residual loads from the data set. The moment backup capacity is installed, it starts covering the residual load from left to right – first covering small residual loads. Therefore, the confidence interval has to be set from left to right rather than from the mean towards the bell curve's ends. This is called a one-tailed confidence interval and is visualised in figure 12. Note that for a 95% one-tailed CI, the remaining 5% of the residual load data is located at the end of one tail of the bell-curve, rather than being divided over the two tails. As a result, the z-score for a 95% one-tailed CI (1.645), is lower than the z-score for a 95% two-tailed CI (2).

Similar as what is visualised in figure 12, this study used a 95% CI, which means that the backup should be able to cover 95% of the residual load left by a VRE portfolio. To be able to do so, the size of a VRE portfolio's backup should be equal to its mean residual load ( $\mu(RL_p)$ ), plus 1.645 times the STD of the portfolio's residual load ( $\sigma(RL_p)$ ) (eq. 3.10). Based on the amount of backup capacity, all the portfolios on the efficient frontier were gauged, and the one that requires the least backup is considered most efficient in meeting demand.

Dispatcable backup capacity =  $\mu(RL_P) + 1.645 * \sigma(RL_p)$  (Eq. 3.10)

#### Example

For this example, the MPT was used to find the VRE portfolios for a 35GW system that minimise the mean residual load and the STD. One of the portfolios on the efficient frontier is comprised 30% solar PV and 70% wind, and has a mean residual load of 5,000 MW and a STD of 4,000 MW. Hence, the amount of dispatchable back required to ensure 95% electricity security is equal to 5,0000+1.645\*4,000=11,580 MW. So, when a 35 GW VRE system would be comprised of 35% solar PV (10.5 GW) and 70% wind (24.5 GW), it would require a backup capacity of 11.58 GW to ensure 95% energy security.



#### 3.3 Energy generation costs

Besides its required backup capacity, the portfolios on the efficient frontier were also gauged and compared based on their energy generation costs. The energy system with the lowest energy generation costs is considered to be most efficient in meeting demand. Hence, there is a VRE portfolio that it most efficient in terms of its required backup capacity and a most cost-efficient system, these are not necessarily the same portfolios.

The energy generation costs were computed for the entire energy system, so for both the VRE portfolio and the backup capacity that is required to ensure energy security. Hence, the backup capacity was added to the 35GW VRE system and the new portfolio shares were determined. Subsequentially, the new portfolio shares were multiplied with each technology's individual energy generation costs. Although numerous studies have estimated technologies' energy generation costs, this study computed them manually. This was done to acquire a thorough understand of the role of certain cost parameters and ensure that the same costs were included for each technology, making the results comparable. The technologies' energy generation costs were computed using the levelized cost of energy (LCOE). A technology's LCOE is the nett present value (NPV) of the costs over its lifetime divided by the NPV of the electricity generated over its lifetime and is expressed in €/MWh [44] (eq. 3.11).

t = period ranging from year 1 to year n

 $C_t = capital \ costs \ in \ period \ t$ 

 $r = discount \ rate$ 

n = final year of operations

$$C_{t} = \text{capital costs in period } t$$

$$O_{t} = \text{fixed operating costs in period } t$$

$$E_{t} = \text{energy generated in period } t$$

$$V_{t} = \text{variable operating costs}$$

$$LCOE\left[\frac{\epsilon}{MWh}\right] = LC_{t} = \sum_{t=1}^{n} \frac{\frac{C_{t} + O_{t} + V_{t}}{(1+r)^{t}}}{\frac{E_{t}}{(1+r)^{t}}}$$
(Eq. 3.11)

Most input parameter for the LCOE calculation are self-explanatory, just note that the variable operating costs  $(V_t)$  are only applicable to the dispatchable backup capacity, as VRE technologies do not use any fuels or emit CO2 when electricity is generated. Apart from the amount of electricity generated over a technology's lifetime, all the input paraments were derived from the literature. The amount of electricity produced over a VRE technologies' lifetime was determined based on its historical output data that was collected. As elaborated in section 3.1.2, from the historical data, each VRE technology's hourly capacity factors were determined. The mean of the hourly capacity factors indicates how much electricity, on average, is produced per MW installed. When a technology's average capacity factor it multiplied with its lifetime in hours, the amount of electricity a technology produces over its lifetime was found (eq. 3.12);

$$E_t[MWh] = average\ capacity\ factor\ [\%] * technology's\ lifetime\ [h]$$
 Eq. 3.12

Regarding the backup system, it is slightly more complicated to determine its capacity factor, as it depends on the characteristics of the VRE portfolio (mean residual load and STD), and thus differs for each portfolio. As elaborated in section 3.1.2, the capacity factor is the amount of electricity produced divided by the installed capacity. The installed dispatchable backup is known, as this was used as a performance indicator to determine a VRE portfolio's ability to meet demand. However, the amount of electricity produced is not known. At first, one would assume that the amount of electricity produced by the backup system is equal to a VRE portfolio's mean residual load. However, the residual load also includes negative values, namely; when more electricity is produced by the VRE system then is consumed. As the dispatchable backup generator cannot store any electricity, only generate, setting the backup system's electricity output equal to a VRE portfolio's mean residual load would yield erroneous results.



To overcome this issue, all the negative residual loads were set to zero, and the average of all the non-negative residual loads was computed. The average of the, non-negative, residual loads is equal to the amount of electricity produced by the backup. In practice, this means that the average electricity output from the backup system is slightly higher than the VRE portfolio's mean residual load. Subsequently, the VRE portfolio's mean, non-negative, residual load was divided by the backup system's size. The resulting capacity factor was used to determine a backup system's LCOE. This was done individually for each portfolio on the efficient frontier.

Finally, the LCOE of each energy system located on the efficient frontier was computed by taking the sum of all the portfolio weights  $(X_i)$  multiplied with the technologies' LCOEs  $(LC_i)$  (eq. 3.13). Subsequentially, all the portfolios' LCOEs were compared in order to find the VRE system that is most costs-efficient in meeting demand.

$$E(LC_p) = \sum_{i=1}^{i=n} X_i * LC_i$$
 (Eq. 3.13)

#### Example:

Using the same example as in section 3.2; a 35 GW VRE system comprised of 30% solar PV and 70% wind with a mean residual load of 5,000 MW and STD of 4,000 MW. The required dispatchable backup capacity was found to be 11,580 MW. Using equation 3.11, the LCOE of solar PV and wind are determined and are 67.31 and 50.27~€/MWh. Additionally, it was found that the average, non-negative, residual load of the VRE portfolio is 4,500 MW, which means that the backup's capacity factor is equal to 4,500 MW / 11,580 MW = 0.39 (39%). Using equation 3.11 a LCOE of 73.85 €/MWh was found.

Before the system's total energy generation costs are determined, the new portfolios shares are computed. The total system's size is 35,000 MW VRE + 11,580 backup = 46,580 MW. So the new portfolio shares are ;

Solar PV: (0.3\*35,000)/46,580=0.23 (23%) Wind: (0.7\*35,000)/46,580=0.53 (53%) Backup: 11,580/46,580= 0.24 (24%)

So, the system's total energy generation costs are;

23% \* 67.31 €/MWh + 53% \* 50.27 €/MWh + 24%\*73,85 €/MWh = 59.84 €/MWh



## 4 Case study: The Netherlands

The novel methodology described in chapter 3 was applied to the case study of The Netherlands in order to find the VRE portfolios that are most efficient in meeting electricity demand. Besides VRES already deployed in The Netherlands – solar PV and wind – a novel energy-generating technology was included in this case study; Dynamic Tidal Energy (DTP). Therewith this case study served three purposes. Firstly, it enabled the validation of the novel application of the MPT and the assessment of whether including demand-variability in the MPT affects the selection of efficient VRE portfolios. Secondly, by determining the most efficient VRE portfolios, this study provides tangible information Dutch energy planners can use to develop a roadmap towards an efficient decarbonised energy system. Thirdly, it provides new insights into whether DTP has a positive effect on a VRE system's ability to efficiently meet demand.

This chapter elaborates the case study, in particular, the data used for the optimisation model. Section 4.1 and 4.2 discuss the supply side of the optimisation model. Section 4.1 elaborates on the VRE technologies currently deployed in the Netherlands (solar PV and wind), while section 4.2 discusses Dynamic Tidal Power. The model's demand side is discussed in section 4.3. Section 4.4 elaborates on the energy generation costs. The last section provides an overview of the different scenarios and configurations that were optimised.

### 4.1 Electricity supply solar PV and wind

This section discusses the electricity supply from currently deployed VRE technologies, including solar PV, offshore wind and onshore wind. As visualised by figure 13, throughout the years, renewable energy technologies have acquired a more dominant role in The Netherlands' electricity mix. Especially the installed capacity of solar PV has increased dramatically since the end of 2016. The installed capacity of onshore wind has also slightly increased, whereas offshore wind has remained the same over the last four years. However, the latter is about to change as The Netherlands aims to increase the installed capacity of offshore wind to 11GW by 2030 [45]. The installed capacity of solar PV and onshore wind is also bound to increase, as The Netherlands has set the target to increase the electricity generation from onshore renewable energy technologies to 35TWh per year by 2030 [46].

The two following sections look into the electricity output from solar PV and wind. Section 4.1.1 first elaborates how the electricity output data that was obtained. In section 4.1.2 the electricity output profiles of solar PV and wind are visualised and discussed.

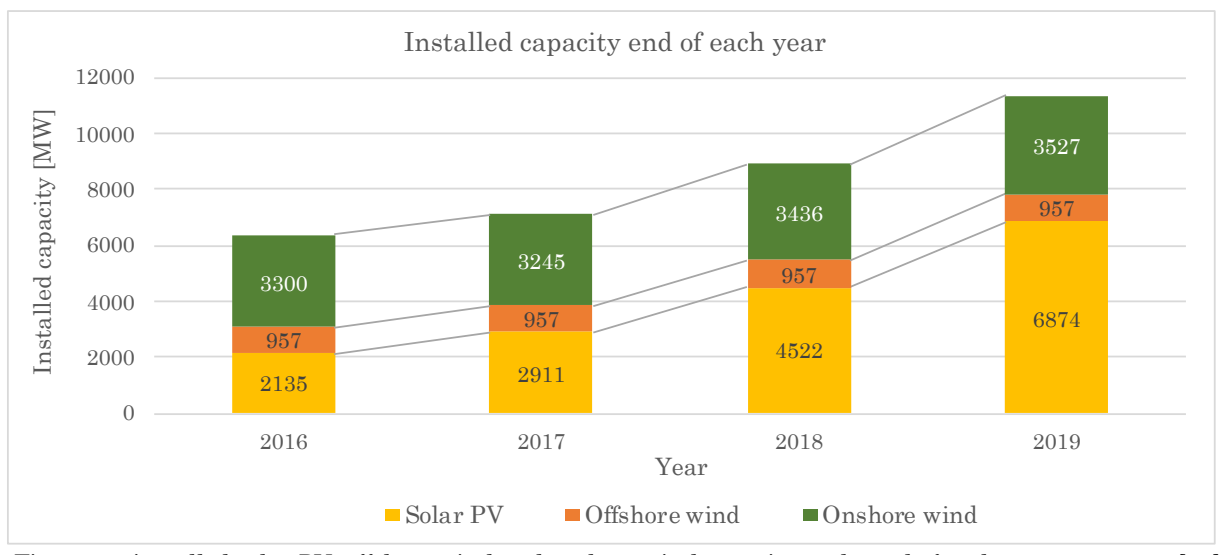


Figure 13: installed solar PV, offshore wind and onshore wind capacity at the end of each year 2016-2019 [90].



#### 4.1.1 Data collection

This section elaborates on the method used to collect the electricity output data of solar PV and wind. The electricity output data of solar PV, onshore wind and offshore wind was collected from the ENTSO-E transparency platform over three years (2017-2019). The historical electricity output was measured for each quarter of an hour, which results in 140.160 data points. To make the dataset more manageable, these 15-minutes intervals were merged into hourly intervals by taking the average of the four intervals that comprise an hour. The resulting 26.280 data points for each technology – equal to the number of hours in three years – still capture the daily and yearly seasonality of the technologies' electricity outputs.

The ENTSO-E Transparency Platform distinguishes between; the actual generated output, the day-ahead forecasted output and the intra-day forecasted output. For this study, the actual generated output was used as it best captures the actual (re-)occurring weather patterns rather than the predicted weather patterns. However, one-third of 2019's actual PV output data was not yet available on the ENTSO-E platform. 2019's forecasted PV output data, on the other hand, was already published on the ENTSO-E Platform. To determine how accurately the forecasted output data corresponded with the actual output, and whether it could be used to substitute the missing data, 2017 and 2018's forecasted PV output data was compared with the actual output data. This was done by calculating the Normalised Root Mean Square Error (RMSE).

The NRMSE is the deviation of the prediction errors divided by the range of the observed data (eq. 4.1). The NRMSE is frequently used in climatology, forecasting, and regression analysis to measure the difference between values predicted by a model (i.e. forecasted electricity output) and the values actually observed from the environment that is being modelled (i.e. actual electricity output) [47].

$$\begin{array}{l} \textit{Xi = actual output} \\ \textit{Yi = forecasted output} \\ \textit{n = number of data points} \\ \textit{Ymax = Higest observed data point (2296MW)} \\ \textit{Ymin = Lowest observed data point (0MW)} \end{array} \\ \begin{array}{l} \textit{NRMSE} = \frac{\sqrt{\sum_{i=1}^{n}\frac{(xi-yi)^2}{n}}}{Ymax-Ymin} \\ \textit{Eq. 4.1} \end{array}$$

The lower the NRMSE, which can vary from zero to one, the smaller the prediction error is. Regarding 2017 and 2018's forecasted PV data, only, 3,7% of all data points deviated relative to the actual electricity output. More importantly, the NRMSE was 0,012, which indicates a very small prediction error. Hence, the model used very accurately predicted the actual electricity output from solar PV cells. Assuming 2019's predictions are equally accurate, 2019's forecasted PV data was used to substitute 2019's missing actual electricity output data.

Though filling the blanks in 2019's actual PV output with the forecasted output significantly reduced the amount of missing data, another 34 (0,13%) wind and 99 (0,38%) solar PV data points were missing. To ensure smooth and continuous output curves, these blanks in the historical data were also filled. Solar irradiation is characterised by a repeating daily and seasonal pattern. Therefore, the blanks were filled using the average hourly electricity output during that month. E.g. the missing data on 20-12-17 was filled with the average electricity output profile of December. On the other hand, wind speeds are more random and, unlike solar irradiation, not characterised by a specific daily pattern. Hence, the method used to substitute the missing solar PV data could not be used to fill the missing wind data. However, unlike the missing PV data, there were no large gaps in the wind data set (max. 15 hours). Additionally, based on the hours prior and after the missing data points, a clear electricity output trend over the missing hours was identified. Therefore, the missing wind data was subsisted by assuming that the electricity output changed linearly over the hours for which no data was available.



#### 4.1.2 Electricity output solar PV and wind

In this section, the electricity output profiles of solar PV and wind are visualised and discussed. To allow for comparability among the energy-generating technologies' hourly electricity outputs, the electricity output data was normalised by the installed capacity. Figure 13 illustrates the installed capacity of solar PV, offshore wind and onshore wind at the end of each year. For the sake of simplification, this study assumed that the in- or decrease of installed capacity over each year was linear. For example, over 2017 (the end of 2016 to the end of 2017), the installed solar PV capacity increased with 776 MW, which means that on the scale of analysis used in this study – hours – the installed capacity increased with 88,6 KW. The change in the hourly installed capacity was added to the initially installed capacity. Subsequentially, the technologies' hourly capacity factors were obtained by dividing the electricity output by the linear increasing installed capacity. The hourly capacity factors indicate how much units of electricity are produced per unit of installed capacity.

Visualising the hourly capacity factors results in electricity output profiles. A small section of these output profiles are illustrated in figure 14. The vertical axis indicates the date and time and the vertical axis the hourly capacity factors for four random days in 2019. As there is no solar irradiation during the night, PV cells only produce electricity during the day, which makes their generation profiles fairly predictable. Only the magnitude of solar PV's electricity output varies depending on the day-to-day circumstances (solar irradiation, temperature). Wind speeds, on the other hand, are much more erratic compared to solar irradiation, making their electricity output highly variable and difficult to predict.

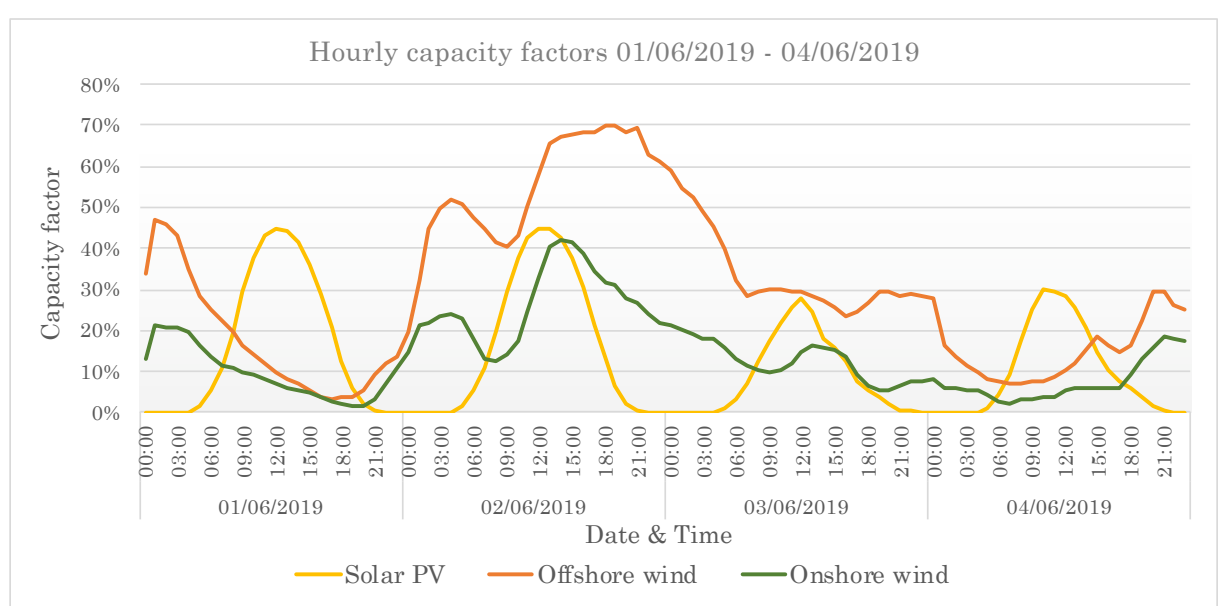


Figure 14: hourly electricity output per unit installed for 4 random days in 2019 [21].

To illustrate the seasonality of solar irradiation and wind speeds, each month's average capacity factors for the years 2017-2019 were visualised in figure 15. It is clear that both solar irradiation and wind speeds are characterised by repeating patterns. Wind speeds tend to peak during autumn and winter (Oct. – Mar.), while solar irradiation peaks during spring and summer (Apr. – Sep.). Figure 15 also illustrates that, the average electricity output from solar PV cells is significantly lower than those from wind turbines. Although off- and onshore wind speeds are characterised by similar yearly profiles, on average, offshore wind turbines generate more electricity than wind turbines located on land.



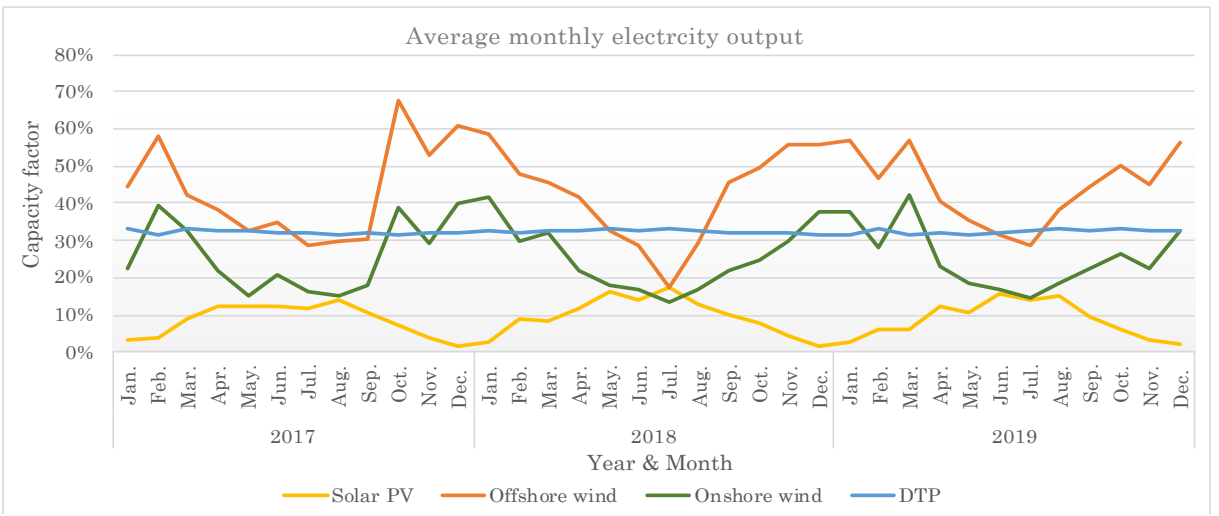


Figure 15: Average monthly capacity factors for 2017-2019 [21].

### 4.2 Electricity supply Dynamic Tidal Energy

Apart from currently deployed VRES, this case study also included Dynamic Tidal Power (DTP), a novel renewable energy technology that generates electricity utilising the North Sea's tidal currents. This section first explains the mechanisms behind tidal currents and how they can be captured to generate electricity. Subsequently, section 4.2.1 elaborates on the data collection method and section 4.2.2 visualises and discuss the electricity output profiles.

Tidal currents are driven by the rise and fall of the astronomic tides [8], which are slow and long-period waves that move through the oceans in response to the gravitational pull of the sun and in particular the moon [48]. The gravitational pull of the sun and moon's causes the ocean to "bulge" outwards on opposite sides of the earth, which causes a rise in the water level in places that are aligned with the moon and sun, and a decrease in water levels halfway between those two places (fig. 16) [49]. During every lunar day, which is 50 minutes longer than a solar day, the earth rotates through two tidal "bulges" [49]. Hence, The Netherlands experience two high and two low tides every 24 hours and 50 minutes, with a period of 6 hours and 12.5 minutes between high and low tide [50].

Besides the earth's rotation around its axis, the moon also revolves around the earth. The moon orbits in the same direction as the earth rotates around its axis, which explains why the earth takes 50 minutes to catch up to the moon [49]. A lunar phase cycle (from new moon to new moon) is 29.5 days. During this cycle the earth, sun, and moon align twice (full moon and new moon), during which the gravitational pull of the sun is added to the gravitational pull of the moon (fig. 17) [51]. Two days later, this results in spring tide; during which high tides are a little higher and low tides are a little lower than average [50]. Approximately seven days after each spring tide, during the first and third quarter moon, the sun and moon are at right angles to each other, which partially cancelling out each other's gravitational pull. During this period of neap tides, high tides are a little lower and low tides are a little higher than average.

As the North Sea is too small to be effected by the sun and moon's gravitational pull, its tides are mainly driven by the Atlantic Ocean' tidal waves [52]. Figure 18, illustrates that this tidal wave starts from the Atlantic Ocean and moves through the English Channel along the Dutch coastline into the North Sea. During high tide, water follows this path to flow into the North Sea. A brief slack period follows, the current switches direction, the velocity increases and the water flows out again [53]. This periodically alternating water flow parallel to the Dutch coastline is referred to as tidal currents [8]. Tidal currents peak four times a day, in between high and low tide. During spring tide, when the magnitude between high and low tide is the greatest, tidal currents in front of the Dutch coast can reach speeds of 0.8-1.2 m/s [9].



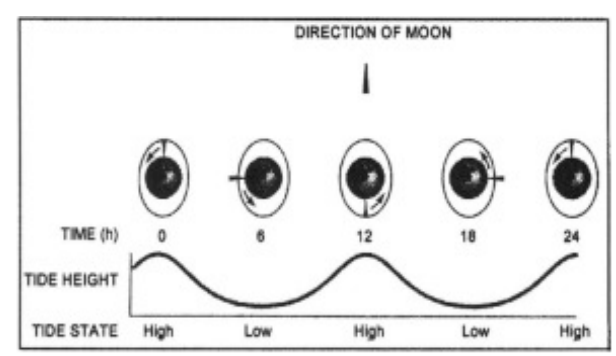


Figure 16: tidal variation due to the rotation of the earth [51].

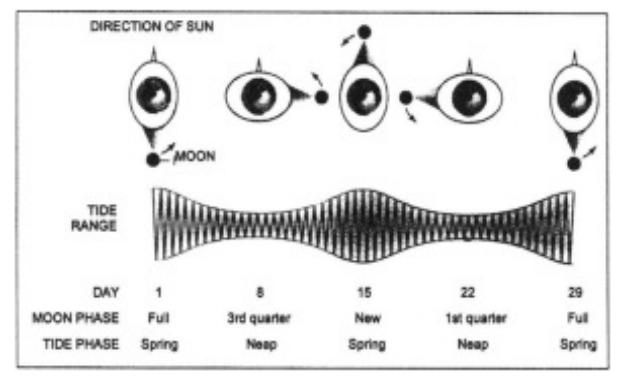


Figure 17: tidal variation due to the moon revolving around the earth [51].

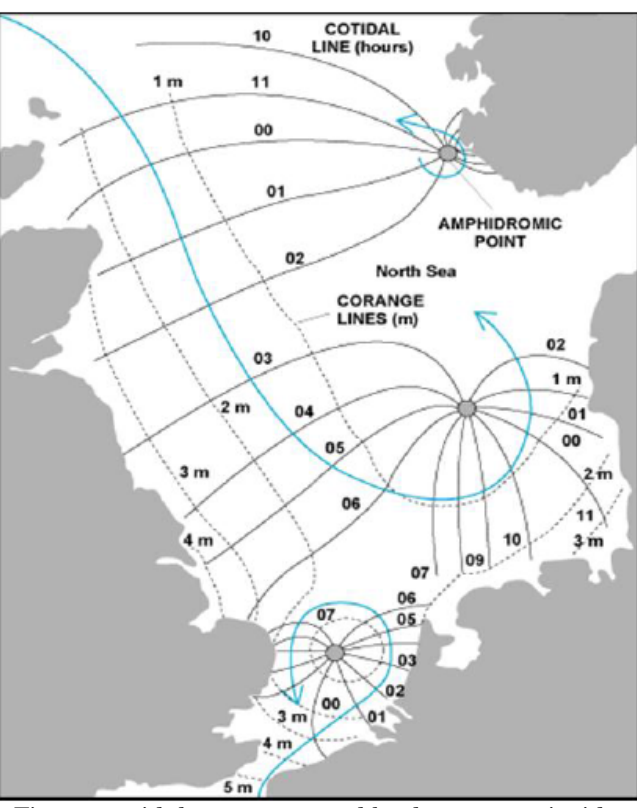


Figure 18: tidal currents caused by the astronomic tides [86].

However, to generate electricity from these tidal currents, most power converters require a minimum flow speed of 0.5 to 1.0 m/s, but preferably a speed between 1.5 and 3.5 m/s [13]. These ideal water velocities are rarely met in the Dutch territories of the North Sea. Hence, apart from some small-scale initiatives, The Netherlands currently does not utilises the North Sea's tidal currents to produce electricity. However, Dynamic Tidal Power (DTP), a novel tidal stream technology also efficient at low water speeds, enables The Netherlands to harvest the North Sea's energy potential.

DTP captures the North Sea's tidal currents using a 30-70 km long and 60-70 meter wide dam perpendicular to the coastline [54]. The periodically alternating tidal current creates a difference in water level amplitude between both sides of the dam [55]. The extra body of water on one side of the dam increases the water velocity as it flows through the 8 meter wide turbines installed in the dam (fig. 19) [54]. As the turbines can rotate in both directions, they generate electricity regardless of the direction – south to north (high tide) or north to south (low tide) – of the tidal current (fig. 20) [54].

The electricity output from a DTP-dam predominantly depends on the velocity of the tidal currents, the water depth, and the dam's length and design. An increase in tidal current speeds will increase the head over the dam and its electricity output. Similarly, when the water depth or length of the dam increases more water is pushed up against the dam, increasing the water speeds through the turbines (fig. 19) [55]. A design variable that greatly influences DTP's electricity output is the shape of the dam's ends. A coastal dam connected to land on one side yields the highest electricity outputs as the large land mass amplifies the head over the dam. An open sea dam's efficiency can significantly be increasing by equipping the dam with so-called T- or Y shaped ends. Especially a Y-shaped dam, illustrated in figure 21, is very effective in increasing the electricity output [56].



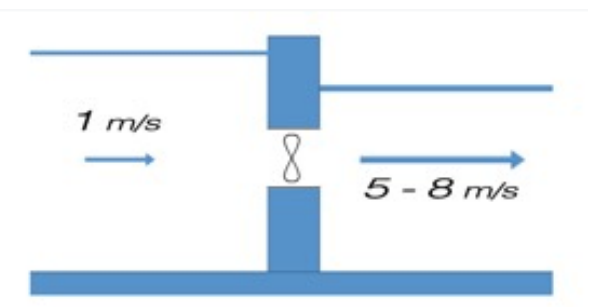


Figure 19: graphical illustration how the head over the DTP-dam increases water velocities [54].

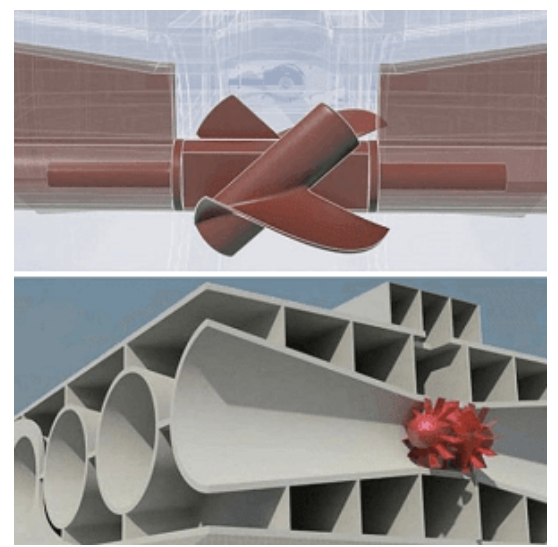


Figure 20; illustration of the 8 meter wide turbines that can rotate in both directions [83].

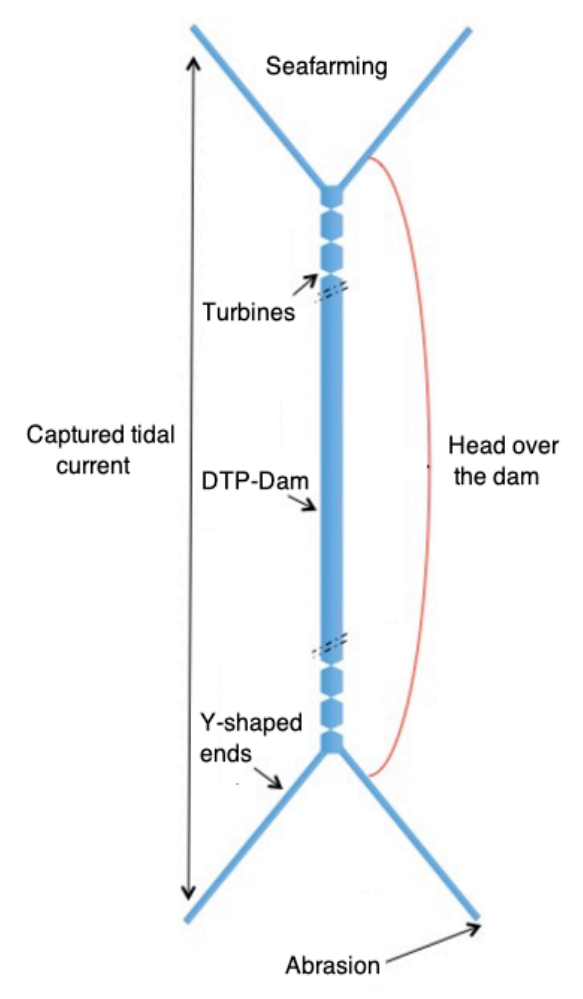


Figure 21: visualisation of a Y-shaped DTP-dam [54]. Text was translated to English.

#### 4.2.1 Data collection

This section elaborates on the data collection method used to obtain the electricity output from DTP. Unlike wind turbines and solar PV cells, there is no DTP-dam from which historical electricity output data can be drawn. Therefore, DTP's hourly electricity profile, capacity factors and installed capacity were mathematically calculated by the DTP foundation using MATHLAB. Since DTP is still under development, important characteristics (i.e. water depth, water velocity, length and design) that determine the dam's efficiency are yet unknown. Hence, generic design parameters and environmental characteristics were used to derive DTP's hourly generation profile.

As a result, DTP's electricity profile was derived modelling a 50 kilometres long dam located in the open North Sea. As explained in the previous section, a coastal dam connected to land would be more efficient. But as it is expected that such a dam would encounter fierce resistance from local communities, the electricity data corresponding with a dam in the open sea was used for this study. To maximise the efficiency of the open-sea dam, the modelled dam was equipped with two Y-shaped ends under an angle of 45 degrees, similar to the ones illustrated in figure 21. The water depth at the dam's location is 35 meters and the tidal currents reach a maximum velocity of 1 m/s. These environmental characterises in combination with the design parameters results in a DTP-dam with an installed capacity of 14,4 GW. The hourly electricity output generated by the DTP-dam was modelled on an hourly interval for 29,5 days, equal to the number of days in one moon cycle. As this cycle continuously repeats itself, the data was duplicated proximately 37 times so it covers three years, similar to the wind and solar PV data derived from the ENTSO-E Transparency Platform.



### 4.2.2 Electricity output DTP-dam

Apart from a single DTP-dam, this optimisation study also included two alternative technical configurations; two geographically dispersed DTP-dams and a DTP-dam with an integrated storage system. DTP is still in its initial phase of development, so including three different technical configurations provides more information useful for further developing DTP. This section will first discuss the electricity output from a single DTP-dam. The other two configurations are discussed in section 4.2.3 and 4.2.4.

Just as for wind and PV, to ensure comparability, DTP's electricity output data was normalised and expressed as a capacity factor by dividing it over the installed capacity (14,4GW). Plotting the hourly capacity factors of DTP for one moon cycle results in the output profile visualised in figure 22. DTP's electricity output perfectly follows the pattern of the tides. The large wave motion is caused by the moon's orbiting around the earth and the resulting spring and neap tides. The earth's rotating around its axis explains the daily fluctuations in electricity output. Four times a day, coinciding with high or low tide, slack water causes the electricity output to drop to almost zero. In between the moments of slack water, flow rates and the electricity outputs peak, with the highest peaks occurring during spring tides and the lowest during neap tides.

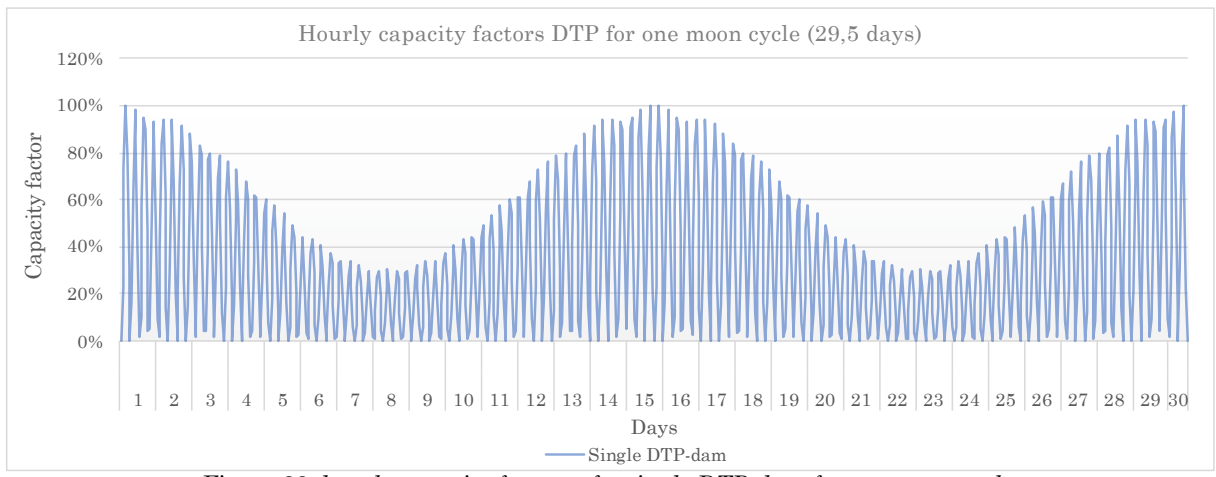


Figure 22: hourly capacity factors of a single DTP-dam for one moon cycle.

When the electricity output from the modelled DTP-dam is compared with the electricity output from wind turbines and solar PV cells in figure 23, it becomes evident how volatile the electricity output from tidal energy is. However, figure 23 also visualises that, unlike wind and solar PV energy, tidal energy is perfectly predictable due to its weather independency.

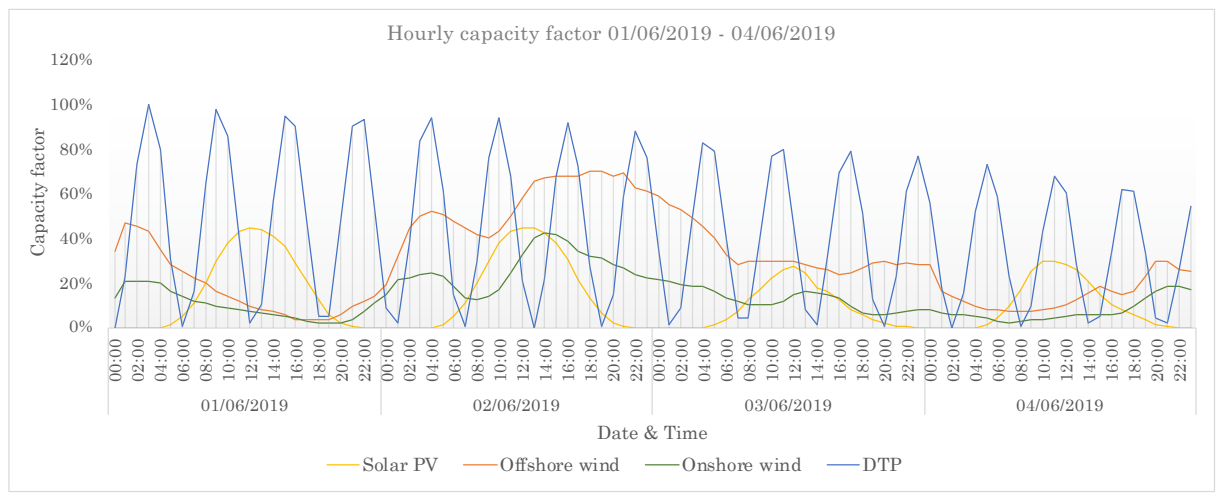


Figure 23: hourly capacity factors solar PV, offshore wind, offshore wind and DTP for 4 random days.



#### 4.2.3 Electricity output two geographically dispersed DTP-dams

For the second technical configuration a second, geographically dispersed, DTP-dam was added to the system. Introducing a second dam creates, what we will call, a natural storage system and reduces DTP's volatile electricity output. As the tidal waves move in from the Atlantic Ocean, high tide first occurs in the South of The Netherlands and then proceeds north. Building a second dam thus offsets the volatility in electricity output caused by high and low tide, which reduces the overall volatility of DTP's electricity output. The period between two electricity peaks is approximately 6 hours, so to offset the tidal effect, the tidal wave would ideally take 3 hours to move from one to the other dam. This scenario could be approached by, for example, building a dam off the coast of Haringvliet in the South of The Netherlands and Texel in the North of The Netherlands. Near Haringvliet high and low tides occur 2 hours and 49 minutes earlier than off the coast of Texel [50]. Whether a DTP-dam at these specific locations is technically feasible is beyond the scope of this study.

To simulate the electricity output from two geographically dispersed DTP-dams, a second output curve is added to the one-dam-scenario and shifted 3 hours. Averaging the cumulative hourly capacity factors results in the output profile shown in figure 24. As expected, a second dam significantly reduces the volatility in electricity output. Only the large wave motion in the output curve, brought about by spring and neap tide, remains. Note that the electricity output data used to compute the two-dam load profile was derived from a 50 kilometre long DTP-dam. However, the dams might be shorter in a two-dam scenario, which will slightly reduce their efficiency. Also, the dams perhaps affect each other's electricity outputs, which was not accounted for in this load profile.

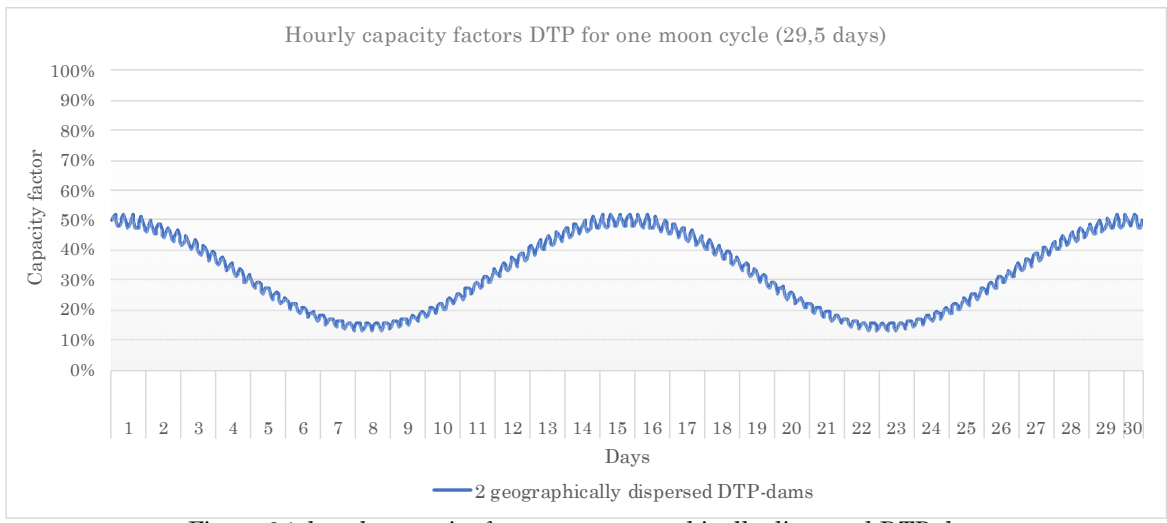


Figure 24: hourly capacity factor two geographically dispersed DTP-dams.

### 4.2.4 Electricity output single DTP-dam with an integrated storage system

The third and last configuration included in this case study equips a DTP-dam with an integrated battery storage system. Due to the short and predictable periods between electricity peaks, a DTP-dam can be equipped with a relatively small storage system to stabilise its electricity system. Such a storage system would store electricity during periods of peak production (high and spring tide) and discharge its stored electricity during periods in which little to no electricity is produced (low and neap tide). For simplification reasons, it is assumed that separate storage systems are used to offset high and low tide, and spring and neap tide. The first, smaller, battery system is used to offset the volatility in electricity supply caused by high and low tide. This storage system should be able to store 0.96 MWh per MW of DTP installed.



The second storage system is much larger and is used to offset the deviations in electricity supply caused by spring and neap tide. The second storage system should be able to store 18.96 MWh per MW DTP installed. The calculation supporting these claims can be found in appendix A.

As visualised in figure 25, due to this integrated storage system, DTP's electricity output is entirely consistent throughout the year. However, storing electricity is characterised by loses in the battery system. As a result, the average capacity factor of a DTP-dam with storage system is 3% lower in relation to a single DTP-dam's capacity factor [57]. The average capacity factor of a single DTP-dam, which was derived from the electricity output data supplied by the DTP-foundation, is 32%. Hence, the capacity factor of a DTP-dam with an integrated storage system is 31%.

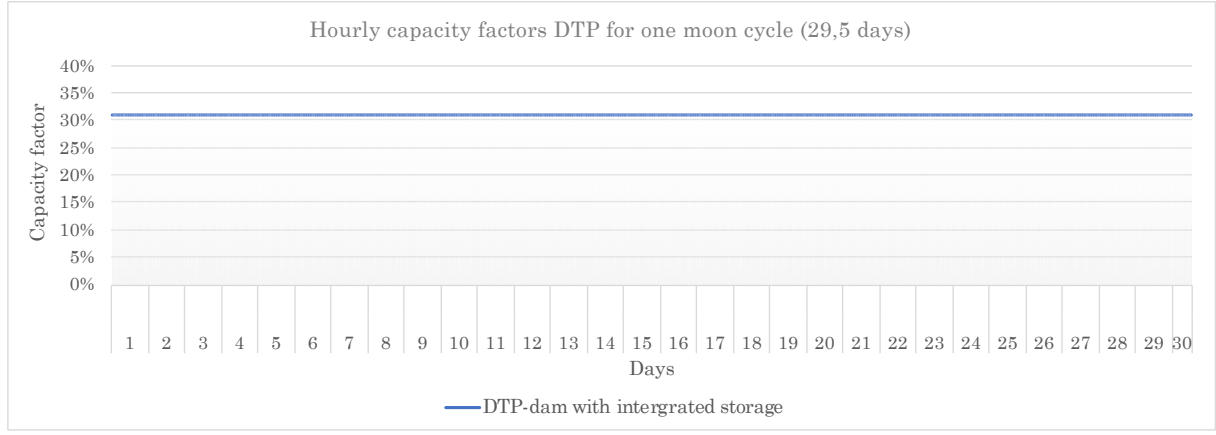


Figure 25: hourly capacity factor of a DTP-dam with an integrated battery storage system.

# 4.3 Electricity demand

In this section, the demand side of the case study is discussed. As stressed by Boßmann et al. [58] "assessing the needs for investments in new electricity generation capacity requires sound assumptions about the future electricity load curve". Therefore, a literature review was conducted in order to forecast if and how the current load profile is expected to change. This has resulted in three different electricity demand scenarios. The different scenarios are visualised in figure 28 and 29 (end of section 4.3) and are elaborated in section 4.3.1, 4.3.2 and 4.3.3.

## 4.3.1 Demand scenario 1: contemporary load profile

The contemporary electricity load profile is the first demand scenario that was included in this optimisation study. Similar to the solar PV and wind output data, the demand data was drawn from the ENTSO-E Transparency Platform from 2017 till 2019 and the fifteen-minute interval data was merged into hourly intervals. Over the three years analysed only three, non-consecutive, data points were missing. These blanks were filled taking the average load of the hours prior and after the missing data points in order to ensure a smooth load curve.

The contemporary electricity demand profile is visualised in figure 28 and 29. The horizontal axis represents the time scale and the vertical axis the amount of electricity demanded from the system, expressed in GW. The different colours correspond with the different demand scenarios; orange represents scenario 1. It is observed that the current electricity load profile is characterised by a repeating pattern. During week and Saturdays, demand peaks in the evenings and mornings. On Sundays, electricity demand is significantly less and only peaks in the evening. Regardless of the day of the week, demand plummets during the night. Similar to wind speeds and solar irradiation, demand is also characteristics by a certain seasonality. So does electricity demand peak during the winter months and significantly decrease towards the summer.



### 4.3.2 Demand scenario 2: increased peak loads due to EV and electric HP

According to Boßmann et al. [58], electrification of specific industries can significantly increase demand and change the shape of the demand curve. In particular electric vehicles (EV) and electric heat pumps (HP) tend to affect the shape of the load curve [58]. Therefore the second demand scenario simulates a situation with an extreme penetration of EV and electric HP.

To determine the demand profile for scenario 2, the load profile of a single EV and HP was derived from the literature [59] and multiplied with EV and HP's potential in The Netherlands. Subsequentially, the extra load was projected on the contemporary load profile.

Figure 26 illustrates the average expected charging profile of a single EV, which was derived from [59]. Since week and weekend day charging profiles differ, a distinction was made. An EV's average daily electricity demand is 3,8 kWh for workdays and 3,1 kWh for the weekend. However, this electricity demand is not evenly distributed throughout the day, which is especially true for weekdays. So is the bulk of charging energy requirements demanded between 5 pm and midnight. On weekdays and in the weekend, electricity demand peaks around 9-10 pm, presumably due to the users charging to prepare for the start of the (working) day. The potential for EV is large in The Netherlands, as only 1,6% of all cars are currently electric [60]. Additionally, it is forecasted that by 2050, in the extreme scenario, the number of cars has increased by 34% relative to 2010 [61]. In 2010 there were approximal 7,62 million cars in The Netherlands [62], which means that it is predicted that there will be 10,21 million cars in 2050. As this scenario tries to represent an extreme situation, it was assumed that everyone drives electric in 2050. Hence, the load curve of a single EV was multiplied by 10,21 million and projected on the load curve.

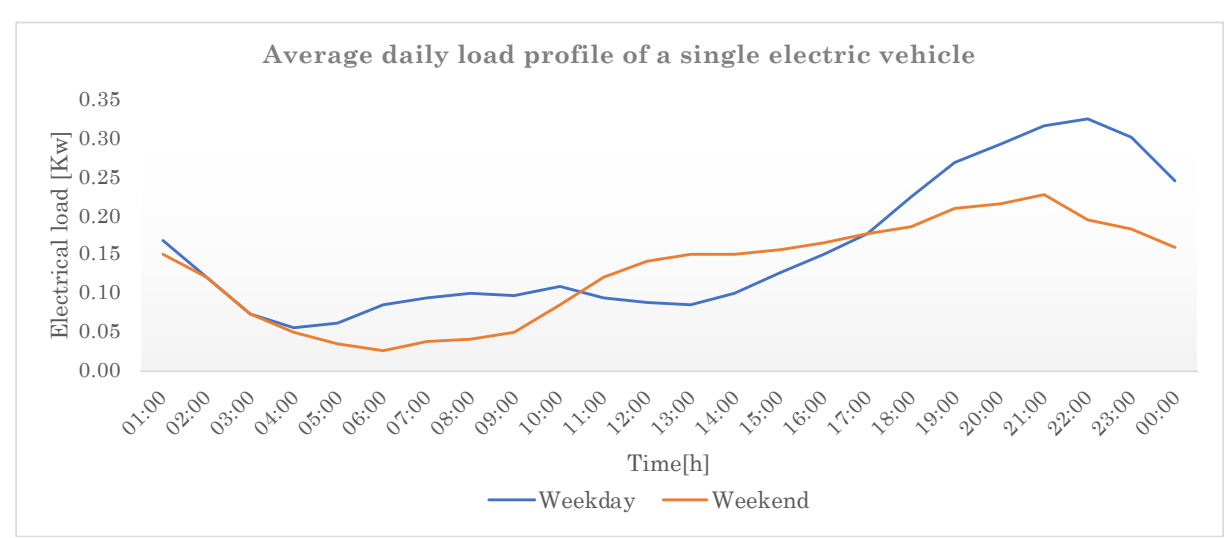


Figure 26: average daily load profile of a single electric vehicle [59]

Figure 27 illustrates the average electricity profile of a single electric HP during different months of the year. The curve was adapted from [59], who used thermal demand data from different UK house types. During winter months, electric HP's average electricity demand is the highest and then gradually decreases as temperatures rise. Regardless of the season, there are definite peaks in electricity demand visible in the morning as people wake up and in the evenings when people return home, both peaks tend to amplify as temperatures drop. According to Kleefkens [63], approximately 5,4 million homes are suitable to be equipped with an electric HP. For this extreme scenario, it was assumed that all these homes have an electric HP.



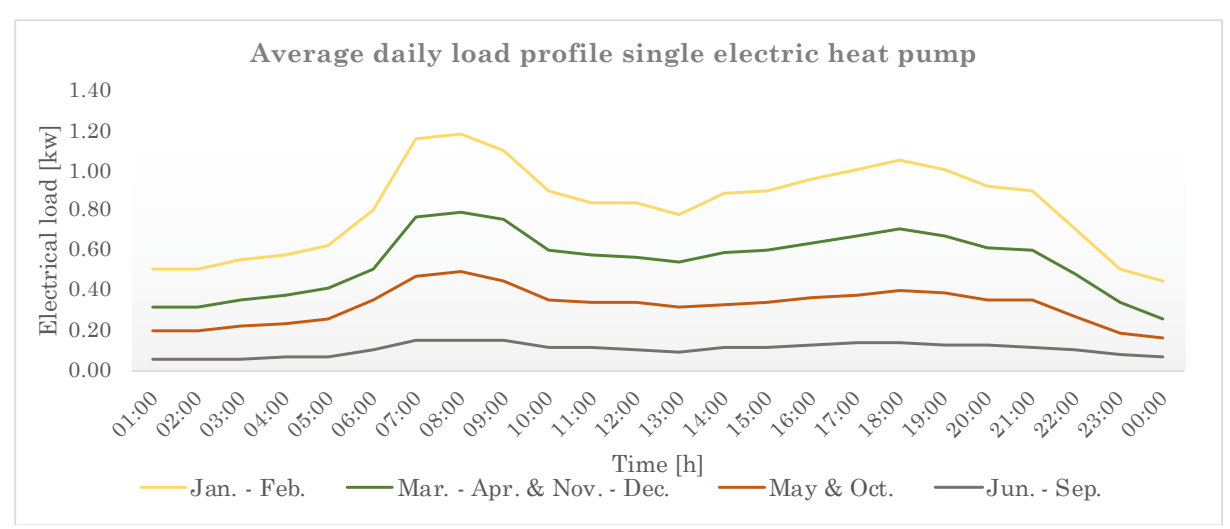


Figure 27: average daily load profile of a single heat pump [59],

Figure 28 and 29 visualise the result when the extreme potentials of EV and HP are projected on the contemporary load profile. The penetration of EV results in significantly higher peaks in electricity demand during the evenings. The extra electricity consumed by electric HP causes electricity demand during the winter months to increase. Heat pumps also tend to have a small effect on morning peaks, as they appear more distinct than in the contemporary load profile. Overall, electric HP have the most effect on the shape of the load curve, especially from a seasonal perspective.

#### 4.3.3 Demand scenario 3: flat load profile due to demand-responsive measures

Østergaard et al. [64] state that EV and HP can potentially be controlled and used to flatten the load curve. This reduction in peak loads can predominately be effectuated in the residential sector (e.g. heating) [65]. Therefore, this third scenario simulates a situation with an extreme penetration of demand-responsive measures. Demand-responsive measures are "changes in electric use by demand-side resources from their normal consumption patterns in response to changes in the price of electricity, or to incentive payments designed to induce lower electricity use at times of high wholesale market prices or when system reliability is jeopardized" [66].

The changes in normal consumption patterns mean that the load will be more evenly distributed over the day, reducing peak hours. Tough there are studies [65] that have estimated the size of the demand-responsive potential in The Netherlands, these studies have not resulted in specific numbers that could be used to derive an hourly load curve required for this study. Therefore, an extreme scenario was simulated in which the load curve completely flattens due to demand-responsive measures. As EV and HP have the potential to shift loads, this scenario has used the load derived after the inclusion of EV and HP (section 4.3.2). Hence this results in a scenario in which there is a high penetration of EV and HP in combination with an extreme penetration of demand-responsive measures. Figure 28 and 29 provide an overview of all the electricity demand scenarios, including the demand profile that was derived in this section. It is important to report that the flat load profile also allows for easy verification of the model later on this research.



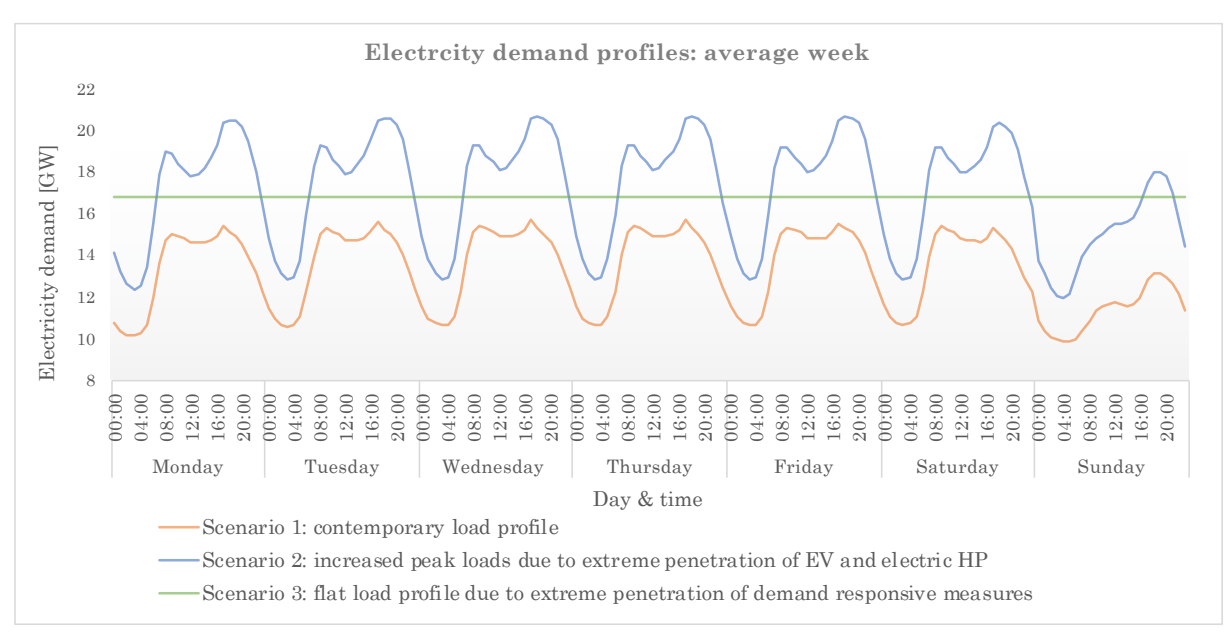
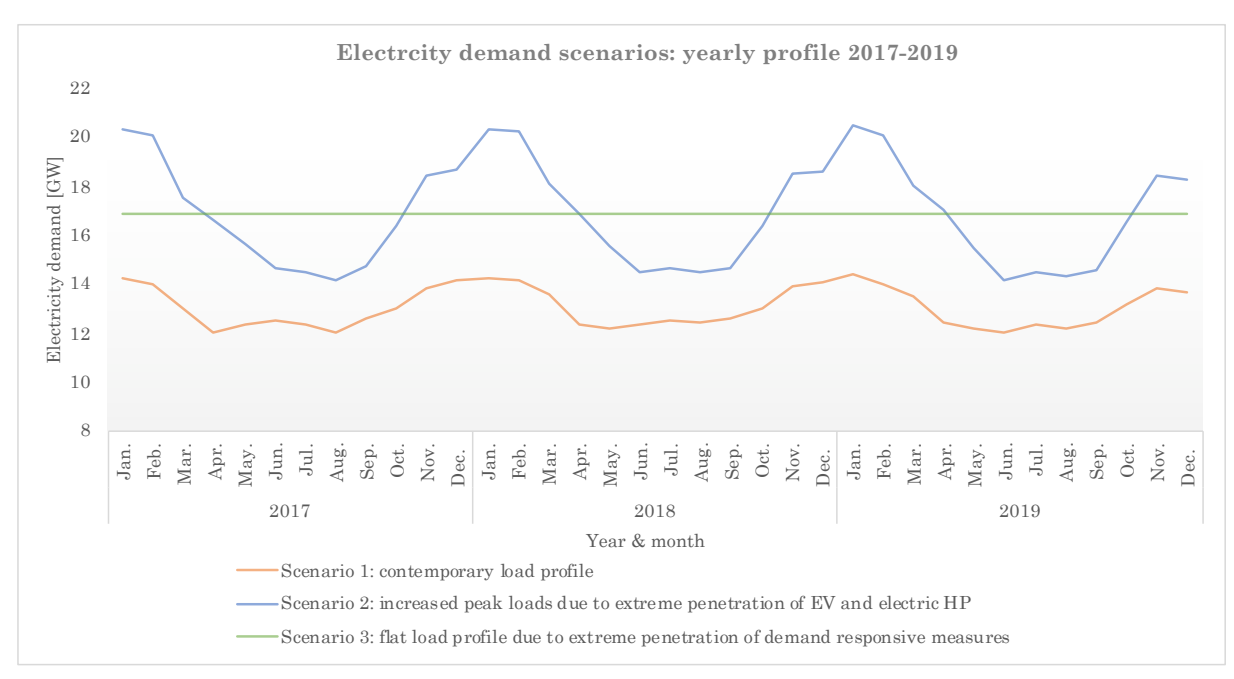


Figure 28: overview of the electricity demand scenarios for an average week.



 $Figure\ 29: overview\ of\ the\ electricity\ demand\ scenarios\ for\ the\ three\ years\ that\ were\ analysed.$ 



## 4.4 Electricity generation costs

As elaborated in section 3.3, the VRE portfolios on the efficient frontier were gauged and compared based on their LCOE. The LCOE is the NPV of the costs over a technology's lifetime divided by the NPV of the technology's electricity output over its lifetime and expressed in €/MWh. Computing a technology's LCOE requires certain costs assumptions, such as; a technologies lifetime, its operation and maintenance (O&M) costs, the overnight capital costs, but also its yearly electricity output. Section 4.4.1 first discusses these input parameters. Subsequently, in section 4.4.2, the LCOEs of the individual VRE technologies and the backup system are determined.

#### 4.4.1 Costs assumptions

A review of the literature discussing costs assumptions relevant to compute the LCOE has revealed a great bandwidth. These deviations in costs parameters appear to be driven by the geographical region. Hence, to most accurately determine the electricity generation costs for The Netherlands, all costs assumptions were derived from studies focusing on The Netherlands. The technologies' average capacity factors, which, as elaborated in section 3.3, determine the electricity output over a technology's lifetime, were derived from the hourly electricity output data.

Table 1 illustrates the costs assumptions that were used to compute the LCOE of each energy-generating technology. This study, does not include learning effects or economies scale, as such the costs of a single and two DTP-dams are assumes to be equal. Most parameters are self-explanatory and have been derived directly from the literature. Two aspects are however worth elaborating on in more detail; the grid connection costs and the flexible CCGT backup system.

Table 1: costs assumptions LCOE calculation

	Solar PV	Offshore wind	Onshore wind	DTP excl. storage	DTP	Flexible CCGT
Overnight capital costs [€/MW]	590,000 [67]	1,750,000 [68]	1,100,000 [69]	1,690,000 [54]	1,690,000 [54]	630,000 [70]
O&M costs [€/MW/y]	11,500 [67]	55,000 [68]	32,524 [69]	23,660 (1,4% of capital costs [54])	23,660 (1,4% of capital costs [54])	40,000 [70]
One-off maintenance costs in year 12 [€/MW]	32,000 [67]	-	-	-	-	-
Offshore grid costs [€/MWh]	-	17.5 [68]	-	5.25	1.75	-
Size battery system [MWh/MW] <sup>1</sup>	-	-	-	-	0.96 (system 1), 18.96 (system 2)	-
Lifetime battery [y] <sup>1</sup>	-	-	-	-	12 (system 1), 60 (system 2)	-
Battery storage costs [€/MWh]	-	-	-	-	100,000 [54]	-
Fuel costs [€/MWh]	-	-	-	-	-	€46.08
CO <sub>2</sub> costs [€/MWh]	-	-	-	-	-	€10.10
Lifetime [y]	25[71]	25[71]	25[71]	60 [54]	60 [54]	25 [70]
Construction time [y]	0.5[71]	1.5[71]	1 [71]	5 [72]	5 [72]	3 [71]
WACC $[\%]^2$	4.3 [71]	4.3 [71]	4.3 [71]	4.5[54]	4.5[54]	4.3 [71]
Average capacity factor [%]	9	43	25	32	$31^{3}$	$0.01 \text{-} 100^4$

<sup>&</sup>lt;sup>1</sup>The battery's size and lifetime was determined in section 4.2.4 and appendix A. System 1 offsets the fluctuations in electricity output as a result of high/low tide. System 2 offsets the fluctuations in electricity output as a result of neap/spring tide.

 $<sup>^2</sup>$ Weighted average cost of capital (WACC) are the expected cost of capital. This is the discount factor used to calculate the NPV of the costs and electricity output.

<sup>&</sup>lt;sup>3</sup>The capacity factor of a DTP-dam with storage system is approximately 3% lower due to electricity loses in the battery system.

<sup>&</sup>lt;sup>4</sup>Capacity factor CCGT varies as it depends on the characteristics of the VRE portfolio's residual load (mean and variance).



#### Flexible combined cycle gas turbine (CCGT)

To cover the erratic residual loads left by VRE portfolios, the backup system should be freely dispatchable. Hence, the dispatchable backup system has to have a high ramp rate<sup>3</sup>. Therefore, this study used the characteristics of a flexible combined cycle gas turbine (CCGT) to derive the costs assumptions for the dispatchable backup system. Opposed to a normal CCGT, the electricity output from a flexible CCGT can easily be ramped up or down, increasing its ability to cover the residual load. However, this flexibility also increases the plant's overnight capital and O&M costs by 40% in relation to a normal CCGT [70]. Additionally, due to its flexibility, its efficiency decreases and more fuel is used to generate one unit of electricity. A conventional CCGT has an efficiency of 60%, while a flexible CCGT's efficiency is 50% [70].

The fuel costs to generate one MWh of electricity are calculated in table 2 and included in the LCOE of the flexible CCGT. Based on a report from The Energy research Centre of the Netherlands (ECN) [73], the natural gas price was estimated to be around  $6.40 \, \text{€/GJ}$ , which results in fuel costs of  $46,08 \, \text{€/MWh}$ .

Unlike renewable energy, burning natural gas to generate electricity emits  $CO_2$ . As elaborated in the literature review (section 2.3), when conventional energy technologies are included in the MPT, the costs associated with the negative externalities of emitting  $CO_2$  should be included in the cost structure. This will reduce the costs distance between polluting technologies and renewables and allows for a fair cost comparison.

The costs of emitting  $CO_2$  from the production of electricity are covered by the EU Emission Trading System (ETS) [74]. Within this trading system companies receive or buy emission allowances, which allows them to emit  $CO_2$ . Companies that have successfully reduced their emissions will sell their surplus of allowances to those companies for which its more costly to reduce its  $CO_2$ -emissions than to by extra allowances. Each year the number of allowances is reduced, which will drive up the price and stimulates more companies to abate  $CO_2$ -emissions [74].

Over the past year (2020),  $CO_2$  allowances were traded for approximately  $25 \text{ €/ton } CO_2$  [75]. Burning natural gas emits 56,10 kg of  $CO_2$  per GJ [76]. As is calculated in table 3, when a flexible CCGT's efficiency is taken into account, 0,4 ton of  $CO_2$  is emitted to produce one MWh of electricity, which results in a  $CO_2$  price of 10.10 €/MWh.

It is important to repeat that the absolute fuel and  $CO_2$  costs are variable costs, which depend on the amount of electricity produced over the CCGT's lifetime. As the flexible CCGT is used to cover the residual load left by the VRE system, the amount of electricity produced by the CCGT depends on the characteristics of the VRE portfolio. As the average residual load increases, the CCGT will have to produce more electricity and its absolute fuel and  $CO_2$  costs will increase.

Table 2: fuel costs CCGT

Table 3: CO<sub>2</sub> costs CCGT

Fuel costs CCGT		${ m CO_2\ costs\ CCGT}$	
Electrical energy [GJ/MWh]	3.60	CO <sub>2</sub> emission factor natural gas [kg/GJ]	56.10[76]
Efficiency CCGT [%]	50 [70]	Energy used to generate 1 MWh [GJ]	7.20
Energy used to generate 1 MWh [GJ]	7.20	CO <sub>2</sub> emission [ton/MWh]	0.40
Natural gas price [€/GJ]	6.40[73]	CO <sub>2</sub> price [Euro/ton]	25.00[75]
Fuel costs [€/MWh]	46.08	CO <sub>2</sub> costs (Euro/MWh)	10.10

-

<sup>&</sup>lt;sup>3</sup> Ramp rate is "the rate at which a power plant can increase or decrease output" [96].



#### Grid connection

Electricity generation technologies located onshore are connected to the existing onshore grid. In most instances, this requires a strengthening of the local electricity grid in order to support the feed-in of electricity. For solar PV, onshore wind and the flexible CCGT these grid costs are included in the O&M costs (solar PV) or overnight capital costs (onshore wind & CCGT) [67] [69] [70].

To utilise the offshore produced electricity, the energy technologies have to be connected to the onshore network by means of an offshore grid. The construction and maintenance of such a grid bear significant investment costs. To advance the energy transition and stimulate market parties to construct offshore wind farms, the Dutch government subsidises Tennet, the transmission system operator (TSO), to build and maintain an offshore electricity grid. Hence, grid connection costs associated with offshore wind and DTP are not included in the overnight capital costs nor in the O&M costs. To allow for a fair comparison among all energy generation technologies, the offshore grid costs were added to the LCOE.

A study [68] that evaluated all Dutch wind farms' gird costs, found that, although the exact costs depend on the specific location - the further ashore the more expensive the gird - grid costs for an offshore wind farm are around 17.5 €/MWh [68].

Grid connection costs for a DTP dam with a storage system are expected to be a tenth of those [54]. Connecting a DTP dam to the onshore grid is less costly, as it requires fewer cables. The electricity output from wind turbines is first clustered at a hub before it is transmitted to land. Connecting all dispersed wind turbines to this hub requires a dense network of cables, which significantly increases the grid costs.

Opposed to a DTP-dam with battery storage, the hourly electricity output from a DTP-dam without a storage system fluctuates. Rather than a consistent capacity factor (31%), the capacity factor of a DTP-dam without storage system fluctuates between 0% and 100%, with an average of 32%. As a result, the offshore grid has to be designed for a capacity factor of 100%, rather than 31%. Therefore, this study assumes that the grid connection costs for a dam without storage system are approximately three times as much as for a dam with a storage system.

### 4.4.2 Levelized costs of energy

Based on the methodology discussed in section 3.3 and the input parameters in table 1 the LCOE for each energy generation technology was determined. The resulting LCOEs can be found in table 4 and the supporting calculations in appendix B. As the capacity factor (CF) of the flexible CCGT varies depending on the VRE portfolio's characteristics, which are currently unknown, a costs range is included in table 4.

Table 4: levelized costs of energy solar PV, wind, DTP and flex CCGT

	Solar PV	Offshore wind	Onshore wind	DTP	DTP incl. storage	Flex CCGT
LCOE [€/MWh]	67.31	65.67	50.27	48.60	92.48	108.06( <i>CF</i> : 20%) – 66.55 ( <i>CF</i> : 100%)

When the LCOEs are analysed the crucial role of the capacity factor becomes evident. Solar PV, which is characterised by the lowest overnight capital costs and O&M costs (table 1), has a relatively high LCOE. This is due to its small capacity factor (9%). The absolute costs of solar PV might be little, as it produces little electricity its costs per MWh are substantial. Similarly is observed for the flex CCGT, its costs increase rapidly as its deployment plummets. The LCOE of a DTP-dam with a storage system is significantly higher than the LCOE of a DTP-dam without storage costs. This is mainly driven by the significant storage costs, but loses in the battery system also play a minor role in the costs difference. Due to losses in the battery system, the capacity factor slightly decreases (-1%), increasing the costs per MWh produced.



## 4.5 Overview demand scenarios and technical configurations

To summarise, this section provides an overview of the scenarios and technical configurations discussed in this chapter, and that were optimised using the novel methodology discussed in chapter 3.

Regarding the supply side, three different variable renewable electricity generation technologies are included; wind energy, solar PV and Dynamic Tidal Power. For wind energy a distinction is made between; offshore and onshore wind. As DTP is still in its initial phase of development, three different design configurations are included in the case study; a single DTP-dam, a single DTP-dam with a storage system and two DTP-dams three tidal hours apart.

To assess the effects of the incorporation of DTP on the contemporary VRE system's performances, wind and solar PV were always the starting point for each scenario. Subsequently, the different DTP configurations were added to the system. This results in the following four scenarios; solar PV and wind (A), solar PV, wind and a single DTP-dam (B), wind, solar PV and two geographically dispersed DTP-dams (C), and solar PV, wind and a single DTP-dam with an integrated storage system (D).

The demand side of the model is characterised by three different scenarios; the contemporary load profile (1), increased peak loads due to a high penetrations of EV and electric HP (2), and a flat load profile due to a high penetration demand-responsive measures (C). Table 5 visualises all the scenarios and configurations for which the most efficient VRE portfolios and associated energy generation costs were determined.

As elaborated in the research outline (section 1.3), to find the most efficient portfolios for each scenario and configuration, this study investigated how 35GW of installed capacity should be distributed among solar PV, offshore wind, onshore wind and DTP to efficiently meet demand. Hence, regardless of the optimised scenario or configuration, the total VRE capacity is always 35GW.

Table 5: overview of all the 35 GW VRE systems that were optimised.

Scenarios:	1. Contemporary load profile	2. Increased peak loads	3. Flat load profile
A. Wind & solar PV	1.A	2.A	3.A
B. Wind, solar PV & a single DTP-dam	1.B	2.B	3.B
C. Wind, solar PV & 2 geographically dispersed DTP-dams	1.C	2.C	3.C
D. Wind, solar PV & a single DTP-dam incl. storage system	1.D	2.D	3.D



## 5 Results

In this chapter, the optimisation results for the different scenarios and technical configurations are presented. The results were obtained by plugging the data, discussed in chapter 4, in the novel methodology elaborated in chapter 3. The results are presented in the same sequence as in which the methodology was discussed. Hence, section 5.1 first presents the MPT optimisation results and the resulting minimum-variance frontiers for the different scenarios and configurations. Subsequentially, in section 5.2, the results of comparing the VRE portfolios on the efficient frontiers in terms of their required backup capacity are discussed. The results of gauging the VRE portfolios on the efficient frontier in terms of their energy generation costs are presented in section 5.3. In section 5.4, the results of sensitivity analysis, in which the VRE system's size, confidence interval (CI) and CO2 costs were changed, are presented.

#### 5.1 Minimum-variance frontiers

This section presents the modified MPT optimisation results and the resulting minimum-variance frontiers for each demand scenario and the technical configurations. Section 5.1.1 presents the result for electricity demand scenario A: the contemporary load profile. In section 5.1.2, the results obtained for demand scenario B (increased peak loads) are discussed. In the final section (5.1.3), the results that correspond with a flat load profile (scenario C) are elaborated.

All three sections are structured the same. First, the proxy variables that were used for the optimisation model are discussed. Subsequentially, the results of the optimisation model – the minimum-variance frontiers – are presented.

### 5.1.1 Demand scenario 1: contemporary load profile

Table 6 represents the proxy variables that correspond with the contemporary electricity load profile (scenario 1) and a 35GW VRE system. The top row indicates the different electricity generation technologies that were included in this optimisation study. The second and third-row represent an energy technologies' mean residual loads and the STD of their residual loads. The mean residual load indicates the amount of electricity that, on average, could not be covered by a particular technology, if 35GW of that particular energy technology is used to cover demand. The STD of the residual load indicates how volatile the residual load left by that energy technology is.

The bottom three rows illustrate the correlation coefficients among the energy technologies their residual loads. The correlation coefficient indicates to what extent two technologies their residual loads tend to move together. If two technologies' residual loads tend to be above or below their mean residual load simultaneously, the two technologies' residual loads move together, and their correlation coefficient is positive. On the other hand, a negative correlation coefficient means that two technologies' residual loads move in opposite directions.

Table 6 shows that solar PV is characterised by a high mean residual load and relatively low STD. Offshore wind, on the other hand, has a high STD, but low mean residual load. To such an extent that offshore wind's residual load is negative, which indicates that a 35GW offshore wind system would, on average, generate more electricity than is demanded. The STD of the residual load left by offshore wind is slightly higher than onshore wind, which indicates that electricity output from offshore wind tends to be more erratic. Though the electricity output profiles of a single DTP-dam and two geographically dispersed DTP-dams are differently shaped (fig. 22 and 24), their average capacity factors and thus residual loads are equal. The STD of the residual load left by DTP rapidly declines when a second dam or a dam with a storage system was introduced into the system.



The correlation coefficients show that the residual loads from solar PV and on-/offshore wind tend to move in the opposite direction as their correlation coefficients are negative. As visualised in section 4.1.2, wind production peaks during the winter, while solar PV outputs peak in summers, which explains their negative correlation. Wind speeds above land and sea tend to follow the same profile, explaining why their residual loads are heavily correlated. Going by figure 23, it is unlikely that the positive correlation among the residual loads left by DTP and solar PV/wind is driven by the shape of their electricity output profiles. As the correlation coefficients increase as DTP's electricity output stabilises due to a second dam or storage system, it seems like the correlations between DTP and solar PV/wind are driven by the shape of the demand profile rather than the shape of their electricity output profiles. The demand profile is the same for all technologies, which explains the positive correlation.

Table 6: proxy variables 35GW VRE system and demand scenario 1: contemporary load profile.

	Solar	Offshore	Onshore	DTP	2 DTP-	DTP incl.
	PV	wind	wind		dams	storage
Mean residual load [MW]	9,913	-2,104	4,119	1,727	1,726	2,079
STD of the residual load [MW]	5,071	10,567	7,838	10,067	4,885	2,130
Correlation coefficients:						
Solar PV		-0.17	-0.12	0.07	0.14	0.31
Offshore Wind			0.83	0.02	0.05	0.08
Onshore wind				0.04	0.09	0.15

Using the proxy variables from table 6 and the MPT optimisation elaborated on in section 3.1.6, the energy generation portfolios that minimise the residual load's STD for each level of mean residual load were computed. This optimisation problem was tackled through an iterative process at which the mean residual load was increased with 500MW, and the corresponding STD was determined using Excel solver. The minimum-variance frontiers, visualised in figure 30 illustrate the outcome of this optimisation problem.

The vertical axis represents a VRE portfolio's mean residual load and the horizontal axis the STD of a portfolio's residual load. The minimum-variance frontiers thus indicate how volatile a portfolio's residual load is for each level of mean residual load. The four minimum-variance frontiers each correspond to one of the four technical configurations; solar PV and wind (A), solar PV, wind and a single DTP-dam (B), solar PV, wind and two geographically dispersed DTP-dams (C), and solar PV, wind and a DTP-dam with storage system (D).

It is observed from figure 30, that the minimum-variance frontiers stretch from a mean residual load of approximately 10,000 MW to -2,000 MW. This corresponds with the maximum mean residual load (solar PV) and minimum mean residual load (offshore wind). The bent shape of the curve is the result of the correlation among technologies their residual loads. As was observed from the proxy variables, the residual loads left by solar PV and wind are negatively correlated. Combining these two electricity generation technologies into one portfolio (configuration A) partly cancels out their volatility, which reduces the overall STD of the portfolio's residual load and explains the bent shape of minimum-variance frontier.

Similar happened when a single DTP-dam was introduced into the system (configuration B). The minimum-variance frontier shifts left, which indicates that the STD of the portfolio's residual load decreases. When two DTP-dams are introduced into the contemporary VRE system, the minimum-variance frontier moves even further left. This is due to the fact that the electricity output from two geographically dispersed DTP-dams is perfectly negative correlated, which significantly reduces the volatility of DTP's residual load. Hence, in configuration C it is not so much the correlation among DTP, solar PV and wind that reduces the STD of the portfolio's residual load, but more the fact that the STD of one of the energy technology has decreased. Similar is observed in configuration D, where a DTP-dam with an integrated storage system was incorporated into the solar PV and wind system. The storage system has completely flattened DTP's electricity output, leaving only the deviation caused by fluctuations in electricity demand. As a result, the STD of the portfolios' residual loads has even further reduced, and the minimum-variance frontier moved left.



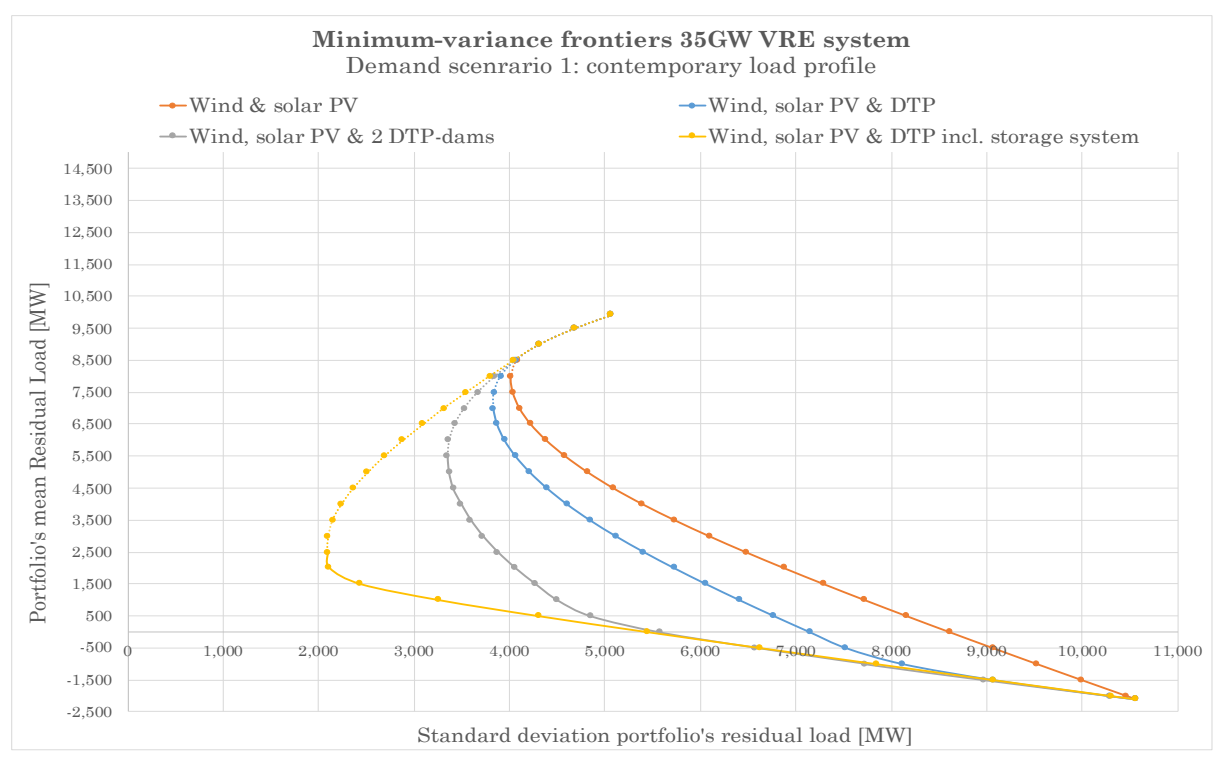


Figure 30: minimum-variance frontiers for a 35GW VRE system and the contemporary electricity demand profile (scenario 1). The solid part of the minimum-variance frontiers indicates the efficient frontier.

As elaborated on in section 3.1.6, all portfolios on the minimum-variance frontiers curtail the STD to the minimum, but they are not equally efficient. The portfolio on the uttermost left point on the four minimum-variance frontiers have the lowest STD and mark the tipping point between the efficient and inefficient part of the minimum-variance frontier. The portfolios located above this tipping point (on the dashed line) are inefficient since other portfolios (on the solid line) have a lower mean residual load for the same STD. To paraphrase, portfolios on the minimum-variance frontiers only minimise the STD, whereas the portfolios on the efficient frontier (solid line) also minimise the mean residual load. This makes these portfolios more efficient to meet demand. Therefore, all the VRE portfolios that are not located on the efficient frontier (solid line) were eliminated.

### 5.1.2 Demand scenario 2: increased peak loads

In the second demand scenario EV and electric HP were introduced into the system. As discussed and visualised in section 4.3.2 this increases the average electricity demand and peak loads, in particular during the winter months. It is important to note that the energy technologies' output profiles have not changed. Hence, any changes in the proxy variables or minimum-variance frontiers in relation to scenario 1 (contemporary demand profile) are solely caused by the altered demand profile.

From table 7, it is observed that the proxy variables have indeed changed due to the new demand profile. As a result of the increased electricity consumption, the mean residual load of all energy technologies has increased with approximately 3,5GW. Except for offshore wind, the volatility of all the technologies' residual loads also slightly increased. The latter is caused by the increased volatility of the demand profile due to the charging profiles from EV and use of electric HP. On the other, the STD of the residual load from offshore wind slightly decreased. This can be explained by the fact that the electricity output from wind turbines, especially those located offshore, tend to peak during winters. As this coincides with the increased electricity consumption from electric HP, the STD of the residual load left by offshore wind decreased.



From table 7, it is observed that all the correlation coefficients have become more positive due to the altered demand profile, which indicates that the residual loads tend to co-move to a greater extent in relation to scenario 1. The increased peak consumption from EV and electric HP has given the demand profile a more pronounced shape. As a result, the shape of the demand profile has a more significant effect on the shape of technologies their residual loads. And as the demand profile is the same for all energy technologies, their residual loads correlate more positively.

Table 7: proxy variables 35GW VRE system and demand scenario 2: increased peak loads.

	Solar PV	Offshore wind	Onshore wind	DTP	2 DTP- dams	DTP incl. storage
Mean residual load [MW]	13,699	1,682	7,905	5.514	5,513	5,866
STD of the Residual load [MW]	6,053	10,560	7,919	10,441	5,605	3,468
Correlation coefficient:						
Solar PV		-0.06	0.03	0.20	0.37	0.60
Offshore Wind			0.82	0.06	0.11	0.15
Onshore wind				0.09	0.17	0.25

The above proxy variables were again plugged into equation 3.8 and 3.9 and Excel Solver was used to solve the optimisation problem and find the portfolios with the lowest STD for each level of mean residual load. The resulting minimum-variance frontiers are illustrated in figure 31.

The most obvious that can be concluded from figure 31, is that the order of the minimum-variance frontiers (left to right) has remained the same, which indicates that, despite the penetration of EV and electric HP, incorporating DTP still reduces the volatility of a VRE system's residual load. However, the distances between the four minimum-variance frontiers have reduced in relation to scenario 1. Due to the deployment of EV and electric HP, electricity peaks have increased, and the technology's residual loads are more positively correlated. As elaborated in section 2.1.3, when the correlation coefficients approach 1, diversification becomes less effective in reducing the STD of a portfolio's residual load. As a result, the minimum-variance frontiers lose their sharp curve, which indicates that the volatility-reducing effects of incorporating DTP into the contemporary VRE mix have slightly diminished.

Apart from the shape of the minimum-variance frontier, its location in the plane has also changed. In scenario A (fig. 30), the minimum-variance frontiers stretched from a mean residual load of 10,000 to -2,000 MW, and in the scenario with EV and electric HP (B) it goes from 14,000 to 3,500MW. This shift is in line with what was observed from the proxy variables, and indicates that the mean residual load has increased, regardless of the energy technologies included in the portfolios. No longer is there any 35 GW VRE portfolio that, on average, produces more electricity than is consumed.

Similar to scenario 1, only those portfolios that minimise both the mean residual load and STD are located on the efficient frontier (solid line) and considered efficient. Hence, the VRE portfolios on the inefficient part of the minimum-variance frontier (dashed line) were eliminated.



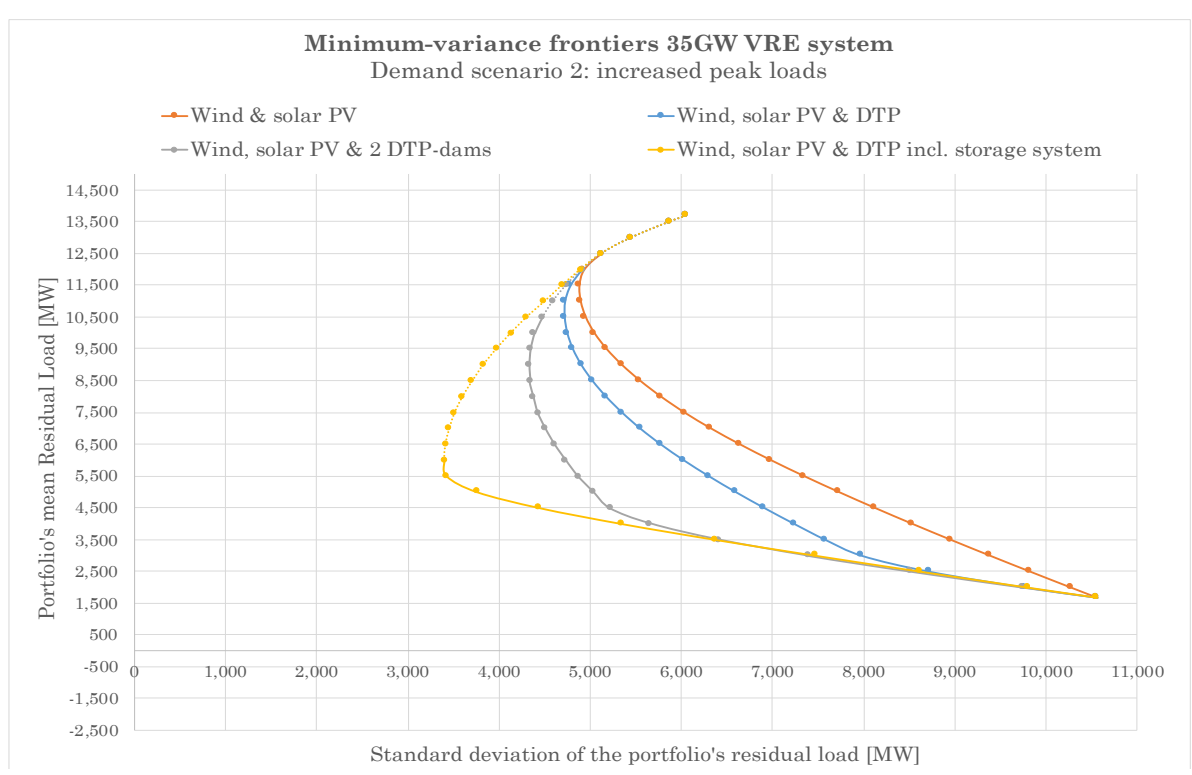


Figure 31: minimum-variance frontiers for a 35GW VRE system and increased peak loads (scenario 2). The solid part of the minimum-variance frontiers indicates the efficient frontier

### 5.1.3 Demand scenario 3: flat load profile

In scenario C, demand-responsive measures are introduced into the system with a high penetration of EV and electric HP (scenario B). As a result of this extreme load shifting, the resulting load profile is completely flat (fig. 28 & 29). Hence, the volatility of the residual loads are entirely the result of deviations in a technology's electricity outputs, and thus any changes in the weather or velocity of the tidal currents.

The effects of this flat load curve can be observed in the table with proxy variables (table 8). Except for offshore wind, the STD of all technologies' residual loads have decreased due to the stabilised electricity demand. In scenario B, electricity output from offshore wind (winter) peaked simultaneously with the increased electricity consumption caused by the use electric HP (winter). However, load shifting has completely flattened the demand curve, which has slightly increased the STD of the residual load left by offshore wind. Since the electricity output from a DTP-dam with storage system is consistent throughout the year, similar to electricity demand, the STD of its residual load equals zero.

The mean residual loads have remained unchanged in relation to scenario B. Although demand-responsive measures have shifted peak loads and changed the shape of the demand curve, the cumulative amount of electricity consumed is the same, it is just better distributed.

Now that the load curve is flat, it no longer affects the STD of the residual load. Therefore, the correlation coefficients are solely affected by the technologies' deviations in electricity output. As a result, the negative correlation between solar PV and wind has increased in comparison to scenario A and B. Furthermore, there is no correlation whatsoever between the electricity output from DTP and any of the other VRES, which confirms that, the in scenario A and B observed, positive correlations were solely driven by the shape of the demand profile.



Table 8: proxy variables 35GW VRE system and demand scenario 3: flat load profile.

	Solar	Offshore	Onshore	DTP	2 DTP-	DTP incl.
	PV	wind	wind	Ъ11	dams	storage
Mean residual load [MW]	13,699	1,682	7,905	5.514	5,513	5,866
STD of the residual load [MW]	4,863	10,606	7,818	9,831	4,383	0
Correlation coefficient:						
Solar PV		-0.19	-0.15	0.00	0.00	0.00
Offshore Wind			0.83	0.00	0.01	0.00
Onshore wind				0.01	0.02	0.00

Using Excel solver, equation 3.8 and 3.9, and the proxy variables the optimisation problem was solved, and the generated minimum-variance is visualised in figure 32. Due to the decreased correlation among the residual loads, the minimum-variance frontiers are characterised by a sharper curve in relation to both scenario A and B. which has increased the distance between the four minimum-variance frontiers. The latter indicates that introducing DTP into a system with a flat load profile has a greater effect on reducing the STD than in a system with average (scenario 1) or high (scenario 2) peak loads. Especially a DTP-dam with an integrated storage system greatly affects the STD of a VRE portfolios' residual load. To such an extent that there is one VRE portfolio on the minimum-variance frontier which residual load bears no deviation whatsoever.

Similar to what was observed from the proxy variables, introducing demand-responsive measures into a scenario with a high penetration of EV and electric HP (scenario 2) has only reduced the STD of the VRE portfolios' residual loads. When scenario 2 (fig. 31) is compared with scenario 3 (fig. 32), it becomes clear that the minimum-variance frontier has not moved up nor down, indicating that the VRE portfolios' mean residual loads have indeed remained the same.

Similar as with the previous two scenarios, only the portfolios on the efficient frontier minimise both the mean residual load and the STD of the residual loads. Therefore, all portfolio that only minimise the STD and are located on the inefficient part of the minimum-variance frontier (dashed lines) are eliminated.

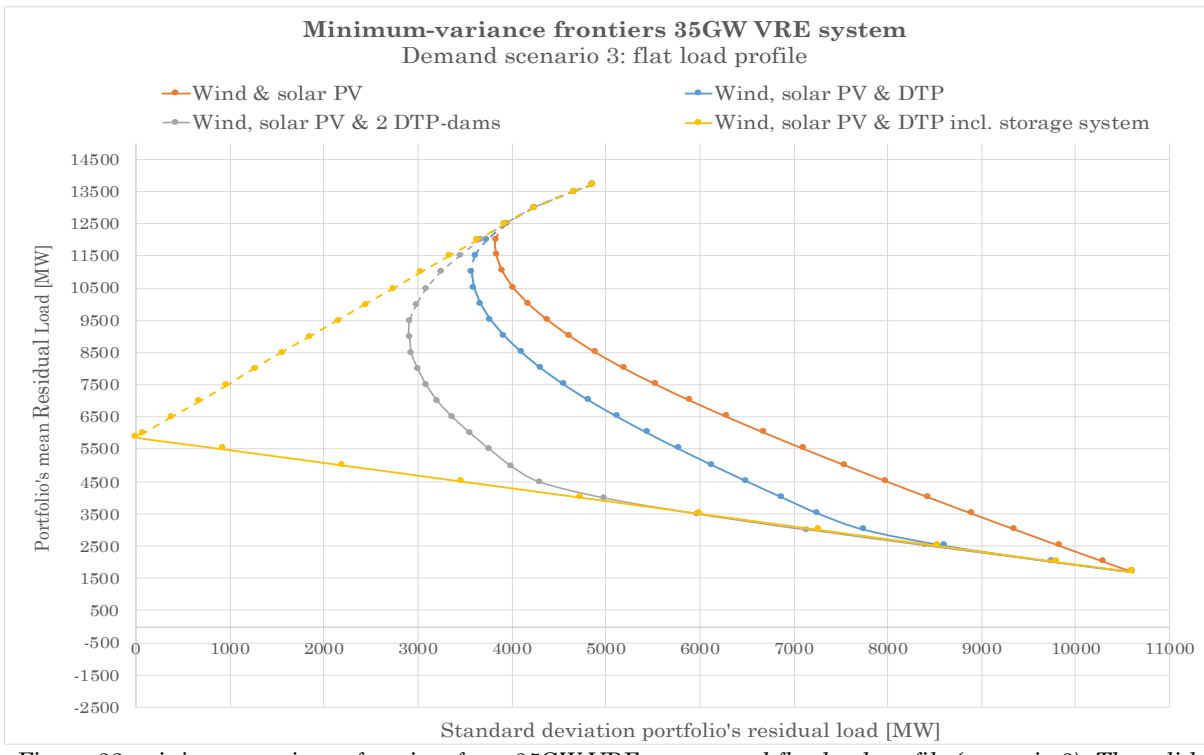


Figure 32: minimum-variance frontiers for a 35GW VRE system and flat load profile (scenario 3). The solid part of the minimum-variance frontiers indicates the efficient frontier



## 5.2 Most efficient portfolios: dispatchable backup capacity

In the previous section, the MPT was used to generate the minimum-variance frontiers for each scenario and configuration. Subsequentially, the portfolios on the inefficient part of the mean-variance frontiers were eliminated, leaving only those VRE portfolios that are located on the efficient frontier. These portfolios minimise both the mean residual load and the STD of the residual load. However, as is visualised by the efficient frontiers, a portfolio's mean residual load and STD are characterised by a trade-off, making it impossible to select which portfolio is most efficient in meeting demand.

Therefore, the dispatchable backup capacity required to cover the residual loads left by each portfolio was determined. This single value indicates how well a portfolio can meet demand and allows for easy comparability among the VRE portfolios. Hence, this enables selecting the most efficient VRE portfolios for each configuration and demand profile. As elaborated in section 3.2, the dispatchable backup capacity is a function of a VRE portfolio's mean residual load, the STD of its residual load and a certain energy security level. For this study, the energy security level was set to 95%.

This section will first discuss all the VRE portfolios' energy generation shares on the efficient frontier and their required dispatchable backup capacity. Subsequentially, for each scenario and configuration, the portfolios that require the least backup capacity, and are considered to be most efficient in meeting demand, are presented.

Figure 33 illustrates the portfolio shares and required dispatchable backup capacity for those VRE portfolios located on the efficient frontier. This particular figure corresponds with a VRE system comprised of solar PV, wind and DTP (configuration B) and the contemporary load profile (scenario 1). However, similar graphs have been generated for all scenarios (1-3) and configuration (A-D), and can be found in appendix C.

The horizontal axis of figure 33 indicates a VRE portfolio's mean residual load (upper value) and STD (lower value). These values thus indicate where on the efficient frontier a certain VRE portfolio is located. The first portfolio (left) marks the efficient frontier's beginning (the utmost left point on the solid line). As one goes down the horizontal axis, the mean residual load decreases and the STD increases, which corresponds with the trade-off visualised by the efficient frontier visualised in figure 30. The left vertical axis represents the portfolio shares and the colours the different energy generation technologies. The right vertical axis indicates the dispatchable backup capacity required to cover 95% of the VRE portfolios' residual load. The portfolio marked with the white dot requires the least backup capacity and is thus considered most efficient for that specific scenario and configuration.

From figure 33, it is observed that the VRE portfolio with the lowest STD (left on efficient frontier) is comprised of different energy technologies, but predominantly solar PV. This illustrates the fundamental idea behind the MPT; to minimise the volatility of a VRE portfolio's residual load one should include energy technologies whose residual loads have a low STD, such as solar PV, and/or technologies whose residual loads negatively correlate (i.e. solar PV and wind). It is observed that a VRE portfolio's STD increases when larger shares of offshore wind are introduced into the system. This is due to the volatile electricity output from offshore wind, but also since the diversification effects with solar PV diminishes. On the other hand, increased penetration of wind decreases the mean residual load of the VRE system. This is due to the high average electricity output (capacity factor) from offshore wind turbines.

From these observations, it can be concluded that both solar PV and offshore wind have a distinguished role in the energy mix. Solar PV tends to stabilise a portfolio's residual load, while offshore wind causes the mean residual load to plummet.

On the other hand, onshore wind only has a minor role in a small number of portfolios on the efficient frontier. The reason for this lies in the electricity output profiles from offshore and onshore wind. As the proxy variables have shown, the electricity output from offshore wind and onshore wind is heavily correlated and tend to follow the same pattern. As elaborated in section 2.1.3, a portfolio that includes two heavily correlated energy technologies, cancels out the diversification



effects, which increases a portfolio's volatility. Hence, it is more efficient to combine either offshore or onshore wind in a portfolio with other, less positively (i.e. DTP) or even negatively (i.e. solar PV) correlating energy technologies. On average, offshore wind produces more electricity than onshore wind and thus has a greater effect on reducing a portfolio's mean residual load. As a result, a VRE portfolio benefits more from the inclusion of offshore wind than onshore wind to reduce its required backup capacity.

As observed from the proxy variables DTP lies somewhere between solar PV and offshore wind in terms of its electricity output and its volatility. As a result, including shares of DTP up to 40% capitalises on the diversification effect, but unlike wind and solar PV, including larger shares yields no significant benefits for the system. However, as can be seen in appendix C. this changes when a second, geographically dispersed DTP-dam was introduced into the system. The second dam causes DTP's electricity output to stabilise to such an extent that its residual load becomes less volatile than that of solar PV. As a result, portfolios shares of DTP up 80% become efficient.

Even though introducing a second dam made DTP superior to solar PV in terms of their mean residual load and volatility, solar PV still plays a minor role in some of the portfolios. This is only because solar PV's electricity output negatively correlates with offshore wind. However, this correlation proves not to be strong enough when DTP is equipped with an integrated storage system. DTP's electricity output becomes entirely consistent, minimising its residual load's volatility and pushing solar PV out of the efficient portfolios.

Regarding the required backup capacity, it is observed that portfolios at both ends of the efficient frontiers require the largest backup to ensure an energy security level of 95%. This can be explained by the fact that portfolios with a high mean residual load (left on efficient frontier), require a substantial amount of backup capacity to compensate the VRE portfolio's low average capacity factor. On the other hand, portfolios whose residual load is highly volatile (right end of the efficient frontier), require a large backup system to compensate the VRE system's erratic capacity factor. On average such backup system produces little electricity, the backup capacity just has to be available to quickly compensate the short but large electricity deficits left by the VRE system.

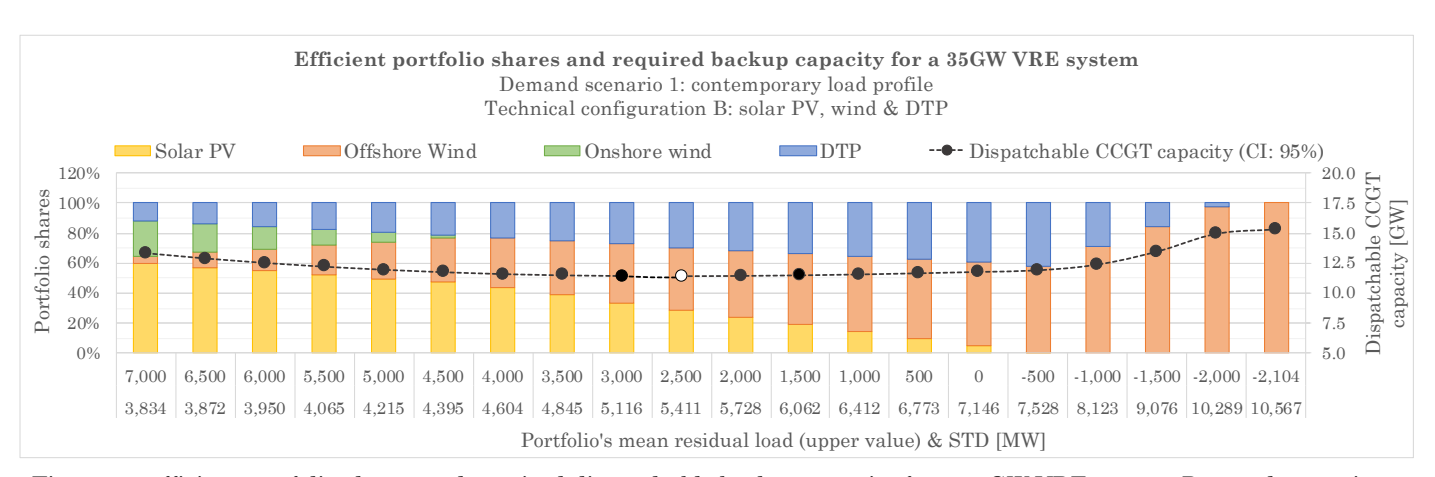


Figure 33: efficient portfolio shares and required dispatchable backup capacity for a 35GW VRE system. Demand scenario 1: contemporary load profile. Technical configuration B: solar PV, wind & DTP.

For each scenario and configuration, the VRE portfolios that require the smallest backup system (marked by the white dot in the figures) were selected. These portfolios are considered most efficient in meeting demand and are visualised in figure 34.

The horizontal axis indicates the different technical configurations (A-D) and the different electricity demand scenarios (1-4). Similar as in the previously discussed figure, the left vertical axis represents the portfolio shares and the right vertical axis the size of the dispatchable backup system required to cover 95% of the residual load left by the VRE system. The colours are also the same as in the previous figure and represent the different energy generation technologies.



What can be observed from figure 34, is that the contemporary VRE system, comprised of solar PV, onshore wind and offshore wind, is best capable of meeting demand when investments are more or less evenly distributed among solar PV and offshore wind. These portfolio shares best utilises the negative correlation among the electricity outputs from solar PV and offshore wind. As a result, the required backup capacity is minimised. When a single DTP-dam is introduced into the system, the diversification effects are maximised by investing approximately 30% in solar PV, 40% in offshore wind and 30% in DTP. As DTP's electricity output stabilises due to the introduction of a second dam (configuration C) or battery storage system (configuration D), its dominance in the efficient VRE portfolios increases and replaces solar PV and offshore wind.

Due to its consistent electricity output, a VRE system comprised of predominately DTP with storage (configuration D) requires the least backup capacity and is thus most efficient in meeting demand. Followed, by the configurations containing two geographically dispersed DTP-dams and a single DTP-dam. A system solely comprised of wind and solar PV requires the largest backup system to meet demand. Hence, in terms of the amount of backup capacity a system requires, it is found that the contemporary VRE system would benefit from the incorporation of DTP, regardless of its technical configuration.

In regards to the electricity demand profile in relation to the VRE portfolio's composition, two major observations can be made from figure 34. Firstly, it is observed that in a scenario were EV and electric HP penetrate the market and increase both the average electricity consumption as well as the peak loads, the VRE system benefits from larger shares of offshore wind. As was observed from the proxy variables and visualised in figure 29, the electricity output from wind, particularly offshore wind, tends to peak in the winter, which coincides with the peak loads from electric HP. Therefore, as the use of EV and especially HP increases, incorporating larger shares of offshore wind decreases the need for dispatchable backup capacity and thus improves a VRE system's ability to meet demand.

Secondly, it is observed that, regardless the technologies included in the VRE system, the use of demand-responsive measures to flatten peak loads caused by EV and electric HP have a backup-reducing effect. Hence, if the use of EV and HP were to increase, the system would benefit if this were to be accompanied by the incorporation of demand-responsive measures to distribute peak loads. This is especially true for a system with a DTP-dam with and incorporated storage system.

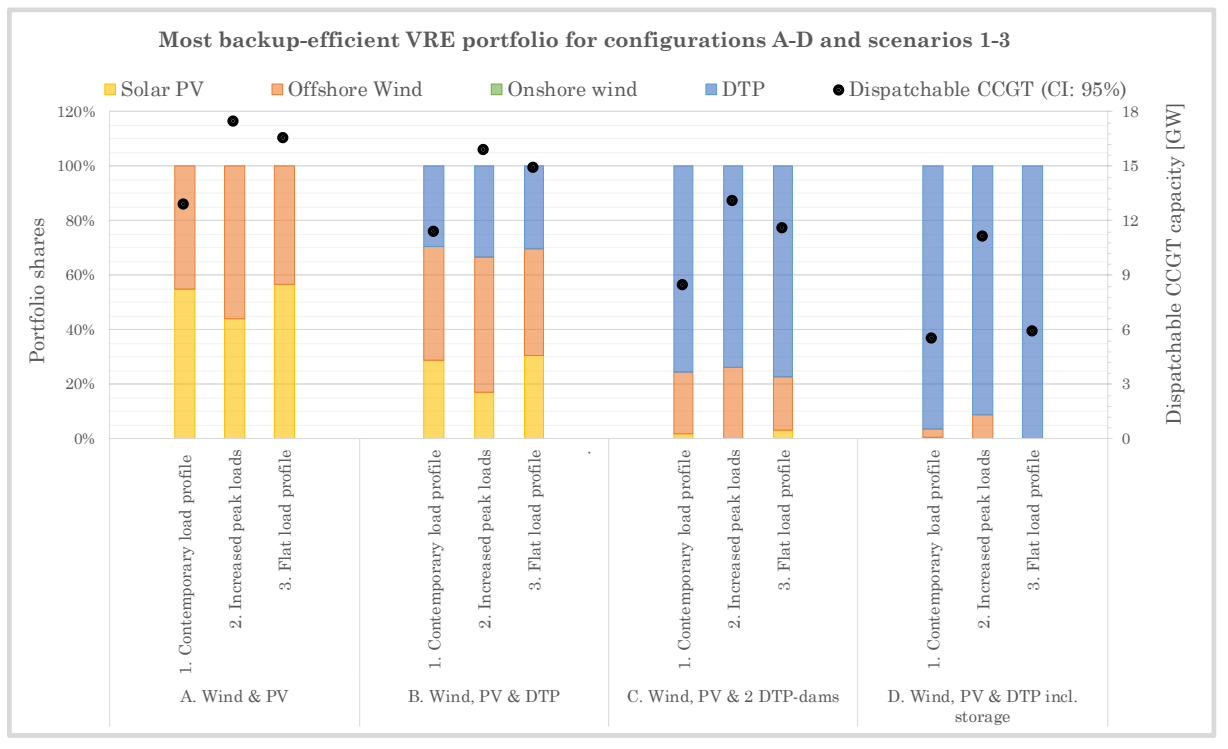


Figure 34: overview of the 35GW VRE portfolios that minimise the required backup capacity.



## 5.3 Most efficient portfolios: electricity generation costs

In the previous section, the portfolios on the efficient frontiers were gauged based on their required backup capacity. In this section, the same VRE portfolios are compared based on their energy generation costs. A VRE portfolio's ability to meet demand together with the electricity generation costs of the entire system provide valuable insights into which VRE portfolio is most efficient.

This section first briefly restates the methodology that was used to determine the system's energy generation costs. Thereafter, the electricity generation costs associated with all the VRE portfolios on the efficient frontiers are discussed. Subsequently, the energy systems that minimise the energy generation cost for each scenario and configuration are presented.

The electricity generation costs were determined for the entire system, including both the VRE system's generation costs and those of the CCGT backup capacity. Hence, the computed backup capacity to cover 95% of the residual load was added to the 35GW VRE system. For most configurations this resulted in a total system size of about 45-55 GW. Due to this increased system size, the portfolio shares changed, and were recomputed. Finally, the system's electricity generation costs were calculated by multiplying the new portfolio shares with each technology's LCOE, which were shown in section 4.4.2.

Though already stressed in section 3.3, it is important to note that the LCOEs of the VRE technologies are consistent regardless of the portfolio composition, while the LCOE of the CCGT backup varies depending on the characteristics of the residual load left by a particular VRE portfolio.

Figure 35 illustrates the results for configuration B (solar PV, wind and DTP) and the contemporary load profile (scenario 1). Similar figures were generated for the other scenarios and configuration and can be found in appendix D.

The horizontal axis indicates a VRE portfolio's mean residual load (upper value) and STD (lower value) and thus marks where a certain VRE portfolio is located on the efficient frontier (fig. 30). The first portfolio (left) corresponds with the uttermost left point of the efficient frontier and as one goes down the horizontal axis the mean residual load decreases and the STD increases, which corresponds with the trade-off visualised by the efficient frontier. On the bottom graph, the left vertical axis represents each technology's installed capacity in GW. The right vertical axis indicates the system's LCOE, expressed in € per MWh of electricity produced. As mentioned before, these costs include both the costs of the VRE system as well as its required backup. The top graph indicates the capacity factor of the CCGT backup.

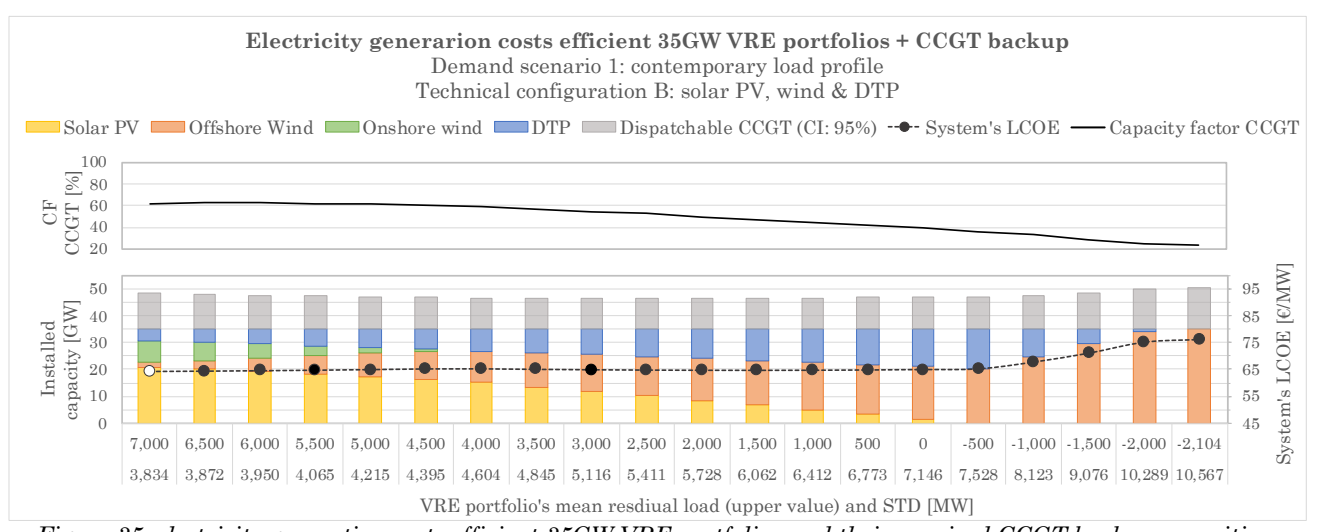


Figure 35: electricity generation costs efficient 35GW VRE portfolios and their required CCGT backup capacities.

Demand scenario 1: contemporary load profile. Technical configuration B: solar PV, wind & DTP.



From figure 35 it is observed that the capacity factor of the CCGT plummets as the mean residual load left by a VRE portfolio decreases and its STD increases. Due to the increasing STD, the backup system becomes increasingly larger to ensure a certain level of energy security (95%), while on average less electricity is generated by the CCGT. As a result, the amount of electricity produced per unit installed – the capacity factor – decreases.

Something else that is observed from figure 35 is that the CGGT's declining capacity factor coincides with rising electricity generation costs. When a declining amount of electricity is produced per unit installed, the initial investment and fixed O&M costs are distributed among fewer units of electricity. This drives up the generation costs per unit produced by CCGT, which explains the increasing system's costs. As a result of this phenomena, the system that bears the lowest electricity generation costs — marked by the white dot in figure 35 — is characterised by a CCGT with a high capacity factor.

The reason why the electricity generation costs stay relatively consistent at the beginning of the efficient frontier (left), despite the decreasing capacity factor of CCGT, is two-folded. Firstly, the amount of CCGT backup capacity decreases, causing the increasing generation costs to weigh less heavily on the total system's costs. Secondly, the generation costs of solar PV are higher than those of offshore wind, but in particular higher than those of DTP. Hence, when the share of solar PV decreases and is replaced by DTP, the generation costs of the VRE system slightly decrease. The decreasing cost of the VRE system partly offsets the increasing generation cost from the CCGT.

The graphs in appendix D support the notion that the phenomes described above apply to all the configurations, except configuration D, which includes a DTP-dam with an integrated storage system

Figure 36 illustrates the electricity generation costs for a system comprised of solar PV, wind and a DTP-dam with an integrated storage system (configuration D). Similar to the previously discussed results, this figure corresponds with electricity demand scenario 1 (the contemporary demand profile). The costs-graphs for demand scenario 2 and 3 can be found in appendix D.

What strikes from figure 36, is that opposed to configuration A, B and C, the system's costs curve and the CCGT's capacity factor curve move together. The costs decrease while the capacity factor inflates, which is counterinitiative considering what was observed in the other configuration. However, this can be explained by the fact that in configuration D the system's costs are no longer driven by the generation costs of CCGT, but by DTP's electricity storage costs. Due to its storage system the residual load left by a system comprised almost entirely of DTP is very stable (STD of 2,090 MW). This causes the CCGT's capacity factor to reach almost 100%, driving down its electricity generation costs. However, DTP's storage costs are so substantial, that the costs-reduction caused by the CCGT's high capacity factor is completely offset. As a result, it is more cost-efficient to have an inefficient backup system (low capacity factor) than to incorporate large shares of DTP with integrated battery storage.

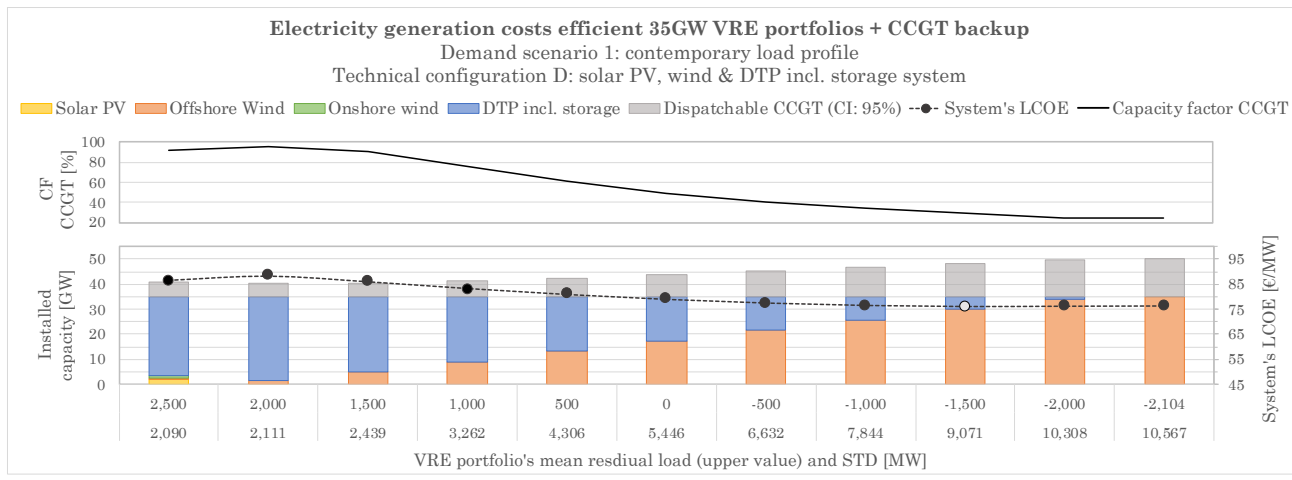


Figure 36: electricity generation costs efficient 35GW VRE portfolios and their required CCGT backup capacities. Demand scenario 1: contemporary load profile. Technical configuration D: solar PV, wind & DTP incl. storage.



The most cost-efficient systems were selected for all technical configurations (A-D) and demand scenarios (1-3). These portfolios are visual in figure 37. The horizontal axis indicates the different configurations and demand scenarios. The bottom's graph right and left axis represents the system's installed capacities and electricity generation costs. The top graph marks the capacity factors of the CCGT backup system.

Its observed, that regardless of the electricity demand profile, configuration C is most cost-efficient. Configuration C is followed by configuration A, B and finally D. Hence, it can be concluded that introducing a single DTP-dam and, to an ever greater extent, two geographically dispersed DTP-dams, into the contemporary VRE systems drives down the energy generation costs. Incorporating a DTP-dam with integrated storage system, on the other hand, would significantly increase the system's costs.

The most cost-efficient portfolio shares differ dramatically compared with the VRE portfolio shares that required the least backup capacity (fig. 34). In regards to configuration A and B, offshore wind is almost entirely replaced by onshore wind. This is partly due to the fact that the energy generation costs of onshore wind are lower than those of offshore wind. However, this shift in portfolio shares is predominantly driven by the fact that the CCGT backup produces more electricity per unit installed (higher capacity factor) in a VRE system comprised of solar PV and onshore wind. And as was concluded from figure 35, a high CCGT capacity factor drives down the electricity generation costs of the total system.

However, the greatest change in portfolio shares is observed in configuration D. Due to its high battery storage costs, DTP is replaced by offshore wind, even though this significantly reduces the CCGT's capacity factor. Hence, it can be concluded, that in terms of the energy generation-costs, including a DTP-dam with an integrated storage system is not efficient.

On the other hand, the composition for the most efficient portfolios for configuration C have remained exactly the same in relation to the portfolio shares that required the least backup capacity (fig. 34).

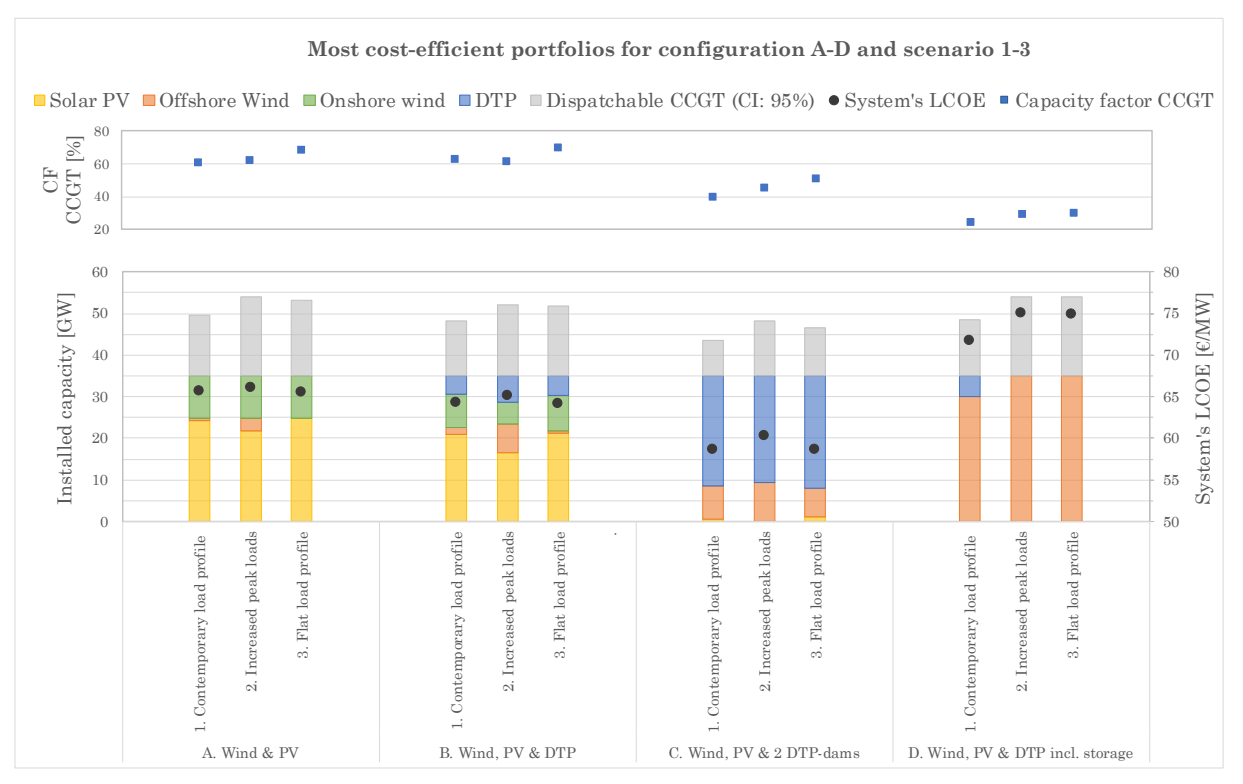


Figure 37: overview of the 35GW VRE portfolios + CCGT backup that minimise the energy generation costs.



From figure 37, it is observed that the shape of the load curve has a small effect on the composition of the efficient portfolios. Similar as observed in section 5.2, when the average electricity consumption and peak loads increase due to EV and electric HP (scenario 2) a small increase in offshore wind is observed in configuration A and B. The electricity output from offshore wind tends to follow the peaks in electricity consumption of electric HP. Hence, increased shares of offshore wind reduce the residual load's volatility. This increases the CCGT's capacity factor and drives down the system's electricity generation costs.

In configuration C, the different load profiles have little effect on the electricity generation costs or portfolio compositions. Increased peak loads tend to slightly increase the generation costs. This is a result of increased size of the CCGT back system, which causes the high costs of the CCGT to weigh heavier on the system's total costs. However, these increased costs do not affect which portfolio shares are most efficient. In every demand scenarios, the three most efficient portfolios are comprised of approximately 25% offshore wind and 75% DTP.

The changes in the demand profiles also resulted in some changes in configuration D. In demand scenario 1, DTP still plays a minor role in the most cost-efficient portfolio, while DTP is completely replaced by offshore wind as the average electricity demand increases in scenario 2 and 3. This is due to the fact that offshore wind tends to produce more electricity per unit installed than DTP, and thus reduces the amount of electricity that is produced by the CCGT



### 5.4 Sensitivity analysis

To acquire a thorough understanding of how the optimisation model reacts to certain changes in the input parameters, a sensitivity analysis was conducted. For this sensitivity analysis, merely electricity demand scenario 1 – the contemporary load profile – was used. The sensitivity analysis includes all the technical configuration (A-D).

For this sensitivity analysis, three different variables were adjusted; the system size, the confidence interval of the backup system and the CO₂ price. Section 5.4.1 discusses the effects of changing the VRE system's size from 35GW to 25 and 45GW. In section 5.4.2, the effects of increasing the confidence interval from 95% to 99% are presented. Finally, the CO₂ price was increased from 25 to 200 €/ton CO₂, the results of this are presented in section 5.4.3.

### 5.4.1 System size

The results presented so far are based on a 35GW VRE system, equal the size of the contemporary electricity system in The Netherlands. To evaluate whether the system's size affects the composition of the portfolios and the amount of backup capacity required, the system size was adjusted. The system size in changed from 35 GW to 25 and 45GW.

In- and decreasing the VRE system's size results in the proxy variables illustrated in table 9 and 10. The table shows the mean residual load and STD, if the VRE system were to be comprised of 25 or 45GW of solely one of the six energy technologies. The bottom three rows represent the correlation coefficients among technology's residual loads.

It is observed that for all energy technologies, the mean residual load decreases as the systems size increases. This is simply due to the fact that when more VRE capacity is installed, on average, more electricity is generated, which reduces the mean residual load.

On the contrary, for all technologies expect a DTP-dam with storage system, the STD of the residual loads increase when the system was enlarged. The electricity output from a certain technology deviates between a certain range. For example, if 25GW of solar PV were to be installed, its electricity output could deviate between 0 and 25 GW, depending on the amount of solar irradiation. When the installed capacity is increased to 45 GW, the range in which the electricity output from solar PV can fluctuate expands, which increases the STD and that of its residual load.

The electricity output from a DTP-dam with storage system does not fluctuate. Hence increasing its installed capacity does not affect its volatility in electricity output. The STD of the residual load left by a DTP-dam with storage system (2,130 MW), is solely the result of the fluctuations in electricity demand and thus does not change when the system's size is adjusted.

From the correlation coefficients, it is observed that the residual loads tend to be more negatively correlated when the system's size increases. The smaller the system's size, the more the correlation among the residual loads is dominated by the shape of the load curve. As the load curve is the same for each technology, their residual loads tend to be more positively correlated. But when the system's size increases, the shaping-effect of the load profile on the residual load diminishes and the correlation is predominately driven by the volatility in electricity output.

Table 9: proxy variables 25GW VRE system and demand scenario 1: contemporary load profile.

	Solar PV	Offshore wind	Onshore wind	DTP	2 DTP- dams	DTP incl. storage
Mean residual load [MW]	10,803	2,221	6,665	4,957	4,956	5,209
STD of the residual load [MW]	3,852	7,622	5,719	7,345	3,797	2,130
Correlation coefficient:						
Solar PV		-0.11	-0.04	0.13	0.26	0.45
Offshore Wind			0.83	0.05	0.10	0.16
Onshore wind				0.08	0.16	0.25



Table 10: proxy variables 45GW VRE system and demand scenario 1: contemporary load profile.

	Solar PV	Offshore wind	Onshore wind	DTP	2 DTP- dams	DTP incl. storage
Mean residual load [MW]	9,022	-6,429	1,572	-1,503	-1,504	-1,050
STD of the residual load [MW]	6.360	13,549	10,007	12,825	6,037	2,130
Correlation coefficient:						
Solar PV		-0.19	-0.15	0.04	0.08	0.22
Offshore Wind			0.82	0.01	0.03	0.04
Onshore wind				0.02	0.05	0.09

The proxy variables were used to generate the minimum-variance frontiers for each technical configuration and system size. From figure 38, it is observed that the efficient frontiers reach further into the negative values as the installed capacity increases. This indicates that a larger number of VRE portfolios on the minimum-variance frontier, on average, produce more electricity than is consumed. Additionally, the efficient frontiers move to the right when the system's size is increased. This visualises what was observed from the proxy variables; when more capacity is installed the volatility increases.

As was elaborated in section 5.1.1, changes in the correlation coefficients affect the sharpness of the curve in the mean-variance frontier. As was observed from the proxy variables, the larger the VRE system, the more negatively the technologies' residual loads tend to correlate. This is also observed in figure 38, the curve in the minimum-variance frontier tens to sharpen when the system's size increases.

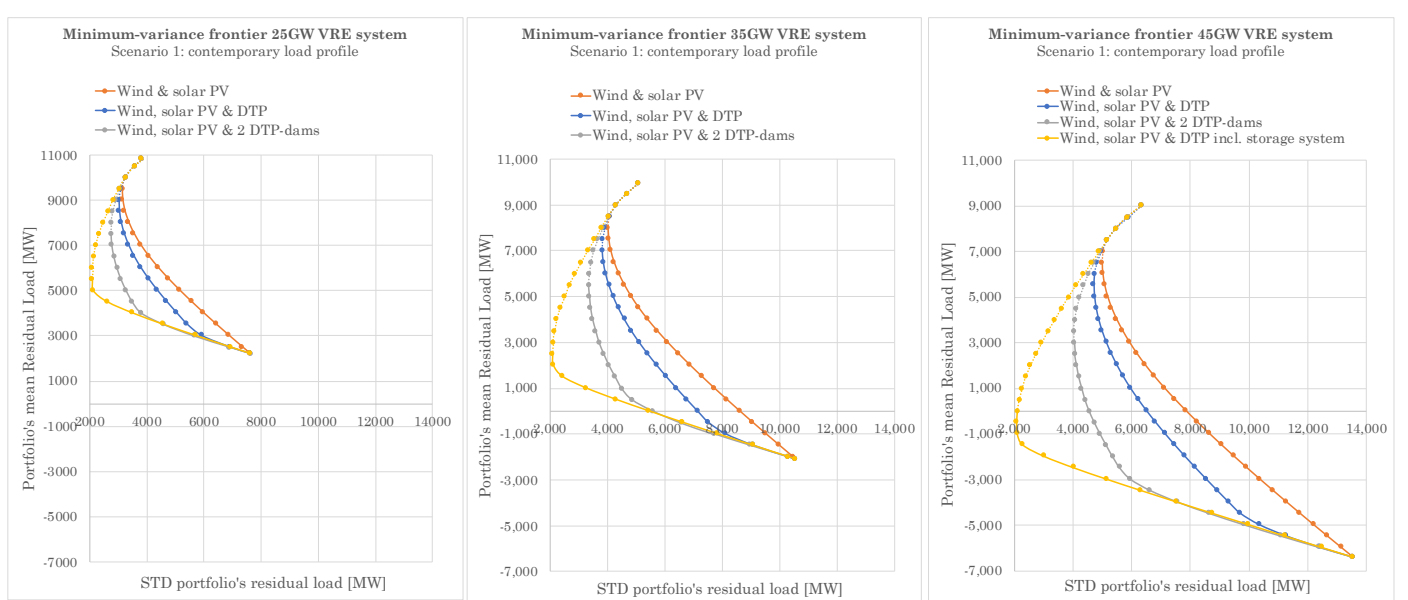


Figure 38: overview minimum-variance frontiers for a 25, 35 and 45 GW VRE system.

Similar to the results of the different demand scenarios, the portfolios on the inefficient part of the minimum-variance frontier (dashed line) were eliminated. The portfolio's shares of the VRE systems on the efficient frontier (solid line) are visualised in bar charts and can be found in appendix E. Subsequentially, for those portfolios on the efficient frontier, the backup capacity required to cover 95% of the residual load was determined, and the portfolios that required the least backup were selected. These most efficient portfolios are visualised in figure 39. The horizontal axis marks the different system sizes and configurations, while the vertical axis represents the portfolio shares (left) and required backup capacity (right).



From figure 39 it is observed that, although the characteristics (mean residual load, STD and correlation) of the portfolios changed, the shares of the most efficient portfolio remained the same, regardless system's size. Hence, one could conclude that the system's size has little to no effect on which VRE portfolio shares are most efficient to meet demand.

However, regarding configuration C and D, increasing the system's size significantly reduced the need for dispatchable backup capacity, while little change is observed in configuration A and B. This can be explained by the fact that the electricity output from solar PV, wind and a single DTP dam know periods in which little to no electricity is produced. During these periods all the electricity to foresee in demand is produced by the backup. Increasing the system's size slightly reduces the number of hours in which VRE technologies produce no electricity, however, they are not eliminated. Hence, regardless of the VRE system's size, a system comprised of solely solar PV, wind and a single DTP-dam requires approximately the same amount of backup capacity to ensure a certain level of energy security.

On the other hand, including a second geographically disperse DTP-dam or a DTP-dam with a storage system helps to distribute the electricity outputs, diminishing periods in which little to no electricity is produced. As a result, increasing the installed capacity reduces the need for a backup system. Therefore, it can be concluded that increasing the installed VRE capacity in order to reduce the need for backup capacity is only effective if the VRE system includes perfect negatively correlating VRE technologies (scenario C) or a storage system (configuration D).

Sensitivity analysis: different VRE system sizes 25GW, 35GW and 45GW

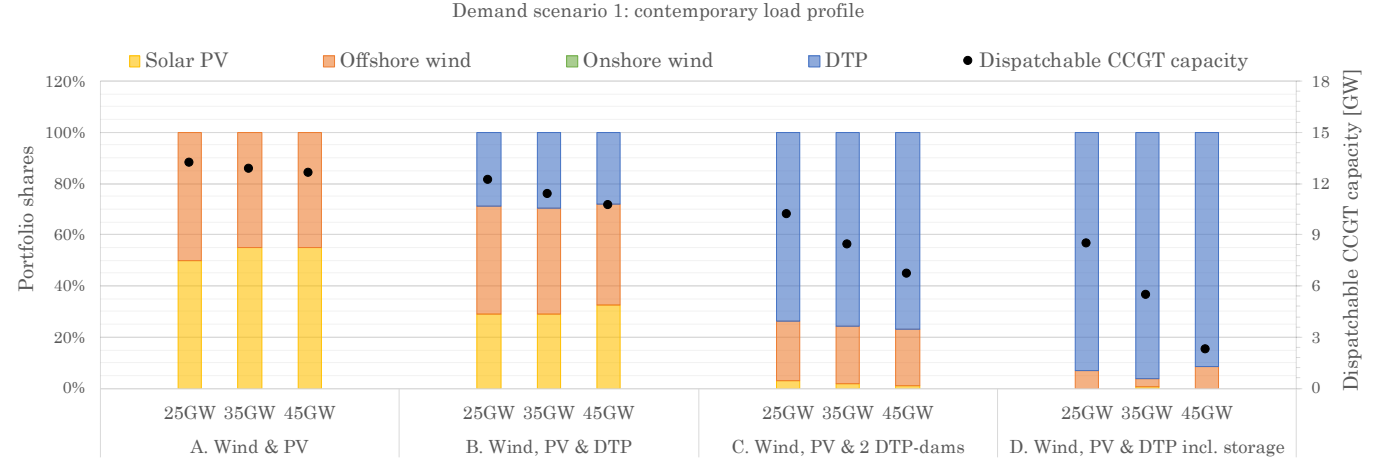


Figure 39: overview most efficient VRE portfolios for different system sizes; 25, 35 and 45GW

## 5.4.2 Confidence interval dispatchable backup system

Until now the confidence interval (CI) of the dispatchable backup system was set to 95%, which means that the backup system should be large enough to cover 95% of the VRE portfolios' residual load. In this sensitivity analysis, the confidence interval is increased to 99%, simulating a scenario with a higher degree of energy security.

As was elaborated in section 3.2, the size of a backup system with a 95% confidence interval corresponds with a VRE portfolio's mean residual load plus 1.645 (z-value) times the STD of the residual load. In order to increase the level of energy security, the z-value was increased so that more outliers are covered by the backup system. For a one-tailed test with a confidence interval of 99%, the z-score is 2.33 [74]. Hence, the equation to determine the size of the backup systems is as following (eq. 5.1);

Dispatcable backup capacity (CI: 99%) =  $\mu(RL_P)$  + 2.33 \*  $\sigma(RL_p)$  (Eq. 5.1)



Figure 40 illustrates the portfolio shares and backup capacity for a system comprised of solar PV, wind and DTP (configuration B). Similar graphs were generated for the other three configurations (A, C and D) and can be found in Appendix F. The horizontal axis indicates a portfolio's mean residual load (upper value) and STD (lower value), and thus mark where on the efficient frontier a portfolio is located (fig. 30). The vertical axis indicates the portfolio shares (left) and the dispatchable backup capacity required (right). The shares of the portfolios on the efficient frontier are not affected by the increased CI, and are thus the same as discussed in section 5.1.1. The red line, which was added to the figure, indicates the backup capacity required to cover 99% of the load left by a VRE portfolio. The white dot on the black and red line indicates which portfolio requires the least backup capacity.

Figure 40 and the figures corresponding with the other configurations (appendix F) show that more backup is required as the level of energy security is increased. Based on the deflecting red line, this effect is the greatest for those VRE portfolios whose residual loads bear high a STD. A high STD indicates that the residual loads are spread out around the mean residual load. As a result, VRE portfolios whose residual loads have a high STD require much extra backup to increase the energy security just a little bit.

On the other hand, when the STD is low, and the residual loads are clustered around the mean, a small increase in dispatchable backup capacity is sufficient to attain a much higher level of energy security. As a result of this disproportional need backup capacity, it is observed that as the CI increases, portfolios with a low STD and high mean residual load tend to become more efficient than portfolios with a high STD and low mean residual load. This phenomenon is also clearly visualised in figure 40, the white dot in the bar chart, which indicates the portfolio that requires the least backup, moves left as the CI increases.

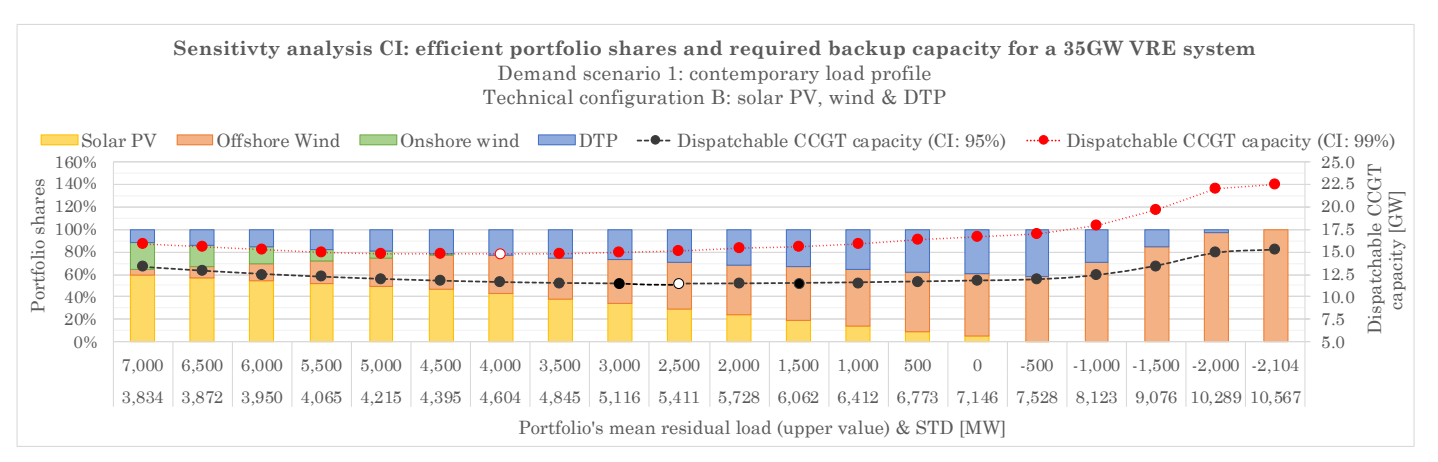


Figure 40: portfolio shares and backup capacity for an increased confidence interval: 95%-99%. Technical configuration B: solar PV, wind & DTP.

Figure 41 illustrates the most efficient VRE portfolios for each configuration and confidence interval. The horizontal axis indicates the four technical configurations (A-D) and the confidence intervals (95% and 99%). The vertical axis illustrate the portfolio shares (left) and the backup capacity required to cover either 95% or 99% of the residual load.

Figure 41, shows that regardless of the technical configuration, the required backup capacity increases as a higher level of energy security is demanded from the system. Something else observed from figure 41, is that the shares of solar PV and onshore wind in the most efficient portfolios for configuration A-C increase when a higher level of energy security is demanded from the system. Onshore wind and in particular solar PV tend to stabilise a portfolio's residual load, which, causes the required backup capacity to increase less rapidly when the CI is increased. Hence, increased levels of energy security require more stable VRE technologies.

The portfolio composition of scenario D does not change when the CI is increased, because there is no portfolio whose residual load bears a lower STD than a portfolio compressed entirely from DTP with an incorporated storage system.



## Sensitivity analysis: increased confidence interval (CI) 95% - 99% Scenario 1: contemporary load profile

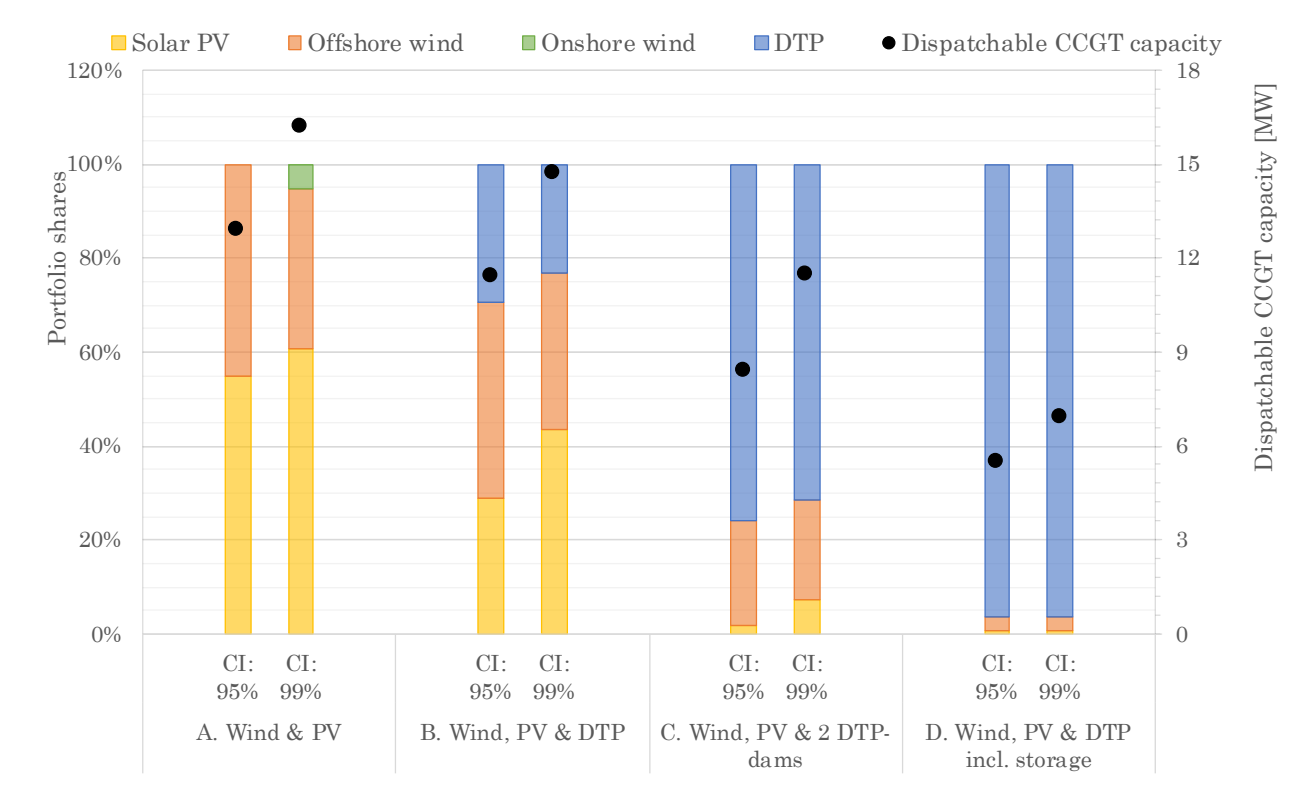


Figure 41: overview most efficient VRE portfolios for different confidence intervals; 95% and 99%.

### 5.4.3 CO<sub>2</sub> price

The results presented so far assumed a  $CO_2$  price of 25 euro per ton of  $CO_2$  emitted, equal to the price for which  $CO_2$  allowances were traded in 2020 [76]. However, as was elaborated in section 4.4.1, the idea behind the Emission Trading System (ETS) is that each year the number of allowances is reduced to drive up the price and stimulate more companies to abate  $CO_2$ -emission. To simulate an extreme reduction in  $CO_2$  allowances, the  $CO_2$  price was increased to  $200 \, \text{€/ton} \, CO_2$  in this sensitivity analysis. Table 11 illustrates that as a result of this increased  $CO_2$  price, the  $CO_2$  costs per MWh produced by the CCGT increase from 10.10 (table 3) to  $80.78 \, \text{€}$ .

Table 11: CO2 costs per MWh for an increased CO2 price

CO <sub>2</sub> costs CCGT	
CO <sub>2</sub> emission factor natural gas [kg/GJ]	56.10 [76]
Energy used to generate 1 MWh [GJ]	7.20
CO <sub>2</sub> emission [ton/MWh]	0.40
CO <sub>2</sub> price [Euro/ton]	200.00
CO <sub>2</sub> costs (Euro/MWh)	80.78

Figure 42 illustrates the effects of the increased  $CO_2$  price on the system's LCOE for technical configuration B. However, similar graphs were generated for the other three configurations (A, C and D) and can be found in appendix G. The dashed black line corresponds with the systems LCOE with  $CO_2$  price of 25  $\ell$ /ton  $CO_2$  and the dashed red line corresponds with a  $CO_2$  price of 200  $\ell$ /ton  $CO_2$ .



From figure 42, it is observed that the systems LCOE has increased regardless of the composition of the VRE system or the size of the backup system. Something else that can be seen from figure 42 is that the most cost-efficient system is no longer located at the end of the efficient frontier, where the capacity factor is the highest, but somewhere halfway. As was concluded in section 5.3, the system's costs of configuration A and B are driven by the capacity factor of the CCGT. When the CO<sub>2</sub> price is relatively low, the CCGT capacity factor should be high so that its investment and fixed O&M costs are spread out. But when the CO<sub>2</sub> costs increase, it becomes increasingly costly to produce electricity, so the overall system's costs are the lowest when little electricity is generated by the CCGT. Hence, it is most cost-efficient when both the capacity factor and the size of the backup system are minimised. This why the most cost-efficient portfolios tend to lie halfway the efficient frontier, where the backup system is the smallest and the capacity factor has decreased.

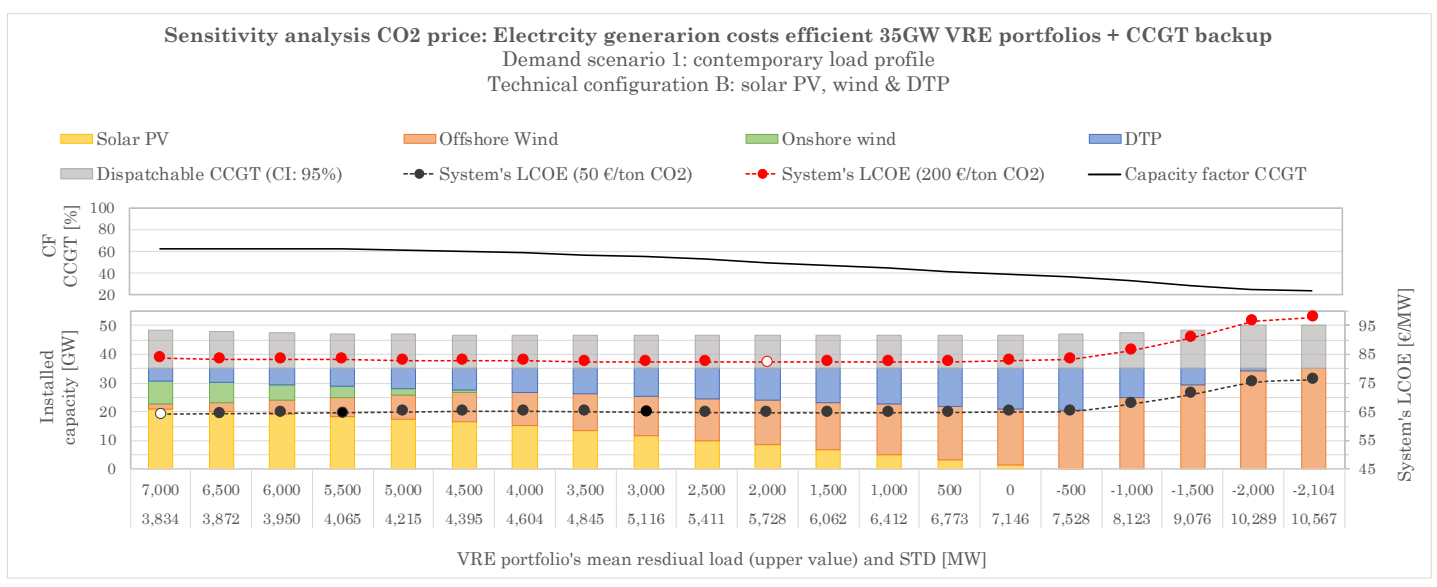


Figure 42: portfolio shares and energy generation costs for an increased CO<sub>2</sub> price. Technical configuration B: solar PV, wind & DTP.

Figure 43 illustrates the most cost-efficient systems for each configuration and  $CO_2$  price. The horizontal axis indicates the four technical configurations (A-D) and the  $CO_2$  prices (25 and 200  $\mbox{\ensuremath{\ensuremath{O}}}$ ). The vertical axis illustrates the installed capacity (left bottom), the capacity factor of the CCGT (left top) and the system's LCOE (right).

The first thing that is observed, is that the order of the most economic configurations has not changed, so is a configuration with solar PV, wind and two geographically dispersed DTP-dams still the most economical. In regards to the portfolio shares of configuration A and B, it is observed that offshore wind and DTP has replaced solar PV and onshore wind as a result of the increased  $CO_2$  price. This is simply explained by the fact that offshore wind and DTP have, on average, a higher capacity factor and thus tend to produce more electricity per MW installed than solar PV and onshore wind. This reduces the total amount of electricity that needs to be produced by the CCGT and thus the system's LCOE

No changes are observed in scenario C as a result of the increased CO<sub>2</sub> price. As shown in appendix G, there is no other portfolio on the efficient frontier that requires a smaller backup system. So in any other systems, the costs of the CCGT weigh more heavily on the system's total LCOE. This outweighs a CCGT with a lower capacity factor.

On the other hand, large changes are observed in configuration D. The share of DTP with storage has increased dramatically due to the increased CO<sub>2</sub> price. This due is to the fact that the system's LCOE is no longer primarily driven by the storage costs, which was the case when the CO<sub>2</sub> price was 25 euro. The increased CO<sub>2</sub> price caused the costs of the CCGT to weigh heavily on the system's total LCOE. As a result, it has become more economical to reduce the size of the backup system by incorporating larger shares of DTP with storage.



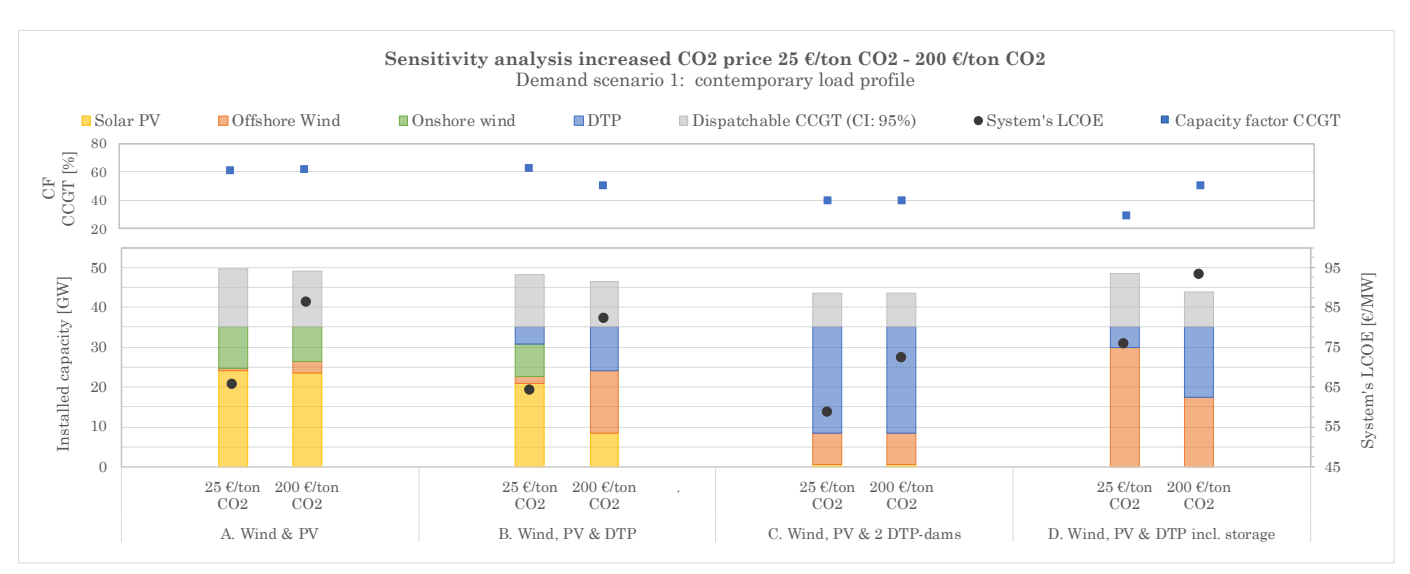


Figure 43: overview most efficient VRE portfolios for different CO₂ prices; 25 & 200 €/ton CO₂.



# 6 Discussion

This chapter reflects on the results presented in the previous chapter and the novel methodology used to obtain the results. Section 6.1 first reflects on the novel application of the MPT and whether it has yielded any new insights. In section 6.2, the interpretation and implications of the main findings are discussed. Also, their relation to the literature and the theoretical background is elaborated. In the last section, the strengths and weaknesses of DTP are discussed, and suggestions for a market entry strategy are provided.

## 6.1 Reflection on the methodology

To fill the knowledge gap identified by Cunha et al. [18] and to find the VRE portfolios that minimise the mean residual load and variance, the MPT was modified. The MPT was modified by including demand-variability, something which was not done before. Subsequentially, for the portfolios that minimise the residual load and variance, the required backup capacity was determined based on the assumption that the residual load data is normally distributed. Thereafter, the portfolios' energy generation costs were computed, and the VRE portfolios were gauged and compared based on these two performance indicators (required backup and costs).

Section 6.1.1 reflects on whether including demand-variability in the MPT has yielded any new insights or unexpected results. In section 6.1.2, the limitations of the methodology developed are discussed.

### 6.1.1 Effects including demand-variability

In total, three different demand profiles were included: The Netherlands' contemporary load profile (1), increased peak loads due to EV and HP (2), and a flat load profile due to an extreme penetration of demand-responsive measures (3). When the results of the different demand scenarios are compared, it becomes evident that the shape of the demand curve only has a limited effect on the composition of the efficient VRE portfolios. Only when peak loads increase due to an extreme penetration of EV and electric HP, does the share of offshore wind in the efficient portfolios slightly increase (2-13%). This effect is the greatest for a portfolio comprised of solely solar PV and offshore wind. Hence, the contemporary VRE system is relatively sensitive for increases in peak demand as it has the greatest effect on which portfolio shares are most efficient.

Although it was expected that changing the demand profiles would have a larger effect on which VRE portfolio shares are efficient, it can be explain why this effect is limited. The deviations in electricity supply from VRE are much larger than the volatility in electricity demand. As a result, the shape of the output profile has a more decisive role which VRE portfolio shares minimise the residual load and its variance. Hence, the changes performed on the demand curve were too little to translate into major changes in the portfolio shares. However, based on the literature review conducted to derive the three demand profiles, it is unlikely that the demand profile will experience larger changes in the future than those simulated in this study. Overall, it can be concluded that including demand-variability in the MPT has a limited effect on the selection of efficient VRE portfolios.

Although demand-variability only has a limited effect on which portfolios shares are most efficient, it significantly affects the magnitude of the residual load left by a VRE portfolio and its volatility. Hence, the amount of backup capacity is greatly affected by changes in demand. The required backup capacity increases when peak loads increase (scenario 2), and decreases when demand stabilises (scenario 3). This effect is the greatest for portfolios that are comprised of a DTP-dam with a storage system.



### 6.1.2 Methodological limitations

This research was the first to apply the novel methodology presented in chapter 3. As such, certain limitation of the methodology emerged when this research was conducted. In this section, these limitations are elaborated, and important aspects that were not included in the methodology are discussed.

First of all, the electricity system that was optimised to derive the results was a simplified representation of real-life and should be treated as such. There are, however, two simplifications that are worth elaborating on. Firstly, DTP's electricity output profile was derived from the perfect astronomic tide, which is a sine function. However, in real-life, the tide is rarely a perfect sine wave, as it is affected by geographical features, such as; local relief on the sea's bottom floor. Hence, DTP's electricity output is affected by its specific location and might be more erratic than was assumed in this study. This also means that in regards to scenario C, where two geographically dispersed dams were introduced into the VRE system, it might not be possible in real-life to find two locations where the dams' electricity outputs perfectly negatively correlate at all times.

Secondly, as elaborated in the research outline (section 1.3), this study treated The Netherlands as a closed electricity system and did not include cross-border electricity trading. However, in real-life, The Netherlands is connected to numerous countries through an international electricity transmission grid. This grid allows for the sale of electricity to neighbouring countries during periods in which more renewable electricity is produced than consumed. On the other hand, during periods of little VRE output, power deficiencies can be compensated by purchasing electricity from other countries, mitigating the need for dispatchable backup capacity.

Hence, increasing the geographical scope of this research and including cross-border electricity trading would not only more accurately represent The Netherlands' real-life electricity system, but is also expected to increase the system's ability to match supply and demand. The extent to which cross-border electricity trading reduces the need for backup capacity depends on the degree to which the VRE outputs from the countries connected through an international grid correlate. If countries' VRE electricity outputs positively correlate, they all face VRE surplus and deficiencies simultaneously, leaving little electricity to trade and offset supply and demand discrepancies. Therefore, one could argue that if the aim is to minimise the need for CO<sub>2</sub>-intensive backup capacity, an international rather than a national approach would be more efficient to allocate investments to VRE technologies.

Another limitation of this research, closely related to the exclusion of cross-border electricity trading, lies in the fact that this study did not include the costs of electricity surplus (negative residual loads) impose on the system. Electricity deficiencies (positive residual loads) were covered by deploying a CCGT backup system. Accordingly, the backup system's costs were included in the electricity system's total energy generation costs. Although this study considered electricity deficiencies and surplus to be equally inefficient to determine the residual load and backup capacity, the costs associated with electricity surplus were not included in this study.

In a closed electricity system with no international electricity trading or storage capacity, as was optimised in this study, VRE surplus are disposed of by curtailment. Curtailment is a deliberate reduction in the electricity output of a generator in order to match supply and demand [77]. For example, when the electricity output from wind turbines exceeds demand (electricity surplus), they can be turned away from the wind, so the blades stop rotating and producing electricity. Such curtailment measures cause a VRE technology to produce less electricity than what it could produce given the available resources. As a result, the costs per unit of electricity generated increases, driving up the VRE system's total costs. As the share of VRE in the electricity system increases, the need to match supply and demand by means of curtailment increases, which causes the curtailment costs to weigh more heavily on the system's total costs. It is expected that if curtailment costs were to be included in the costs structure of this study, VRE technologies that minimise peak outputs, for example, due to the use of a storage system (DTP configuration D) would become increasingly cost-efficient in meeting demand.



However, as discussed before, the Netherlands' real-life electricity system is connected to other countries' electricity systems, allowing for cross-border electricity trading. As a result, electricity surplus can partly be sold to neighbouring countries, which reduces the curtailment costs. It is important to note that the construction and maintenance of an international electricity grid are capital intensive. So even though a wide transmission grid might reduce national curtailment costs, these costs are (partly) replaced by the extra grid costs.

Another cost-related limitation concerns the accuracy of the costs data used to derive DTP's LCOE. For well-established energy technologies, including solar PV and wind, numerous studies have estimated their costs. However, as DTP is an untested technology, obtaining accurate costs data proved to be more difficult. For this study, DTP's cost data was derived from the DTP foundation, which got their information from estimations made by contractors. As a result, it is expected that the DTP's costs data is less accurate than the cost data used for solar PV and wind.

This might partly explain why the LCOE of DTP is lower than those of solar PV and offshore wind. In general, one would expect that the costs of an untested electricity generation technology that has not experienced any learning-effects are higher than those of well-established energy technologies. DTP's low LCOE is predominately driven by its O&M costs, which are estimated to be much lower than those of offshore wind. More research is required to assess whether this is truly the case and increase the overall accuracy of DTP's costs assumptions. Besides a potential underestimation of the O&M costs, DTP's low LCOE is also partly driven by its longer lifetime (60 years) in relations to solar PV and wind (25 years). Due to this longer lifetime, DTP produces more electricity in its lifetime, and the overnight capital costs are divided over more units of electricity, driving down its LCOE.

Moreover, this study did not include any forecasted cost reductions. For example, in this study, battery storage costs were estimated to be 100,000 €/MWh, but it is expected that these costs will drop as batteries are used on a large scale, and technical innovations and/or economies of scale make them less costly to produce [78]. Additionally, the construction of a second DTP-dam (configuration C) might be less costly than the first dam due to the insights that were acquired constructing the first DTP-dam (learning-effects). Similarly, offshore wind and solar PV's electricity generation costs are expected to decline rapidly in the coming years [79] [80]. The LCOE of onshore wind, on the other hand, is expected to stabilise [80]. As the margins between technologies' LCOEs are thin, incorporating these forecasted cost-reductions might yield different results than were found in this study.

To derive a VRE technology's residual load, this study used historical supply and demand data. However, as was stressed by A. Stirling [40] [41], solely using historical data to support the portfolio model might lead to erroneous results (section 2.3). This limitation was partly mitigated by incorporating two alternative electricity demand scenarios. However, in regards to the electricity output profiles only one scenario was included, a technology's contemporary electricity output. Although the output data was derived over three years (2017-2019) in order to minimise the effect of random events on the results, if two of those years were characterised by, for example, below-average wind speeds, the data might be biased. Hence, the accuracy of the outcome could be improved by including different supply scenarios. Including different scenarios would also allow the inclusion of climate change effects on the output from VRE technologies. This was not included in this study but might play a role in the future.

A more practical issue was caused by the choice for the specific demand scenarios. In each scenario, both the average electricity demand and the shape of the demand profile were deviated. Although this has yielded interesting results, it was sometimes difficult to distinguish which changes in the results were caused by the increased electricity consumption and which by the altered shape of the demand profile.

To find the VRE portfolios that are most efficient in meeting demand, this study optimised a 35GW VRE system. Hence, the constraint was the amount of installed capacity, and the trade-off was how much capacity to allocate to each energy generation technology. However, this study did, for example, not restrict the amount of capital that could be invested in the VRE system, nor was there a minimum capacity factor that had to be met by the VRE system.

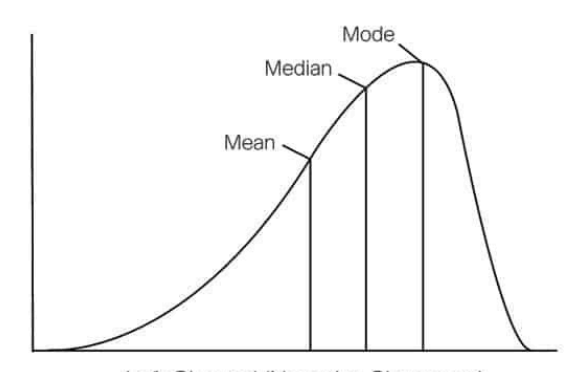


Introducing a budget constraint would significantly reduce the amount of capacity allocated to a DTP-dam with a battery storage, as its capital costs are substantial. On the other hand, a minimum capacity factor would discourage solar PV investments due to its small capacity factor. Hence, setting different constraints or introducing additional constraints might significantly affect the results found in this study.

Another limitation lies in how the size of a VRE portfolios' required backup capacity was determined. Going by the assumption that the residual load data was normally distributed, the backup's size was determined by multiplying a portfolios' mean residual load, the STD of its residual load and the z-value that corresponds with a one-tailed confidence interval (CI) of 95% (1.645). However, when, in the sensitivity analysis the z-value was increased to 2.33 to correspond with a confidence interval of 99%, it is observed (fig. 40) that the backup capacity approaches a size of 22.5 GW, while the maximum electricity load in scenario 1 (the contemporary load profile) is approximately 19GW. Even though the confidence interval was increased, the backup system should not be larger than the maximum amount of electricity that is consumed.

The issue causing this overestimation lies in the fact that, although the residual load data lies within George et al.'s [43] acceptable boundaries for kurtosis and skewness (-2/+2) to be considered normally distributed, the data tends to be negatively skewed. This phenomena is illustrated in figure 44 and means that the left tail of the distribution graph is longer and that more values are concentrated on the right end of the distribution graph. The distribution of the residual loads can be found in appendix H. As a results, there are no actual residual load data points 2.33 standard deviations right from the mean anymore. The value found is larger than the maximum residual load in the data set, which explains the overestimation of the backup's size.

However, data is rarely perfect normally distributed and over- or underestimations are common in statistics when the z-score approach is used. This study in particular highlights this limitation since there is a clear upper boundary to the size of the backup system. Using the z-score thus allows for easy and relative accurate comparability among different portfolios. But if the aim is to determine the exact size of the backup system under extreme levels of energy security, a more comprehensive method should be used



Left-Skewed (Negative Skewness)
Figure 44: visualisation negatively skewed
data set [97].

Overall, the methodology's main benefit is the different steps in which one works towards the outcome. These steps provide clear insights into how specific changes in the parameters translate into the result. On the other hand, these different steps and the fact that all results need to be manually visualised are also the methodology's weaknesses since it is quite a time-consuming process. Therefore, this methodology is most suitable for scientific purposed; to find relations between particular variables and acquire a thorough understanding of diversification effects in the electricity system. Because no expensive software is required, the mythology might also be beneficial for (small) companies, startups or NGO's that are concerned with optimising the electricity systems of small or remote communities, for example, in sub-Saharan Africa. For governmental proposes and actual locating large-scale investments into energy-generating assets, the absolute outcomes generated using this methodology, especially the size of the backup system, may not be accurate enough. However, the theory behind the method (the MPT) could be used as the foundation to build a more sophisticated energy planning tool.



### 6.2 Interpretation of the main findings

This research's main goal was to find the portfolios of solar PV, wind and DTP that are most efficient in meeting The Netherlands' electricity demand. Additionally, this study aimed to evaluate whether DTP improves the current VRE system's efficiency to meet demand.

This section first discusses the key findings and elaborates on the theoretical background supporting these findings and their relation to the existing literature. Subsequently, the findings are compared with The Netherland's current VRE system in order to formulate how future energy investments should be allocated.

From the MPT optimisation, it was found that there are three ways to decrease the volatility of a VRE system's residual load and thus increase its ability to follow the demand curve. Firstly, incorporating VRE technologies whose electricity outputs negatively correlate reduces the overall STD of the portfolio's residual load. Secondly, a system's ability to follow the demand profile can be increased by stabilising the electricity output from an individual energy technology. Third and last, flattening the electricity demand curve also reduces the variance of an energy system's residual load. These findings are in line with the fundamental theory behind the MPT discussed in the literature review (section 2.1), illustrating the validity of the novel application of the MPT.

The rest of this section discusses how these fundamental mechanisms translate into which VRE portfolios are most efficient and what can be implied from these results.

Based on the backup capacities required to ensure 95% energy security, it is observed that the current VRE system (configuration A) would be most efficient in meeting demand when comprised of offshore wind (approx. 45%) and solar PV (approx. 55%). This indicates that including onshore wind deteriorate a system's ability to meet demand. This phenomenon was not found in the literature that was reviewed, which might be due to the fact that not many studies distinguish between on- and offshore wind. It can, however, be explained by the above-described mechanisms of the MPT. The electricity output from on- and onshore wind follow the same pattern and are thus positively correlated. However, the electricity output per unit installed (capacity factor) from offshore wind is much larger. As a result, offshore wind is more negatively correlated with solar PV. Hence, combining solar PV and offshore wind in one portfolio maximises the diversification effects and the amount of volatility that is eliminated, which minimises the required backup capacity.

When DTP was introduced into the VRE system, it is observed that the required backup capacity declines and that the VRE system's ability to meet demand improves. The magnitude of this effect and the share of DTP that is most efficient to include in the VRE system depends on DTP's technical configuration. When a single DTP-dam is introduced, shares up to 30% are most efficient. This result provides an interesting new insight into the effect of tidal energy on an electricity system's ability to follow the load curve. Allan et al. [29], found that tidal energy shares up to 10% have a volatility-mitigating effect, but did not assess whether this positive effect preserved when tidal energy penetration surpassed 10%. This study confirms that this is the case. In fact, the positive diversification effects of incorporating tidal energy are particularly noticeable when larger shares (up to 30%) of DTP are included in the electricity system.

When a second DTP-dam, whose electricity outputs perfectly negatively correlate with the first dam, is introduced into the VRE system, the system's ability to meet demand further increases. It also becomes efficient to introduce larger DTP shares into the VRE system; shares up to 75% are most efficient. In a 35GW VRE system, this would be similar to two 50 kilometre long DTP-dams (each dam has an installed capacity of approx. 14.4 GW). It would be most efficient if the remaining 25% of installed capacity was comprised of offshore wind turbines. DTP's share in the efficient VRE portfolios and the VRE system's ability to meet demand even further increases when DTP is equipped with an integrated storage system to flatten its electricity output profile. To such an extent, that when DTP is equipped with a storage system, it becomes most efficient to comprise almost the entire VRE system out of DTP. To conclude, introducing two, geographically dispersed, DTP-dams (configuration C), but especially a DTP dam with an integrated storage system (configuration D), has a positive effect on a VRE system's ability to match supply and demand.



There is another reason why configuration C and D are more efficient than configuration A and B. From the sensitivity analysis (section 5.4.1) it was observed that in regards to configuration A and B, changing the VRE system's size has little to no effect on the amount of backup capacity that is required to ensure energy security. This means that even if an excessive amount of solar PV, wind or DTP were to be installed, the VRE system would not be able to cover electricity demand on its own. A relative large backup system will always be needed to cover the periods in which there is no solar irradiation, wind and/or tidal currents. Only when a second geographically dispersed DTP-dam (configuration C) or storage system (configuration D) is introduced, does the amount of backup capacity rapidly decrease when more capacity is installed. Hence, in the long-term, investments in two DTP-dams or a DTP-dam with storage system are more efficient to increase the VRE system's ability to meet demand.

The cost analysis shows that the energy generation costs of VRE systems without battery storage (A, B and C) are driven by the CCGT backup required to cover its residual load. More specifically, by the size of the CCGT backup system and the capacity factor of the CCGT. The backup system's size determines how heavily the CCGT costs weigh on the system's total energy generation costs. The capacity factor indicates how much electricity is produced per unit installed. It was found that when  $CO_2$  price is low (25  $\epsilon$ /ton  $CO_2$ ) VRE portfolios whose CCGT have a high capacity factor are most cost-efficient. But when the  $CO_2$  price (200  $\epsilon$ /ton  $CO_2$ ), and thus the marginal costs of the CCGT, increases, a decreasing capacity factor is most economical. This perfectly illustrates the fundamental idea behind the EU ETS that was described in section 3.3 - when the  $CO_2$  price increases due to a declining number of  $CO_2$  allowances, it becomes increasingly costly for  $CO_2$ -intensive generators to produce electricity.

On the other hand, configuration D's energy generation costs are primarily driven by the battery storage costs. As a result, configuration D is characterised by the highest energy generation costs, regardless of the CO<sub>2</sub> price and its portfolio composition. In terms of the costs, configuration D is followed by configuration B, and configuration A. Configuration B is most cost-efficient when comprised of; 60% solar PV, 5% offshore, 23% onshore wind and 12% DTP, and configuration B is most cost-efficient when comprised of 69% solar PV, 2% offshore wind and 29% onshore wind. When the CO<sub>2</sub> price inflates the share of offshore wind in scenario A and B slightly increases as it produces more electricity per unit installed and thus reduces the output from the CCGT. This result confirms that the model correctly translates CO<sub>2</sub> price incentives to the result. Configuration C is the most cost-efficient and its portfolio shares are not affected by changes in the CO<sub>2</sub> price. In fact, the portfolio shares that required the least backup capacity (75% DTP and 25% offshore wind), are also most cost-efficient.

As this study has shown that the size of the VRE system has little to no effect on the composition of the efficient VRE portfolios, above key findings are compared with The Netherlands' current VRE portfolio, even though it is smaller than the 35GW system that was optimised in this study. The Netherlands' current VRE mix (2020) is comprised of 61% solar PV (6874MW), 8% offshore wind (957 MW) and 31% onshore wind (3527 MW).

Hence, if DTP fails to enter the power generation market and The Netherlands relies on solar PV and wind to decarbonise its electricity market (scenario A), it would be most cost-efficient if investments were allocated to solar PV and onshore wind at the expenses of offshore wind. However, if the aim is to minimise the need for backup capacity the share of offshore wind should be increased dramatically (to 45%) and replace all the installed onshore wind capacity and a part of solar PV.

If DTP successfully penetrates the power generation market, this study has shown that investments in DTP increase the current VRE system's ability to meet demand and decrease its energy generation costs. From a costs perspective, the current VRE system would benefit most from the incorporation of two, geographically dispersed, DTP-dams. Especially when combined with offshore wind, in a 75:25 ratio. This configuration would also dramatically reduce the need for backup capacity. Although most costly, the need for backup capacity is minimised when a DTP-dam with an integrated storage system is introduced into the contemporary VRE system.



To conclude, there is no unequivocal VRE portfolio that is both most cost-efficient and requires the least backup capacity. Therefore, other aspects that were not included in this research should also be weighted before deciding whether a DTP-dam should be constructed or how much capital should be allocated to which VRE technology.

For a starter, the electricity balancing costs a VRE technology poses to the electricity system as a whole should be included in a more comprehensive way. This study did include the costs to connect VRE technologies to the existing grid and the costs to compensate for electricity deficiencies by means of a CCGT backup system. However, as elaborated in section 6.1.2, numerous other balancing costs, such as, the costs associated with; electricity curtailment and an international electricity grid were not included in this study. As these costs are expected to weigh heavily on the system's total energy generation costs when VRE penetration increases, they should be quantified and taken into account before any large investments in VRE technologies are made.

Another important costs aspect that should be taken into account was pointed out by De Llano-Paz et al. [23]. The transition from an inefficient to an efficient energy portfolio involves high costs, for which the MPT does not account. Hence, if one aims to significantly deviate from the current VRE investment trajectory, these costs have to be added to the system's total costs and included in the decision-making process. Transition costs could be avoided by setting constraints to the minimum or maximum amount of capacity installed of certain energy technologies. Such constraints were not included in this optimisation study,

Besides more sophisticated costs aspect, it is also important to include certain social aspects in the decision-making process. For example, investments in VRE result in the phase-out of conventional energy generators, which means that certain jobs will disappear. These people should be able to find work in the renewable energy industry or be retrained to work in other sectors. Besides the social impact this has on the people that are let go, this obviously also bears substantial costs. Moreover, social acceptance might play a significant role in the allocation of investments. The degree of social acceptance or the lack of it might favour certain VRE technologies even though they might not be most efficient or economical. Additionally, the effects of VRE technologies on other environmental aspects than CO<sub>2</sub>-emissions should be considered. For example, VRE technologies' impact on the ecology, the recyclability of amortised VRE installation and the environmental effects of the subtraction of minerals and other natural building materials required for the construction VRE installations.

That being said, several arguments supporting the notion that future investments should be allocated to offshore wind and two geographically dispersed DTP-dams. Firstly, the Netherlands aims to phase-out natural gas for heating, which will increase the use of electric HP. As the peaks in electricity consumption of electric HP (winter) coincidence with the peaks in electricity output from offshore wind, increased shares of offshore wind will enable the electricity system to better cope with the phase-out of natural gas. Secondly, offshore wind produces more electricity per unit installed and thus has the potential to abate more CO<sub>2</sub>. This will not only be increasingly important when CO<sub>2</sub> prices increase, the extra electricity might also be useful in the future to produce hydrogen. Thirdly, though a DTP-dam with storage system requires less backup capacity, its substantial energy generation costs make this configuration economical unviable in the contemporary power market. However, introducing two geographically dispersed DTP-dams reduces the need for backup capacity and the energy generation costs and is, therefore, a better alternative. Fourth, unlike a system comprised of solely solar PV and wind, in a VRE system that includes two geographically dispersed DTP-dams, increasing the VRE system's size rapidly declines the need for CO<sub>2</sub>-intensive backup capacity.



### 6.3 Market entry strategy Dynamic Tidal Power

The previous section concluded that DTP would positively affect the current VRE system's costs and the need for backup capacity. Hence, it would be beneficial for the transformation of The Netherlands' electricity system if DTP were to penetrate the energy generation market. Therefore, this section elaborates on some of DTP's strengths and weaknesses in order to increase DTP's chances of successfully entering the power generation market. It also provides some suggestions to highlight or tackle these strengths and weaknesses, which might help develop a market entry strategy. The content discussed in this section is based on information from people spoken with throughout this research process and knowledge obtained from this research and during the master's programme.

Firstly, it was found that two geographically dispersed dams are most cost-efficient. However, as a DTP-dam's efficiency increases exponentially with its length and a DTP-dam thus has to be tens of kilometres long, it is unlikely that two dams will be constructed simultaneously. However, equipping a single dam with a small battery storage system would result in a similar electricity output profile and only slightly increase the energy generation costs. In this research, two battery storage systems were used to offset all the deviations in electricity supply. The first battery system was used to offset the volatility caused by high and low tide, and the second to offset deviations due to neap and spring tide. However, if the latter storage system were to be eliminated, the output profile would be the same as if two geographically dispersed DTP-dams were constructed. Such a storage system would increase DTP's LCOE from 48.60 to 51.37 €/MWh.

Another alternative would be to oversize the storage system, so it could also compensate for deviations caused by other VRES. Actively matching supply and demand could also generate extra cashflows, as electricity can be stored when electricity prices are low and sold during peak hours when prices inflate.

However, such a storage system does not necessarily have to be comprised of batteries. A pumped hydropower storage lake in the North Sea might be an interesting alternative for battery storage. As visualised in figure 45, a pumped hydropower storage lake would require a watertight ringshaped dike in the North Sea that is approximately ten kilometres long and six kilometres wide.

When more VRE is produced than consumed or when the electricity prices are low, seawater is pumped from the lake into the surrounding sea. Subsequentially, when little renewable energy is produced and electricity prices are high, seawater flows back into the lake, driving a turbine that generates electricity. Hence, similar to a battery storage system, a pumped hydropower storage lake can be used to match supply and demand and mitigate curtailment costs.

A lake with a surface of 40 square kilometres and a depth of 32 to 40 meters could store 20,000 MWh of electricity [81]. A 50 kilometres DTP-dam in the open North Sea with an installed capacity of 14,4GW would require 13,824 MWh storage capacity (0.96 MWh/MW installed, appendix A) to offset the volatility in the electricity output caused by high and low tide. Hence, a pumped hydropower storage lake could theoretically offset DTP's volatility in electricity output caused by high and low tide, which would result in a similar output profile as if two geographically dispersed dams were to be deployed.

However, in the current design, the pumped hydropower storage lake's installed capacity is 1,500MW, which is not enough to compensate for the volatility caused by high and low tide. However, when the lake is full, it can generate 1,500MW for at least 12 consecutive hours [81]. Therefore, a pumped hydropower storage lake seems to be more suitable for long term storage, for example, to partly offset DTP's volatility in electricity output caused by neap and spring tide or to store wind energy to compensate for wind-droughts. Unlike battery storage systems, a pumped hydropower storage lake enables sector coupling and is characterised by several positive externalities. So could the storage lake and its surrounding dam facilitate residentials, tourism, fish farming and agriculture [81].





Figure 45: visualisation of a pumped hydropower storage lake in the North Sea [81].

DTP's size also results in strengths and weaknesses that are unrelated to the electricity market. So does its size allow for sector coupling; the Y-shaped ends of the dam could be used for seafaring, or a road on the dam could be used to access a the potential offshore expansion of Schiphol airport. Moreover, wind turbines could be built on top of the dam, or the dam could be used as a base from which maintenance on offshore wind farms is carried out.

The downside of its bulky size is that it is likely that the a DTP-dam greatly affects the surrounding ecology, morphology and shipping. Additionally, due to its size, DTP's overnight capital costs are substantial, which, in combination with its novelty, makes it questionable whether market parties in The Netherlands' liberal electricity market are willing to invest in DTP. Similar issues are, for example, observed in regards to the construction of nuclear power plants. Market parties seem to be inclined to invest in proven renewable technologies, such as; wind and solar PV.

However, while these weaknesses could be tackled by doing excessive research, there is a social issue that is more difficult to address, namely, the social acceptance of DTP. Over the course of the past few years, fierce resistance against numerous renewable energy projects has emerged. Due to its size, possible effects on the local (marine) environment and the fact that a DTP-dam hampers numerous other activities deployed on the North Sea (e.g. fishing, shipping and recreation), it is expected that DTP will also encounter fierce resistance. Therefore, this issue might require more attention than is currently paid to it.

Therefore, as a final note, this research would like to suggest two possible ideas that might increase the social acceptance of DTP. First, it could help to have someone who is known in the media to advocate for DTP. Not only will this start the discussion about DTP, it can also help to move DTP up the political agenda. A colleague from the Ministry of Infrastructure and Water Management (Rijkswaterstaat), suggested to get Ed Nijpels, former politician, involved.

Secondly, a study [82] in Germany has proven that co-ownership significantly increases the social acceptance of renewable energy projects. By comparing two wind farms in East Germany villages, the social acceptance regarding wind energy was measured through a survey. In Zschadraß, a wind park was for 20% owned by community organisations, while in Nossen the wind farm was owned by 54 individual stockholders, of whom only two lived in Nossen. The researchers found that 62% of the people in Zschadraß were positive towards the local wind farm, opposed to 26% in Nossen [82]. Perhaps co-ownership could also mitigate the potential social resistance against DTP. Parties that might be interested in co-ownership are; the Dutch government, community organisations, climate organisations, power plant constructors, or even commercial companies aiming for a sustainable image. Afterall, who does not want to be the co-owner of the world's first DTP-dam.



#### 7 Conclusion and recommendations

This chapter first provides the answers to the research questions presented in section 1.3 and the conclusions drawn from this study. Subsequentially, section 7.2 provides recommendations and suggestions for future research.

#### 7.1 Conclusion

To keep global warming well below 2°C above pre-industrial levels, The Netherlands aims to reduce its CO<sub>2</sub>-emissions and decarbonise its power generation industry. To bring about this transition, CO<sub>2</sub>-intensive energy generators have to be phased out and replaced by renewables. Currently, investments aiming to decarbonise the power generation industry are predominately allocated to solar PV, offshore wind and onshore wind. But due to the development of Dynamic Tidal power (DTP), The Netherlands might soon be able the harvest the currently unutilised North Sea's tidal currents to generate clean electricity. However, the intermitted nature of solar irradiation, wind speeds, and tidal currents makes it increasingly difficult and costly to match demand and supply as their penetration in the electricity mix increase.

Therefore, this research's main objective was to determine the efficient portfolios of solar PV, offshore wind, onshore wind, and DTP to meet electricity demand. This research also asked how including DTP affects The Netherlands' current VRE system's efficiency to meet electricity demand. To achieve these objectives a modified version of the Modern Portfolio Theory (MPT) was used. The MPT was modified by including demand-variability, something that had not been done before. Hence, by assessing to what extent including demand variability in the MPT affects the selection of efficient VRE portfolios, this study filled a gap in the literature.

Firstly, it is concluded that DTP improves The Netherlands' current VRE system's efficiency to meet demand. DTP penetration curtails the number of hours in which little to no electricity is generated by the VRE system, which diminishes the need for dispatchable backup capacity. This effect is significantly enhanced when a second, geographically dispersed, DTP-dam is introduced into the electricity system. A second dam mitigates the deviation in electricity supply caused by high and low tide and thus reduces the need for backup capacity. A DTP-dam with an integrated storage system eliminates all deviations in electricity supply, which maximises DTP's positive effect on a VRE system's ability to meet demand.

Depending on its technical configuration, DTP also positively affects the current VRE system's energy generation costs. The inclusion of a single DTP-dam has a moderate cost-reducing effect. This cost reduction is driven by the declining amount of backup capacity required to ensure energy security and the more consistent electricity output from the backup system. However, it is most cost-efficient to introduce two, geographically dispersed, DTP-dam into the current VRE system. On the other hand, a DTP-dam with a battery storage system large enough to offset all the deviations in electricity supply would significantly increase the current VRE system's energy generation costs. This this due to the fact that battery storage costs are currently still substantial.

Regarding the question of which portfolios shares of solar PV, offshore wind, onshore wind, and DTP are most efficient to meet electricity demand, there is no unequivocal conclusion. From a costs perspective, a VRE portfolio comprised of (two) geographically dispersed DTP-dams, and offshore wind in a 75:25 ratio would be most efficient to meet demand. However, in terms of the amount of dispatchable backup capacity a system requires to ensure electricity security, a system comprised entirely of DTP with an integrated battery storage system is most efficient. Hence, to make a weighted decision regarding the allocation of capital to VRE technologies, aspects not investigated in this research, such as, the costs associated with electricity surplus, the degree of social acceptance, and the environmental and ecological effects should also be included.



From the three different demand scenarios for which the VRE portfolios were optimised, it is concluded that including demand-variability in the MPT has a limited effect on the selection of efficient VRE portfolios. In a scenario with increased peak loads due to an extreme penetration of electric vehicles (EV) and heat pumps (HP), the efficient VRE portfolios tend to be characterised by slightly larger offshore wind shares. This is because peak demands of HP coincide with peak outputs from offshore wind turbines. Apart from that, demand-variability has little effect on the composition of efficient VRE portfolios. The variability in electricity demand is relatively limited in relation to the volatility in electricity outputs from VRES. Hence, selecting efficient VRE portfolios predominately revolves around finding energy technologies that minimise the deviation in electricity supply when combined in a portfolio.

However, demand-variability does affect the amount of dispatchable backup capacity a VRE portfolio requires to ensure energy security. When electricity demand is better distributed, and the demand profile flattens, the required dispatchable backup capacity dwindles.

### 7.2 Recommendations and suggestions for future research

This section lists some recommendations and suggestions for future research, which are derived from both this report and the relevant literature that was reviewed for this study.

Firstly, this study treated the Netherlands as a closed energy system and did not include electricity transmission among neighbouring countries. To assess its effect on the need for backup capacity, it would be interesting if future research were to increase the scope and include cross-border electricity trading. Increasing the scope would also allow for the inclusion of geographically dispersed solar PV and wind farms, which might increase the systems' ability to meet demand.

In terms of the electricity output from VRE, this study only included a single scenario. To increase the results' robustness, it would be valuable if future research were to include multiple supply scenarios. One aspect recommended to include is the effect of climate change on the output from VRE technologies. Additionally, future research should also include forecasted cost reductions due to learning effects, economies of scale and technical innovations. Including different economic scenarios would increase the sustainability and timelessness of the results.

To find the most efficient VRE portfolios, the total amount of installed VRE capacity was restricted (35GW) in this study, and the aim was to optimise its distribution among different energy generation technologies. However, it would be interesting if future research applying a similar methodology would consider different or additional constraints. For example, a limitation on the total amount capital invested in a VRE system or an average capacity factor that must be met by the VRE system.

Additionally, future research aiming to include demand-variability in the MPT should deviate the demand profiles by either increasing the mean load or the shape of the load profile. Simultaneously changing both the mean load and the shape of the load profile has proven to make it difficult to interpret the results.

One of the limitations of the methodology used was that it overestimated the backup system's size when the level of energy security was increased. Future research could aim to improve this methodology or develop a more sophisticated approach to estimate the size of the required backup system.

In this study, it was found that the shape of the electricity demand curve has a limited effect on the composition of the efficient VRE portfolios. Therefore, when the aim is to find efficient VRE portfolios, it is recommended to primarily focus on comprising portfolios that include energy technologies whose electricity outputs negatively correlate.



It is recommended that the DTP-foundation focuses on the development of a DTP-dam that offsets the volatility in electricity supply caused by high and low tide. This can be achieved by deploying two geographically dispersed dams whose electricity outputs negatively correlate or by introducing a small storage system. The development of a DTP-dam with a battery storage system large enough to offset all variability in electricity output (high/low tide and neap/spring tide) is discouraged, as battery storage costs are currently still too high.

In regards to the storage system, this study only included a battery storage system. As there are numerous other storage systems (e.g. a pumped hydropower storage lake), future research should also assess the viability of a DTP-dam in combination with other means of electricity storage. Additionally, this study's battery storage system was solely used to offset the deviation in electricity supply from the DTP-dam. However, as such a system could also be used to actively match supply and demand and generate extra cashflows, future research should include an autonomous storage system and assess its viability.

And finally, to enrich the discussion-making process regarding the allocation of investments to VRE technologies, future research should aim to quantify all the balancing costs (e.g. electricity curtailment, grid expansion and storage systems) attributed to specific VRE technologies. These costs, in combination with the costs to switch over from an inefficient to an efficient energy portfolio, should also be included in the decision-making process before investments in VRE technologies are made.

In line with this, future research could focus on developing a pricing mechanism, similar to a carbon-pricing system, that ensures that VRE generators are financially held accountable for the balancing costs they impose on the system. This would ensure that negative externalities (balancing services) imposed on third parties (the TSO) are remunerated and might also encourage technical innovations aiming to reduce the need for balancing services



## 8 Personal reflection and acknowledgements

This thesis research has allowed me to perform my own research, which has taught me many things, some of which I would like to share in this section. As I could not have done this research without some people, I would also like to take this opportunity to gratefully thank them.

My thesis research preparation started as early as in December 2019, when I got in touch with Bas Jonkman and Walther Walraven for the first time to discuss the possibility to write my thesis about Dynamic Tidal Power. Thanks to them my enthusiasm for DTP was fueled, and even after writing so much about it I am still greatly interested in it. In March, when I returned from my Erasmus programme, the aim was to start with my thesis straight away. However, a frustrating period followed as it was rather difficult to gather a graduation commission in the middle of a pandemic. I experienced it to be quite challenging to get in touch with the right professors, not being able to meet face-to-face as the greatest barrier. However, after several changes in my graduation commission, I eventually got my kick-off form signed and could officially start.

Since that moment, it was quite a smooth process. Contact with my first, second and external supervisor was good, and I have the feeling that we really established a relation of the past six months. I really enjoyed the weekly meetings with Rob Stikkelman. He looked at things from a different perspective than I do myself, which really helped me to increase my thesis's overall quality. Working and studying from home; it was pleasant to also be able to talk about other things than my thesis during our weekly meetings. Therefore, I would like to gratefully thank Rob Stikkelman for all the guidance he provided and the time he invested in me and my research. I am also pleased with the way in which Enno Schröder helped me, especially in regards to a units issue in my thesis. Though not being my first supervisor, he spent quite some time helping me, for which I would like to thank him.

Having Bas Jonkman and Walther Walraven involved in my research process brought so much knowledge and two whole different perspectives to the table. Both really helped me grasp the idea behind DTP and provided me with so much relevant information and indispensable data. Regarding the latter, I would like to thank Walther Walraven in particular; he provided most of the DTP data used in this study.

Though I am sure that all the different perspectives on my research have increased the quality, I also experienced it to be quite challenging from time to time. Everyone had its own perspective on my research, and I was sometimes struggling to choose which trajectory to follow. This has also taught me to be more direct in my communication and better manage expectations. In line with this, if I were to do a similar research again, I would probably choose to either develop a new methodology or include a novel technology. Doing both simultaneously in one study perhaps made the scope too large. From a more practical standpoint, it also resulted in quite the workload, especially since I also worked for the Dutch government (Rijkswaterstaat) throughout the process. Apart from that, I feel that I have acquired so much new knowledge, not only about the electricity market, DTP or modelling but also how to conduct a proper scientific research and how to defend your research choices.

Last but not least, I would like to thank my family and friends for the mental support. Having people around me with whom I could share successes and difficult moments really helped me.



## References

- [1] Business Wire, [Online]. Available: https://mms.businesswire.com/media/20170619006072/en/593434/5/SterlingWilsonImage.j pg?download=1 . [Accessed 15 02 2021].
- [2] Paint, [Online]. Available: https://www.paint.org/wp-content/uploads/2020/01/josh-spires-dronenr-70R6ZJ0XGXg-unsplash-scaled.jpg. [Accessed 15 02 2021].
- [3] EL-PRO-CUS, [Online]. Available: https://www.elprocus.com/types-and-working-functionality-of-hydroelectric-energy-power-plants/. [Accessed 15 02 2021].
- [4] M. O. D. W. S. F. A.-D. W. C. S. H. M. K. J. K. N. M. Y. M. R. P. M. W. a. K. Z. Allen, "Framing and Context," in Global Warming of 1.5°C. An IPCC Special Report on the impacts of global warming of 1.5°C above pre-industrial levels and related global greenhouse gas emission pathways, in the context of strengthening the global response to the threat of climate changet, In Press, 2018, p. 51.
- [5] I. Dincer and A. Abu-Rayash, "Chapter 1 Fundamental aspects of energy, environment, and sustainability Author links open overlay panelIbrahimDincer," *Energy Sustainaility*, pp. 1-18, 2020.
- [6] CBS, "Uitstoot broeikasgassen 3 procent lager in 2019," 07 05 2020. [Online]. Available: https://www.cbs.nl/nl-nl/nieuws/2020/19/uitstoot-broeikasgassen-3-procent-lager-in-2019. [Accessed 11 2020].
- [7] Rijksoverheid, "Meer duurzame energie in de toekomst," 15 07 2020. [Online]. Available: https://www.rijksoverheid.nl/onderwerpen/duurzame-energie/meer-duurzame-energie-in-de-toekomst. [Accessed 08 2020].
- [8] CBS, "Elektriciteit en warmte; productie en inzet naar energiedrager," 23 06 2020. [Online]. Available: https://opendata.cbs.nl/statline/#/CBS/nl/dataset/80030NED/table?fromstatweb. [Accessed 16 10 2020].
- [9] G. Lavidas and H. Polinder, "Wave energy in the Netherlands: Past, Present and Future perspectives," in *Proceedings of the 13th European Wave Energy and Tidal Conference (EWTEC 2019)*, Napels, 2019.
- [10] A. Owen, "Chapter 16: Tidal Current Energy: Origins and Challenges," in *Future Energy*, vol. 2, Aberdeen, 2014.
- [11] E. Segura, R. Morales and J. Somolinos, "A strategic analysis of tidal current energy conversion systems in the European Union," *Applied Energy*, vol. 212, pp. 527-551, 08 12 2017.
- [12] Sustainable Energy Ireland (SEI), "Tidal & Current Energy Resources in Ireland," Glasnevin.
- [13] K. Haas and Z. Define, "So What? Tidal Stream Resource Potential," Berau of Ocean Energy Management.
- [14] E. van Druten and K. Kruit, "Perspectieven elektriciteit uit water," Deventer, 2019.
- [15] Z. William, M. Junginger and M. van den Broek, "Is a 100% renewable European power system feasible by 2050?," *Applied Energy*, pp. 1027-1050, 12 09 2018.
- [16] W.-P. Schill, "Residual load, renewable surplus generation and storage requirements in Germany," *Energy Policy*, vol. 73, pp. 65-79, 10 2014.
- [17] S. Awebuch, "Portfolio-Based Electricity Generation Planning: Implications for Renewables and Energy Security," *Mitigation and Adaptation Strategies for Global Change*, vol. 11, 04 2004.
- [18] J. Cunha and P. Ferreira, "Designing electricity generation portfolios using the meanvariance approach," *International Journal of Sustainable Energy Planning and Management*, vol. 04, 27 02 2015.
- [19] J. Berk and P. DeMarzo, "Chapter 11: Optimal Portfolio Choice and the Capital Asset Pricing Model," in *Corporate Finance: The Core*, vol. 4, Harlow, Essex: Pearson Education Limited, 2016.



- [20] C. Janse van Vuren, H. Vermeulen and M. Groch, "Optimal Siting of Wind Energy Capacity for Minimum Residual Load Variance," in *International Conference on Power and Energy Systems (ICPES)*, Perth, 2019.
- [21] ENTSO-E, "Electricity Market Transparency," [Online]. Available: https://www.entsoe.eu/data/transparency-platform/. [Accessed 11 2020].
- [22] H. Markowitz, "Portfolio selection," Journal of Finance, vol. 7, pp. 77-91, 1952.
- [23] F. De Llano-Paz, A. Calvo-Silvosa, S. I. Antelo and I. Soares, "Energy planning and modern portfolio theory: A review," *Renewable and Sustainable Energy Reviews*, vol. 77, 28 04 2017.
- [24] J. Berk and P. DeMarzo, "Chapter 3: Financial Decision Making and the Law of One Price," in *Corporate Finance: The Core*, vol. 4, Harlow, Essex: Pearson Eduction Limited, 2016.
- [25] J. Berk and P. DeMarzo, "Chapter 10: Capital Markets and Pricing of Risk," in *Corporate Finance: The Core*, vol. 4, Harlow, Essex: Pearson Eduction Limited, 2016.
- [26] L. Zhu and Y. Fan, "Optimization of China's generating portfolio and policy implications based on portfolio theory," *Energy*, vol. 35, pp. 1391-1402, 04 2010.
- [27] E. Elton, M. Gruber, S. Brown and W. Goetzmann, in *Modern Portfolio Theory and Investment Analysis*, John Wiley & Son, 2010.
- [28] D. Bar-Lev and S. Katz, "A portfolio approach to fossil fuel procurement in the electric utility industry," *J Finance*, vol. 3, pp. 933-947, 1976.
- [29] G. Allan, I. Eromenko, P. McGregor and K. Swales, "The regional electricity generation mix in Scotland: a portfolio selection approach incorporating marine technologies. Energy Policy," *Energy Policy*, vol. 39, pp. 6-22, 2011.
- [30] G. Escribano Francés, J. M. Marín-Quemada and E. San Martín González, "RES and risk: Renewable energy's contribution to energy security. A portfolio-based approach," *Renewable and Sustainable Energy Reviews*, vol. 26, pp. 549-559, 2013.
- [31] J. Stempien and S. Chan, "Addressing energy trilemma via the modified Markowitz Mean-Variance Portfolio Optimization theory," *Applied Energy*, vol. 202, pp. 228-237, 2017.
- [32] L. Losekann, G. Marreco, F. Ramos-Real and E. Almeida, "Efficient power generating portfolio in Brazil: Conciliating cost, emissions and risk," *Energy Policy*, vol. 62, pp. 301-314, 11 2013.
- [33] Y. S. Awerbuch S., "Efficient electricity generating portfolios for Europe: maximising energy security and climate change mitigation," *European investment bank papers*, vol. 12, pp. 8-37, 2007.
- [34] O. H. O. M. Doherty R., "Generation portfolio analysis for a carbon constrained and uncertain future," *Elsevier*, pp. 150-165, 2008.
- [35] C. de Jonghe, E. Delarue and W. D'haeseleer, "Determining optimal electricity technology mix with high level of wind power penetration," *Applied Energy*, pp. 2231-2238, 2011.
- [36] F. Roques, C. Hiroux and M. Saguan, "Optimal wind power deployment in Europe A portfolio approach," *Energy Policy*, vol. 38, pp. 3245-3256, 2010.
- [37] Y. Rombauts, E. Delarue and W. D'haeseleer, "Optimal portfolio-theory-based allocation of wind power: taking into account cross-border transmission-capacity constraints," *Renewable Energy*, vol. 9, pp. 2374-2387, 2011.
- [38] M. Arnesano, A. Carlucci and D. Laforgia, "Extension of portfolio theory application to energy planning problem The Italian case," *Energy*, vol. 39, pp. 112-124, 04 2012.
- [39] F. DeLlano-Paz, F. Inglesias, S. Calvo and I. Soares, "The European Low-Carbon Mix for 2030: the role of renewable energy sources in an environmentally and socially efficient approach," *Renewable Sustainable Energy Review*, vol. 48, pp. 49-61, 2015.
- [40] S. A., "A general framework for analyzing diversity in science, technology and societ," *Journal of The Royal Society Interface*, vol. 15, pp. 707-20, 2007.
- [41] S. A., "Diversity and ignorance in electricity supply investment: addressing the solution rather than the problem," *Energy Policy*, vol. 3, pp. 195-216, 1994.
- [42] ,. W. J. Huang Y.H., "A portfolio risk analysis on electricity supply planning," *Energy Policy*, vol. 36, pp. 627-41, 2008.



- [43] George and Mallery, SPSS for Windows Step by Step: A Simple Guide and Reference 17.0 Update., 2010.
- [44] J. Aldersey and T. Rubert, "Levelised cost of energy A theoretical justification and critical assessment," *Energy Policy*, vol. 124, pp. 169-179, 2019.
- [45] Rijksoverheid 2, "Wind op zee," 2020. [Online]. Available: https://www.rijksoverheid.nl/onderwerpen/duurzame-energie/windenergie-op-zee.
- [46] Rijksoverheid 3, "Overheid bevordert groei zonne-energie," 2020. [Online]. Available: https://www.rijksoverheid.nl/onderwerpen/duurzame-energie/zonne-energie.
- [47] "Model Evaluation Methods," [Online]. Available: http://hydropedia.blogspot.com/2014/06/model-evaluation-methods.html. [Accessed 11 2020].
- [48] J. Horten, "How Ocean Currents Work," [Online]. Available: https://science.howstuffworks.com/environmental/earth/oceanography/ocean-current4.htm. [Accessed 11 2020].
- [49] National Ocean Service Education (NOAA), "Welcome to Tides and Water Levels," 2004.
- [50] Rijkswaterstaat, "Getij," [Online]. Available: https://www.rijkswaterstaat.nl/water/waterdata-en-waterberichtgeving/waterdata/getij/index.aspx. [Accessed 11 2020].
- [51] A. McLachlan and A. Brown, "The Physical Environment," in *The Ecology of Sandy Shores*, vol. 2, Academic Press, 2006.
- [52] J. Sündermann and T. Pohlmann, "A brief analysis of North Sea physics," *Oceanologia*, vol. 3, no. 53, pp. 663-689, 17 09 2014.
- [53] National Ocean Service, "Tidal Currents 1," [Online]. Available: https://oceanservice.noaa.gov/education/tutorial\_currents/02tidal1.html. [Accessed 11 2020].
- [54] Dynamic Tidal Power, "Kengetallen," [Online]. Available: https://www.dynamictidalpower.eu/DTP-ontwikkeling/SWOT/Kengetallen/index.html. [Accessed 11 2020].
- [55] K. Hulsbergen, R. Steijn, G. van Banning, G. Klopman and A. Fröhlich, "Dynamic Tidal Power (DTP) A new approach to exploit tides," in *2nd International Conference on Ocean Energy*, Brest, France, 2008.
- [56] L. Qlulln, "Hydrodynamic Study of Phase-Shift Power System wit Y-Shaped Dams," *Journal of Hydraulic Research*, 27 08 2015.
- [57] W. Walraven, Interviewee, *Email contact about battery storage system*. [Interview]. 12 10 2020.
- [58] T. Boßmann, B. Pfuger and M. Wietschel, "The shape matters! How structural changes in the electricity load curve affect optimal investments in generation capacity," in *International Conference on the European Energy Market*, Stockholm, 2013.
- [59] UK Power Networks, "Impact of Electric Vehicle and Heat Pump Loads on Network Demand Profiles," 2014.
- [60] CBS, "Number of all-electric cars has doubled," 10 05 2019. [Online]. Available: https://www.cbs.nl/en-gb/news/2019/19/number-of-all-electric-cars-has-doubled. [Accessed 11 2020].
- [61] T. Manders and C. Kool, "Nederland in 2030 en 2050: Twee referentiescenario's," Den Haag, 2015
- [62] CBS, "Motorvoertuigenpark; inwoners, type, regio, 1 januari," 26 06 2019. [Online]. Available: https://opendata.cbs.nl/statline/#/CBS/nl/dataset/7374hvv/table?fromstatweb. [Accessed 11 2020].
- [63] O. Kleefkens, "Status Rapportage Warmtepompen".
- [64] P. A. Østergaard, F. M. Andersen and P. S. Kwon, "Energy Systems Scenario Modelling and Long Term Forecasting of Hourly Electricity Demand," *International Journal of Sustainble Energy Planning and Management*, vol. 7, pp. 99-116, 2015.



- [65] H. C. Gils, "Assessment of the theoretical demand response potential in Europe," *Energy*, vol. 67, pp. 1-18, 2014.
- [66] Federal Energy Regulation Comission, "2010 assessment of demand response and advance metering," Washington DC, 2011.
- [67] L. Beurkens, J. Lemmers and H. Elzenga, "CONCEPTADVIES SDE++ 2020: Zonne-energie," Planbureau voor de Leefomgeving, The Hague, 2019.
- [68] Algemene Rekenkamer, "Kosten wind op zee," Algemene Rekenkamer, The Hague, 2018.
- [69] E. Mast and I. Pisca, "CONCEPTADVIES SDE++ 2020; Windenergie op land," The Hague, 2019.
- [70] A. van Dril and H. Elzenga, "Referentieraming Energie en Emissies 2005-2020," Enegieonderzoek Centrum Nederland, 2005.
- [71] ENCO, "Possible Role of Nuclear in the Dutch Energy Mix in The Future," ENCO, 2020.
- [72] W. Walraven, Interviewee, Question asked by email. [Interview]. 14 01 2021.
- [73] A. Seebregts, H. Snoep, J. van Deurzen, S. Lensink, A. van der Welle and W. Wetzels, "Brandstofmix elektriciteit 2020," Energieonderzoek Centrum Nederland, 2009.
- [74] European Commission, [Online]. Available: https://ec.europa.eu/clima/policies/ets\_en. [Accessed 01 2021].
- [75] Ember, "Carbon Price Viewer," [Online]. Available: https://ember-climate.org/data/carbon-price-viewer/. [Accessed 09 01 2021].
- [76] H. Vreuls, "The Netherlands: list of fuels and standard CO2 emission factors," Steering Group for Emissions Registration, 2005.
- [77] L. Bird, J. Cochran and X. Wang, "Wind and Solar Energy Curtailment: Experience and Practices in the United States," 2014.
- [78] C. Curry, "Lithium-ion battery costs & market squeezed margins seek technology improvements and new business models," Bloomberg New Energy Finance, 2017.
- [79] IRENA, "Global energy transformation: A roadmap to 2050," International Renewable Energy Agency, Abu Dhabi, 2019.
- [80] IRENA, "FUTURE OF WIND," 2019.
- [81] Deltares, 17 05 2019. [Online]. Available: https://publicwiki.deltares.nl/display/KWI/6.3.2.1.+Energie-eiland+in+de+Noordzee. [Accessed 15 02 2021].
- [82] F. D. Musall and O. Kuik, "Local acceptance of renewable energy—A case study from southeast Germany," *Energy Policy*, vol. 39, p. 3252–3260, 8 03 2011.
- [83] Greener 4 life, "Dynamic Tidal Power: An Amazing Reliable Energy," 2019. [Online]. Available: https://greener4life.com/Blog/Dynamic-Tidal-Power-An-Amazing-Reliable-Energy. [Accessed 11 2020].
- [84] "What are the differences between one-tailed and two-tailed tests?," [Online]. Available: https://stats.idre.ucla.edu/other/mult-pkg/faq/general/faq-what-are-the-differences-between-one-tailed-and-two-tailed-tests/. [Accessed 11 2020].
- [85] "Normal Distribution," [Online]. Available: http://my.ilstu.edu/~gjin/hsc204-eh/Module-5-Summary-Measure-2/Module-5-Summary-Measure-29.html. [Accessed 11 2020].
- [86] R. Dalrymple, "Tidal Depositional System," in Facies Models: Response to Sea Level Changes, St. John's, Nfld., 1992.
- [87] G. Francés, J. Marín-Quemada and E. González, "RES and risk: Renewable energy's contribution to energy security," *A portfoliobased approach, Renewable and Sustainable Energy Reviews*, vol. 26, pp. 549-559, 10 2013.
- [88] A. Bhattacharya and S. Kojima, "Power sector investment risk and renewable energy: A Japanese case study using portfolio risk optimization method," *Energy Policy*, vol. 40, pp. 69-80, 01 2012.
- [89] E. Delarue, C. Jonghe, R. Belmans and W. D'haeseleer, "Applying portfolio theory to the electricity sector: Energy versus power," *Energy Economics*, vol. 88, 2011.



- [90] CBS, 29 07 2020. [Online]. Available: https://opendata.cbs.nl/statline/#/CBS/nl/dataset/82610NED/table?dl=1ACA6. [Accessed 11 2020].
- [91] Kalender 365, "Maankalender december 2019," [Online]. Available: https://www.kalender-365.nl/maankalender/2019/december.html. [Accessed 11 2020].
- [92] P. Wang, "Minimum-Variance Portfolio and Monte Carlo Simulation on Selected Stocks' Returns," University of Connecticut, 10 12 2016. [Online]. Available: http://datascience.uconn.edu/index.php/projects/students-work/item/51-minimum-variance-portfolio-and-monte-carlo-simulation-on-selected-stocks-returns. [Accessed 30 10 2020].
- [93] V. N. Gudivad, "Chapter 2: Data Analystics: Fundamentals," *Data Analytics for Intelligent Transportation Systems*, pp. 31-67, 7 04 2017.
- [94] Rijksoverheid, "meer-duurzame-energie-in-de-toekomst," 2020. [Online]. Available: https://www.rijksoverheid.nl/onderwerpen/duurzame-energie/meer-duurzame-energie-in-de-toekomst. [Accessed 07 2020].
- [95] Rijksoverheid 1, "Klimaatbeleid," 2020. [Online]. Available: https://www.rijksoverheid.nl/onderwerpen/klimaatverandering/klimaatbeleid.
- [96] Wärtsilä, "Combustion engine vs gas turbine ramp rate," [Online]. Available: https://www.wartsila.com/energy/learn-more/technical-comparisons/combustion-engine-vs-gas-turbine-ramp-rate. [Accessed 20 01 2021].
- [97] R. Sharma, "Skewed data a problem to your statistical model," 30 07 2019. [Online]. Available: https://towardsdatascience.com/skewed-data-a-problem-to-your-statistical-model-9a6b5bb74e37. [Accessed 25 01 2021].
- [98] O. C. Ibe, Fundamentals of Applied Probability and Random Processes, 2014.
- [99] KIVI Engineering Society, "Dynamic Tidal Power," 2008. [Online]. Available: https://www.kivi.nl/afdelingen/regio-utrecht/activiteiten/activiteit/dynamic-tidal-power. [Accessed 10 02 2021].
- [100] L. Hoekstra, "Dynamic Tidal Power: golven zorgen voor duurzame energie," 27 02 2020. [Online]. Available: https://www.detechniekachternederland.nl/article/energie/gebruik-duurzame-energie/dynamic-tidal-power-golven-voorzien-nederland-van-duurzame-energie. [Accessed 10 02 2021].
- [101] Dutch Water Sector, 23 12 2013. [Online]. Available: https://www.dutchwatersector.com/news/power-group-enters-crucial-phase-with-feasibility-study-for-large-dynamic-tidal-power-in-china. [Accessed 15 02 2021].



## Appendix A: Battery system DTP

To manually calculate the size and lifetime of the battery system required to flatten out DTP's electricity output, the battery system will be divided into two systems. The first system is used to offset the fluctuation in electricity output as a result of high and low tide which is caused by the rotations of earth. The second battery system stores electricity during spring tide to discharge it in during neap tide in order to offset the fluctuation in electricity output caused by the orbiting of the moon. Both systems together will create a consistent flow of electricity. For this calculation the following input parameters visualised in table 12 were used.

Table 12: input parameters for battery storage calculation

Input parameters battery system		
Lifetime battery [charging cycles] 18,000 [54		
Capacity factor DTP	$0,32^{1}$	

<sup>&</sup>lt;sup>1</sup>Derived from electricity output data provide by the DTP foundation.

#### Battery system 1: to offset daily fluctuation in electricity output caused by high and low tide

According to the DTP foundation a battery system to offset the fluctuations of high and low tide should have a size of 12,5% of the daily electricity output [54]. Hence, the battery system should need to have a size of;

Daily electriity output = 
$$0.32 * 24h = 7.68 \frac{MWh}{MW installed}$$

Size battery system = 
$$7.68 \text{ MWh} * 12\% = 0.96 \frac{\text{MWh}}{\text{MW installed}}$$

Based on 4 charging cycles per day (fig. 46), the battery's lifetime is;

$$Lifetime\ battery\ system = \frac{18,000}{4*365} = 12.33\ years$$

So, the battery system should have a size of 0.96 MWh per MW of DTP installed and has a lifetime of 12 years.

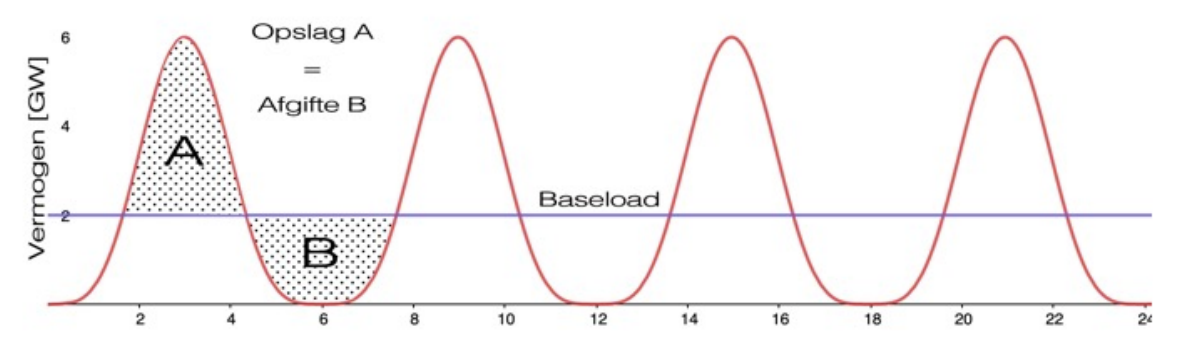


Figure 46: visualisation of the storage system to offset the fluctuations in electricity output caused by high and low tide [54].



#### Battery system 2: to offset daily fluctuation in electricity output caused by spring and neap tide

The size of the battery system in relation to its production has not been determined by the DTP foundation yet. Hence, this will be calculated manually using the electricity output data provided by the DTP foundation. Figure 47 represents the electricity output curve after the daily fluctuations have been flattened out due to battery system 1. The red line represent the capacity factor of a DTP-dam after the its electricity output has been flattened. The blue line is a DTP-dam's average capacity factor. The aim to compute the area between the red and blue line; that is the amount of electricity that needs to be stored and discharged.

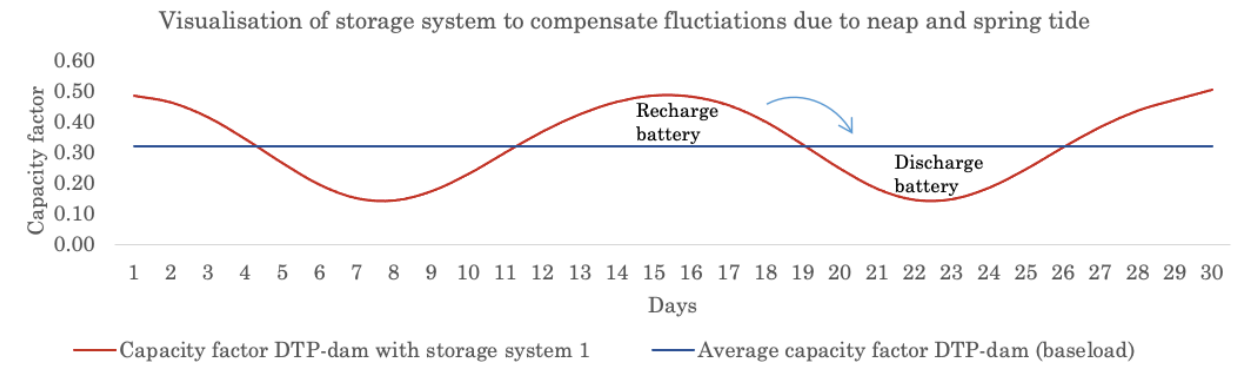


Figure 47: visualisation of the storage system to offset the fluctuations in electricity output caused by neap and spring tide.

Table 13 represent the daily capacity factors that are visualised in figure 47. The orange shaded rows is the area underneath the red line and above the blue line, during which the battery is discharging its electricity to compensate neap tide. The green shaded cells is the area above the red line and underneath the bleu one, during which the battery is recharging.

The cumulative area underneath the graph is 0.79 MW/MW installed. As each day has 24 hours, the total area underneath the red line, and size of the battery system, is;

Size battery system = 
$$0.79 * 24h = 18.96 \frac{MWh}{MW Installed}$$

So the size of the storage system to offset the fluctuations in electricity output caused by spring and neap tide should be 18.86 MWh per MW of DTP installed. As can be seen in figure 47, the system has 2 charging cycles per 29,5 days (moon cycle). Hence, the lifetime of the battery will be long enough to cover the 60 years lifetime of the dam.



Table 13: daily capacity factors of a single DTP -dam for one moon-cycle (29,5 days). The green shaded rows mark the values above the mean capacity factor and the red shaded rows the values below the mean capacity factor.

	Day	Capacity factor DTP- dam with storage system 1	Average capacity factor DTP-dam (baseload)	Area under/above graph	Cumulative area under/above graph
	1	0.48	0.32	0.16	
	2	0.46	0.32	0.14	
	3	0.41	0.32	0.09	
	4	0.34	0.32	0.02	
Discharging	5	0.26	0.32	-0.06	-0.79
electricity	6	0.19	0.32	-0.13	
from storage	7	0.15	0.32	-0.17	
system	8	0.14	0.32	-0.18	
	9	0.17	0.32	-0.15	
	10	0.23	0.32	-0.09	
	11	0.30	0.32	-0.02	
Recharging	12	0.37	0.32	0.05	0.83
battery	13	0.42	0.32	0.10	
system	14	0.46	0.32	0.14	
	15	0.48	0.32	0.16	
	16	0.48	0.32	0.16	
	17	0.45	0.32	0.13	
	18	0.40	0.32	0.08	
	19	0.32	0.32	0.00	
Discharging	20	0.24	0.32	-0.08	-0.78
electricity	21	0.18	0.32	-0.14	
from storage	22	0.14	0.32	-0.18	
system	23	0.15	0.32	-0.17	
	24	0.18	0.32	-0.14	
	25	0.24	0.32	-0.08	
	26	0.32	0.32	0.00	
	27	0.38	0.32	0.06	
	28	0.43	0.32	0.11	
	29	0.47	0.32	0.15	
	30	0.50	0.32	0.18	



# Appendix B: LCOE calculation

# Appendix B1: Solar PV

Input parameters	
Overnight capital costs [€/MW]	590,000
O&M costs [€/MW/y]	11,500
One-off maintenance costs in year 12 [€/MW]	32,000
Lifetime [y]	25
Construction time [y]	0.5
WACC	4.3%
Capacity factor	0.09

Outcome		
NPV costs [€]	777,885	
NPV output [MWh]	11,557	
LCOE [€/MWh]	67.31	

NPV costs					
Year	Overnight capital	O&M costs [€]	One-off maintenance	Discount	PV of
rear	costs [€/MW]	Octivi costis [c]	costs [€]	factor	costs [€]
Entry	590,000				590,000
1		5,750		95.88%	5,513
2		11,500		91.92%	10,571
3		11,500		88.13%	10,135
4		11,500		84.50%	9,718
5		11,500		81.02%	9,317
6		11,500		77.68%	8,933
$\frac{7}{2}$		11,500		74.47%	8,565
8		11,500		71.40%	8,212
9		11,500		68.46%	7,873
10		11,500		65.64%	7,548
11		11,500	22.000	62.93%	7,237
12		11,500	32,000	60.34%	26,247
13		11,500		57.85%	6,653
14		11,500		55.47%	6,378
15		11,500		53.18%	6,116
16 17		11,500 11,500		50.99% 48.88%	$\frac{5,863}{5,622}$
18		11,500		46.87%	$\frac{5,622}{5,390}$
19		11,500		44.94%	$\frac{5,390}{5,168}$
$\frac{19}{20}$		11,500		43.08%	$\frac{5,166}{4,955}$
$\frac{20}{21}$		11,500		41.31%	$\frac{4,955}{4,750}$
$\frac{21}{22}$		11,500		39.60%	$\frac{4,750}{4.555}$
23		11,500		37.97%	$\frac{4,355}{4,367}$
$\frac{23}{24}$		11,500		36.41%	4,367
$\frac{24}{25}$		11,500		34.91%	4,014

NPV costs [€] 777,885

NPV electrcity output				
Year	Yearly electrity output [MWh]	Discount factor	PV of output [MWh]	
Entry				
1	394	95.88%		
2	788	91.92%	725	
3	788	88.13%	695	
4	788	84.50%	666	
5	788	81.02%	639	
6	788	77.68%	612	
7	788	74.47%		
- 8	788	71.40%	563	
9	788	68.46%	540	
10	788	65.64%	517	
11	788	62.93%	496	
12	788	60.34%		
13	788	57.85%		
14	788	55.47%	437	
15	788	53.18%	419	
16	788	50.99%	402	
17	788	48.88%		
18	788	46.87%	370	
19	788	44.94%	354	
20	788	43.08%	340	
21	788	41.31%	326	
22	788	39.60%	312	
23	788	37.97%	299	
24	788	36.41%	287	
25	788	34.91%	275	

NPV output [MWh]

11,557



# Appendix B2: Offshore wind

Input parameters	
Overnight capital costs [€/MW]	1,750,000
O&M costs [€/MW/y]	55,000
Offshore grid costs [€/MWh]	17.5
Lifetime [y]	25
Construction time [y]	1.5
WACC	4.3%
Capacity factor	0.43

Outcome		
NPV costs [€]	3,393,846	
NPV output [MWh]	51,680	
LCOE [€/MWh]	65.67	

	NPV costs					
	Overnight capital	O&M	Offshore grid	Discount	PV of costs	
Year	costs [€]	costs [€]	costs [€]	factor	[€]	
Entry	1,750,000				1,750,000	
1		0		95.88%	0	
2		27,500	16,480	91.92%	40,428	
3		55,000	65,919	88.13%	106,572	
4		55,000	65,919	84.50%	102,178	
5		55,000	65,919	81.02%	97,965	
6		55,000	65,919	77.68%	93,927	
7		55,000	65,919	74.47%	90,054	
8		55,000	65,919	71.40%	86,342	
9		55,000	65,919	68.46%	82,782	
10		55,000	65,919	65.64%	79,369	
11		55,000	65,919	62.93%	76,097	
12		55,000	65,919	60.34%	72,960	
13		55,000	65,919	57.85%	69,952	
14		55,000	65,919	55.47%	67,068	
15		55,000	65,919	53.18%	64,303	
16		55,000	65,919	50.99%	61,652	
17		55,000	65,919	48.88%	59,110	
18		55,000	65,919	46.87%	56,673	
19		55,000	65,919	44.94%	54,337	
20		55,000	65,919	43.08%	52,096	
$\frac{21}{22}$		55,000	65,919	41.31%	49,949	
22		55,000	65,919	39.60%	47,889	
23		55,000	65,919	37.97%	45,915	
24		55,000	65,919	36.41%	44,022	
25		55,000	65,919	34.91%	42,207	

NPV costs [€] 3,393,846

NPV electrcity output				
<b>X</b> 7	Yearly electriity	Discount	PV of output	
Year	output [MWh]	factor [%]	[MWh]	
Entry				
1	0	95.88%	0	
2	1,883	91.92%	1,731	
3	3,767	88.13%	3,320	
4	3,767	84.50%	3,183	
5	3,767	81.02%	3,052	
6	3,767	77.68%	2,926	
7	3,767	74.47%	2,805	
8	3,767	71.40%	2,690	
9	3,767	68.46%	2,579	
10	3,767	65.64%	2,472	
11	3,767	62.93%	2,371	
12	3,767	60.34%	2,273	
13	3,767	57.85%	2,179	
14	3,767	55.47%	2,089	
15	3,767	53.18%	2,003	
16	3,767	50.99%	1,921	
17	3,767	48.88%	1,841	
18	3,767	46.87%	1,765	
19	3,767	44.94%	1,693	
20	3,767	43.08%	1,623	
21	3,767	41.31%	1,556	
22	3,767	39.60%	1,492	
23	3,767	37.97%	1,430	
24	3,767	36.41%	1,371	
25	3,767	34.91%	1,315	

NPV output [MWh] 51,680



# Appendix B3: Onshore wind

Input parameters		
Overnight capital costs [€/MW]	1,100,000	
O&M costs [€/MW/y]	32,524	
Lifetime [y]	25	
Construction time [y]	1.0	
WACC	4.3%	
Capacity factor	0.25	

Outcome		
NPV costs [€]	1,561,174	
NPV output [MWh]	31,053	
LCOE [€/MWh]	50.27	

	NPV costs						
37	Overnight capital	O&M	Discount	PV of costs			
Year	costs [€]	costs [€]	factor	[€]			
Entry	1,100,000			1,100,000			
1		0	95.88%	0			
2		32,524	91.92%	29,898			
3		32,524	88.13%	28,665			
4		32,524	84.50%	27,483			
5		32,524	81.02%	26,350			
6		32,524	77.68%	25,264			
7		32,524	74.47%	24,222			
8		32,524	71.40%	23,224			
9		32,524	68.46%	22,266			
10		32,524	65.64%	21,348			
11		32,524	62.93%	20,468			
12		32,524	60.34%	19,624			
13		32,524	57.85%	18,815			
14		32,524	55.47%	18,039			
15		32,524	53.18%	17,296			
16		32,524	50.99%	16,583			
17		32,524	48.88%	15,899			
18		32,524	46.87%	15,244			
19		32,524	44.94%	14,615			
20		32,524	43.08%	14,013			
21		32,524	41.31%	13,435			
22		32,524	39.60%	12,881			
23		32,524	37.97%	12,350			
24		32,524	36.41%	11,841			
25		32,524	34.91%	11,353			

NPV costs [€] 1,561,174

	NPV electrcity output				
37	Yearly electriity	Discount	PV of output		
Year	output [MWh]	factor	[MWh]		
Entry					
1	0	95.88%	0		
2	2,190	91.92%	2,013		
3	2,190	88.13%	1,930		
4	2,190	84.50%	1,851		
5	2,190	81.02%	1,774		
6	2,190	77.68%	1,701		
7	2,190	74.47%	1,631		
8	2,190	71.40%	1,564		
9	2,190	68.46%	1,499		
10	2,190	65.64%	1,437		
11	2,190	62.93%	1,378		
12	2,190	60.34%	1,321		
13	2,190	57.85%	1,267		
14	2,190	55.47%	1,215		
15	2,190	53.18%	1,165		
16	2,190	50.99%	1,117		
17	2,190	48.88%	1,071		
18	2,190	46.87%	1,026		
19	2,190	44.94%	984		
20	2,190	43.08%	944		
21	2,190	41.31%	905		
22	2,190	39.60%	867		
23	2,190	37.97%	832		
24	2,190	36.41%	797		
25	2.190	34.91%	764		

NPV output [MWh] 31,0



# Appendix B4: DTP

Input parameters			
Overnight capital costs [€/MW]	1,690,000		
O&M costs [€/MW/y]	23,660		
Offshore grid costs [€/MWh]	5.3		
Lifetime [y]	60		
Construction time [y]	5.0		
WACC	4.5%		
Capacity factor	0.32		

Outcome		
NPV costs [€]	2,313,548	
NPV output [MWh]	47,602	
LCOE [€/MWh]	48.60	

	NPV costs					
Year	Overnight capital	O&M	Offshore grid	Discount	PV of costs	
	costs [€]	costs [€]	costs [€]	factor	[€]	
Entry	1,690,000	_	_		1,690,000	
$\frac{1}{2}$		0	0	95.69% 91.57%	0	
3		0	0	87.63%	0	
4		0	0	83.86%	0	
5		00000	14.717	80.25%	0	
<u>6</u>		$\frac{23,660}{23,660}$	$\frac{14,717}{14,717}$	76.79% 73.48%	$\frac{29,469}{28,200}$	
8		23,660	14,717	70.32%	26,986	
9		23,660	14,717	67.29%	25,824	
10 11		$\frac{23,660}{23,660}$	$\frac{14,717}{14,717}$	64.39% 61.62%	$\frac{24,712}{23,648}$	
$\frac{11}{12}$		23,660	14,717	58.97%	$\frac{25,048}{22,629}$	
13		23,660	14,717	56.43%	21,655	
14		23,660	14,717	54.00%	20,722	
$\frac{15}{16}$		$\frac{23,660}{23,660}$	$\frac{14,717}{14,717}$	51.67% 49.45%	$\frac{19,830}{18,976}$	
17		23,660	14,717	47.32%	18,159	
18		23,660	14,717	45.28%	17,377	
19		23,660	14,717	43.33%	16,629	
20 21		$\frac{23,660}{23,660}$	$\frac{14,717}{14,717}$	41.46% 39.68%	$\frac{15,913}{15,227}$	
22		23,660	14,717	37.97%	14,572	
23		23,660	14,717	36.34%	13,944	
$\frac{24}{25}$		$\frac{23,660}{23,660}$	$\frac{14,717}{14,717}$	34.77% 33.27%	$\frac{13,344}{12,769}$	
$\frac{25}{26}$		23,660	14,717	31.84%	12,709	
27		23,660	14,717	30.47%	11,693	
28		23,660	14,717	29.16%	11,190	
29		23,660	14,717	27.90%	10,708	
30 31		$\frac{23,660}{23,660}$	$\frac{14,717}{14,717}$	$\frac{26.70\%}{25.55\%}$	$\frac{10,247}{9,805}$	
32		23,660	14,717	$\frac{24.45\%}{24.45\%}$	9,383	
33		23,660	14,717	23.40%	8,979	
$\frac{34}{35}$		$\frac{23,660}{23,660}$	$\frac{14,717}{14,717}$	22.39% 21.43%	$\frac{8,592}{8,222}$	
36		23,660	14,717	20.50%	7,868	
37		23,660	14,717	19.62%	7,529	
38		23,660	14,717	18.78%	7,205	
39 40		$\frac{23,660}{23,660}$	$\frac{14,717}{14,717}$	17.97% 17.19%	$\frac{6,895}{6,598}$	
41		23,660	14,717	16.45%	6,314	
42		23,660	14,717	15.74%	6,042	
43 44		$\frac{23,660}{23,660}$	$\frac{14,717}{14,717}$	$\frac{15.07\%}{14.42\%}$	$\frac{5,782}{5,533}$	
$\frac{44}{45}$		23,660	$\frac{14,717}{14,717}$	13.80%	$\frac{5,333}{5,295}$	
46		23,660	14,717	13.20%	5,067	
47		23,660	14,717	12.63%	4,848	
$\frac{48}{49}$		$\frac{23,660}{23,660}$	$\frac{14,717}{14,717}$	12.09% 11.57%	$\frac{4,640}{4,440}$	
50		23,660	14,717	11.07%	4,249	
51		23,660	14,717	10.59%	4,066	
52		23,660	14,717	10.14%	3,891	
$\frac{53}{54}$		$\frac{23,660}{23,660}$	14,717 14,717	9.70% 9.28%	$\frac{3,723}{3,563}$	
55		23,660	14,717	8.88%	3,409	
56		23,660	14,717	8.50%	3,263	
57		23,660	$\frac{14,717}{14,717}$	8.14% 7.78%	3,122	
$\frac{58}{59}$		$\frac{23,660}{23,660}$	$\frac{14,717}{14,717}$	7.45%	$\frac{2,988}{2,859}$	
60		23,660	14,717	7.13%	$\frac{2,736}{2,736}$	

NPV costs [€] 2,313,548



	NPV electrcity output						
77	Yearly electriity	Discount	PV of output				
Year	output [MWh]	factor	[MWh]				
Entry							
1	0	95.88%	0				
$\frac{2}{3}$	,	91.92% 88.13%	0				
4		84.50%	0				
5		81.02%	0				
6 7	2,803 2,803	77.68% 74.47%	$\frac{2,177}{2,088}$				
8		71.40%	$\frac{2,088}{2,002}$				
9	2,803	68.46%	1,919				
10	-,000	65.64%	1,840				
11 12	2,803 2,803	62.93% 60.34%	$\frac{1,764}{1.691}$				
13		57.85%	1,622				
14	2,803	55.47%	1,555				
$\frac{15}{16}$		53.18% 50.99%	1,491 1,429				
$\frac{16}{17}$	2,803	48.88%	$\frac{1,429}{1,370}$				
18	2,803	46.87%	1,314				
19		44.94%	1,260				
$\frac{20}{21}$	2,803 2,803	43.08% 41.31%	$\frac{1,208}{1,158}$				
$\frac{21}{22}$		39.60%	1,110				
23		37.97%	1,064				
24		36.41% 34.91%	1,021				
$\frac{25}{26}$		$\frac{34.91\%}{33.47\%}$	$\frac{978}{938}$				
$\frac{25}{27}$		32.09%	899				
28		30.76%	862				
29		29.50%	$\frac{827}{702}$				
30 31	2,803 2,803	$\frac{28.28\%}{27.11\%}$	793 760				
32	2,803	26.00%	729				
33		24.92%	699				
$\frac{34}{35}$		23.90% 22.91%	$\frac{670}{642}$				
36		$\frac{22.91\%}{21.97\%}$	616				
37	2,803	21.06%	590				
38	2,803	20.19%	566				
39 40		19.36% 18.56%	$\frac{543}{520}$				
41	2,803	17.80%	499				
42	2,803	17.06%	478				
43	0.000	16.36% 15.69%	459 440				
45		15.04%	422				
46	2,803	14.42%	404				
$\frac{47}{48}$		13.82% 13.25%	$\frac{388}{372}$				
49		12.71%	356				
50	2,803	12.18%	342				
51		11.68%	$\frac{327}{214}$				
52 53		$\frac{11.20\%}{10.74\%}$	314 301				
54		10.30%	289				
55	2,803	9.87%	277				
56		$\frac{9.46\%}{9.07\%}$	$\frac{265}{254}$				
$\frac{57}{58}$		9.07% 8.70%	$\frac{254}{244}$				
59	2,803		234				
60		8.00%	224				

NPV output [MWh] 47,602



# Appendix B5: DTP incl. storage system

Input parameters				
Overnight capital costs [€/MW]	1,690,000			
O&M costs [€/MW/y]	23,660			
Offshore grid costs [€/MWh]	1.8			
Size battery system [MWh/MW]	0.96 (system 1), 19.00 (system 2)			
Lifetime battery [y]	12 (system 1), 60 (system 2)			
Battery storage costs [€/MWh]	100,000			
Lifetime [y]	60			
Construction time [y]	5			
WACC	4.5%			
Capacity factor	0.31			

Outcome		
NPV costs [€]	4,264,920	
NPV electricty output [MWh]	46,115	
LCOE [€/MWh]	92.48	

			NPV co			
Year	Overnight capital costs [€]	O&M costs [€]	Offshore grid costs [€]	Battery storage costs [€]	Discount factor	PV of costs [€]
Entry	1,690,000	505 to [0]	- CO	1,992,000	140001	3,682,00
<u>лигу</u> 1	1,080,000	0	0	1,334,000	95.69%	5,064,00
$\frac{1}{2}$		0	0		91.57%	
3		0	0		87.63%	
4		0	0		83.86%	
5		0	0		80.25%	
6		23,660	4,752		76.79%	21,81
7		23,660	4,752		73.48%	20,87
8		23,660	4,752		70.32%	19,97
9		23,660	4,752		67.29%	19,11
10		23,660	4,752		64.39%	18,29
11		23,660	4.752	0.0.00	61.62%	17.50
12		23,660	4,752	96,000	58.97%	73,36
13		23,660	4,752		56.43%	16,03
14		23,660	4,752		54.00% 51.67%	15,34
15 16		$\frac{23,660}{23,660}$	$\frac{4,752}{4,752}$		49.45%	14,68 14,04
$\frac{16}{17}$		23,660	$\frac{4,752}{4,752}$		49.45%	13.44
18		23,660	4,752		45.28%	12,86
19		23,660	4,752		43.33%	12,31
20		23,660	4,752		41.46%	11,78
21		23,660	4,752		39.68%	11,27
22		23,660	4,752		37.97%	10,78
23		23,660	4,752		36.34%	10,32
24		23,660	4,752	96,000	34.77%	43,25
25		23,660	4,752		33.27%	9,45
26		23,660	4,752		31.84%	9,04
27		23,660	4,752		30.47%	8,65
28		23,660	4,752		29.16%	8,28
29		23,660	4,752		27.90%	7,92
30		23,660	4,752		26.70%	7,58
31		23,660	4,752		25.55%	7,25
32		23,660	4,752		24.45%	6,94
33 34		$\frac{23,660}{23,660}$	$\frac{4,752}{4,752}$		23.40% 22.39%	6,64 6,36
$\frac{34}{35}$		23,660	$\frac{4,752}{4,752}$		21.43%	6,08
36		23,660	$\frac{4,752}{4,752}$	96,000	20.50%	25,50
37		23,660	4,752	00,000	19.62%	5,57
38		23,660	4,752		18.78%	5,33
39		23,660	4,752		17.97%	5,10
40		23,660	4,752		17.19%	4,88
41		23,660	4,752		16.45%	4,67
42		23,660	4,752		15.74%	4,47
43		23,660	4,752		15.07%	4,28
44		23,660	4.752		14.42%	4.09
45		23,660	4,752		13.80%	3,92
46		23,660	4,752		13.20%	3,75
47		23,660	4,752	00.000	12.63%	3,59
$\frac{48}{49}$		$\frac{23,660}{23,660}$	$\frac{4,752}{4,752}$	96,000	12.09% 11.57%	$\frac{15,04}{3,28}$
50		23,660	4,752		11.07%	3,14
$\frac{50}{51}$		23,660	4,752		10.59%	$\frac{5,14}{3,01}$
$\frac{51}{52}$		23,660	4,752		10.14%	2,88
53		23,660	4,752		9.70%	2,75
$\frac{53}{54}$		23,660	4,752		9.28%	2,63
55		23,660	4,752		8.88%	$\frac{2,06}{2,52}$
56		23,660	4,752		8.50%	
57		23,660	4,752		8.14%	2,31
58		23,660	4,752		7.78%	2,21
59		23,660	4,752		7.45%	2,11
60		23,660	4,752		7.13%	

91



Year	Vacala alastasitas	_	
Year	Yearly electrity	Discount	PV of output
	output [MWh]	factor	[MWh]
Entry			L ]
1	0	95.88%	0
2		91.92%	0
3	-	88.13%	0
$\frac{4}{5}$		84.50% 81.02%	0
6		77.68%	2.109
7	2,716	74.47%	2,022
8	2,716	71.40%	1,939
9		68.46%	1,859
10		65.64%	1,782
11 12	$\frac{2,716}{2,716}$	62.93% 60.34%	$\frac{1,709}{1,639}$
13		$\frac{57.85\%}{}$	1,571
14		55.47%	1,506
15	2,716	53.18%	1,444
16		50.99%	1,385
17	,	48.88% 46.87%	1,327 $1,273$
$\frac{18}{19}$		46.87%	$\frac{1,273}{1.220}$
20		43.08%	$\frac{1,220}{1.170}$
21	2,716	41.31%	1,122
22		39.60%	1,076
23		37.97%	1,031
24		36.41%	989
$\begin{array}{c} 25 \\ 26 \end{array}$		$\frac{34.91\%}{33.47\%}$	948 909
$\frac{20}{27}$		32.09%	871
28		30.76%	835
29		29.50%	801
30	2,716	28.28%	768
31	2,716	27.11%	736
32 33		26.00%	706
		24.92% 23.90%	677 649
35		$\frac{23.30\%}{22.91\%}$	622
36	2,716	21.97%	597
37	2,716	21.06%	572
38		20.19%	548
39 40		19.36% 18.56%	$\frac{526}{504}$
41		17.80%	483
42	2,716	17.06%	463
43	2,716	16.36%	444
44		15.69%	426
$\frac{45}{46}$		$\frac{15.04\%}{14.42\%}$	$\frac{408}{392}$
$\frac{40}{47}$		13.82%	$\frac{392}{375}$
48		13.25%	360
49	2,716	12.71%	345
50		12.18%	331
51	2,716	11.68% 11.20%	317
52 53		11.20%	$\frac{304}{292}$
53 54		10.74%	$\frac{292}{280}$
55	2,716	9.87%	$\frac{260}{268}$
56	2,716	9.46%	257
57	2,716	9.07%	246
58	2,716	8.70%	236
59 60		8.34% 8.00%	$\frac{227}{217}$
60	NPV out	9.00% put [MWh]	46,115



## Appendix B6: Flexible CCGT

Input parameters		
Overnight capital costs [€/MW]	630,000	
O&M costs [€/MW/y]	40,000	
Fuel costs [€/MWh]	46.08	
CO2 costs [€/MWh]	10.10	
Lifetime [y]	25	
Construction time [y]	3.0	
WACC	4.3%	
Capacity factor *	0.50	

Outcome		
NPV costs [€]	4,171,109	
NPV output [MWh]	54,220	
LCOE [€/MWh]	76.93	

<sup>\*</sup>Capacity factor varies (0.01-1.00) as it depends on the characteristics of the residual load. For this exemplary calculation a capacity factor of 0.50 is used.

NPV costs							
Year	Overnight capital costs [€]	O&M costs [€]	Fuel costs [€]	CO2 costs [€]	Discount factor	PV of costs [€]	
Entry	630,000					630,000	
1		0	0	0	0.00%		
2		0	0	0	0.00%		
3		0	0	0	0.00%	0	
4		40,000	201,830	44,229	84.50%		
5		40,000	201,830	44,229	81.02%		
6		40,000	201,830	44,229	77.68%	222,203	
7		40,000	201,830	44,229	74.47%	213,043	
8		40,000	201,830	44,229	71.40%	204,259	
9		40,000	201,830	44,229	68.46%		
10		40,000	201,830	44,229	65.64%		
11		40,000	201,830	44,229	62.93%		
12		40,000	201,830	44,229	60.34%		
13		40,000	201,830	44,229	57.85%	165,486	
14		40,000	201,830	44,229	55.47%		
15		40,000	201,830	44,229	53.18%	152,122	
16		40,000	201,830	44,229	50.99%	145,850	
17		40,000	201,830	44,229	48.88%	139,837	
18		40,000	201,830	44,229	46.87%		
19		40,000	201,830	44,229	44.94%		
20		40,000	201,830	44,229	43.08%		
21		40,000	201,830	44,229	41.31%		
22		40,000	201,830	44,229	39.60%	113,293	
23		40,000	201,830	44,229	37.97%	108,622	
24		40,000	201,830	44,229	36.41%	104,144	
25		40,000	201,830	44.229	34.91%	99,850	

NPV costs [€] 4,171,109

NPV electrcity output							
37	Yearly electriity	Discount	PV of output				
Year	output [MWh]	factor	[MWh]				
Entry							
1	0	95.88%	0				
2	0	91.92%	0				
3	0	88.13%	0				
4	4,380	84.50%	3,701				
5	4,380	81.02%	3,549				
6	4,380	77.68%	3,402				
7	4,380	74.47%	3,262				
8	4,380	71.40%	3,128				
9	4,380	68.46%	2,999				
10	4,380	65.64%	2,875				
11	4,380	62.93%	2,756				
12	4,380	60.34%	2,643				
13	4,380	57.85%	2,534				
14	4,380	55.47%	2,429				
15 16	4,380 4,380	53.18% 50.99%	$\frac{2,329}{2,233}$				
17	4,380	48.88%	2,233				
18	4,380	46.87%	$\frac{2,141}{2.053}$				
19	4,380	44.94%	1,968				
20	4,380	43.08%	1,887				
$\frac{20}{21}$	4,380	41.31%	1,809				
22	4,380	39.60%	1,735				
23	4,380	37.97%	1,663				
$\frac{23}{24}$	4,380	36.41%	1,595				
25	4,380	34.91%	1,529				
	MIDIT	. [3/[37]]	,				

NPV output [MWh] 54,220



## Appendix C: Efficient portfolio shares and backup capacity

## Appendix C1: Demand scenario 1 – contemporary load profile

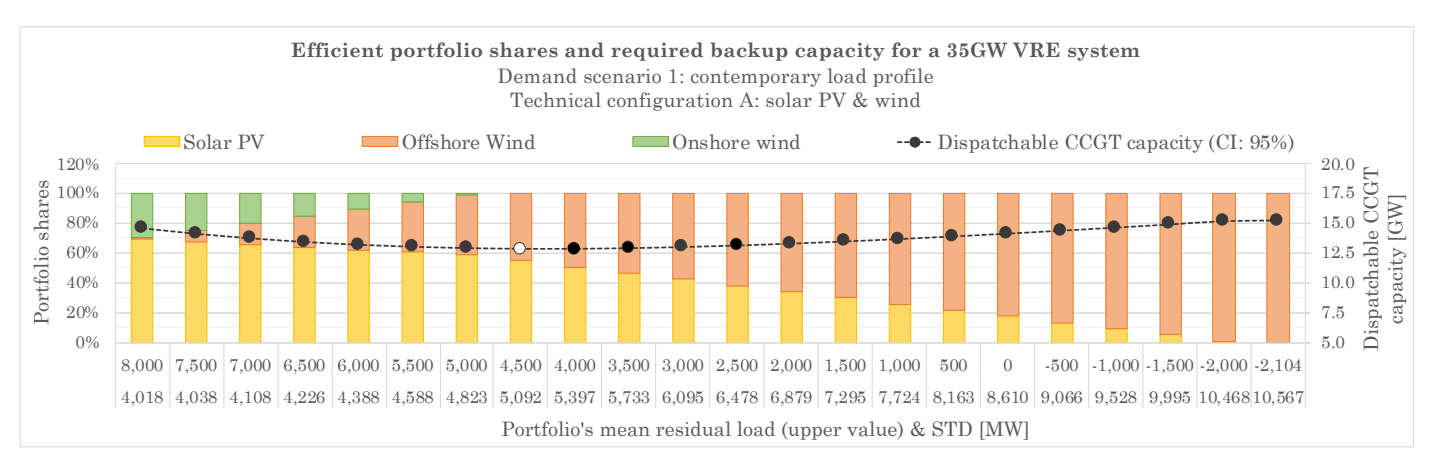


Figure 48: efficient portfolio shares and required dispatchable backup capacity for a 35 GW VRE system. Demand scenario 1: contemporary load profile. Technical configuration A: solar PV & wind. Note; the white dot marks the portfolio that requires the least backup capacity (most efficient).

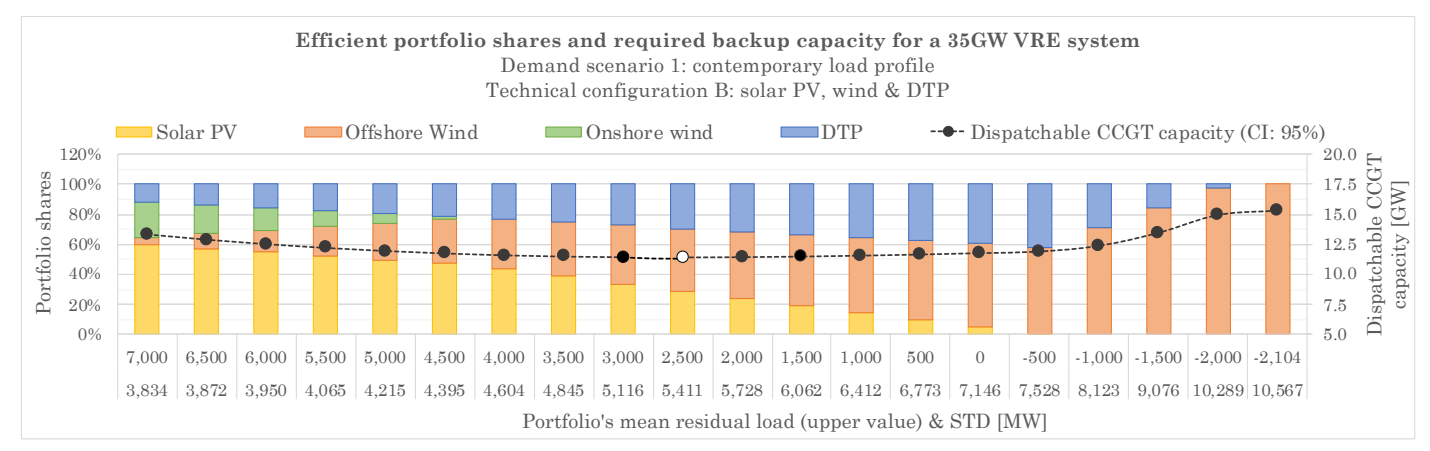


Figure 49: efficient portfolio shares and required dispatchable backup capacity for a 35GW VRE system. Demand scenario 1: contemporary load profile. Technical configuration B: solar PV, wind & DTP. Note; the white dot marks the portfolio that requires the least backup capacity (most efficient).

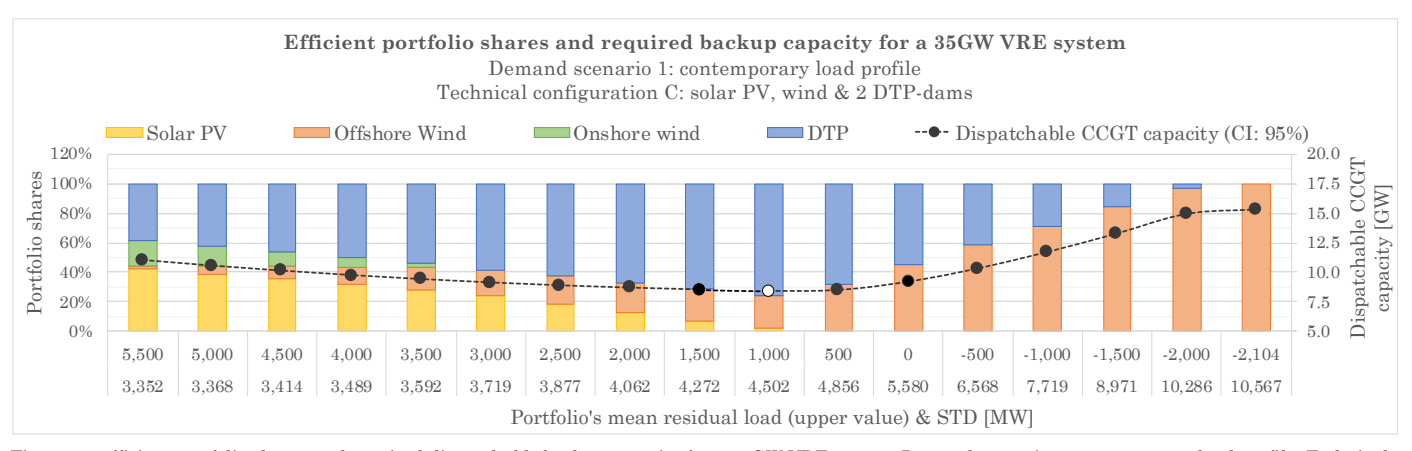


Figure 50: efficient portfolio shares and required dispatchable backup capacity for a 35GW VRE system. Demand scenario 1: contemporary load profile. Technical configuration C: solar PV, wind & 2 DTP-dams. Note; the white dot marks the portfolio that requires the least backup capacity (most efficient).



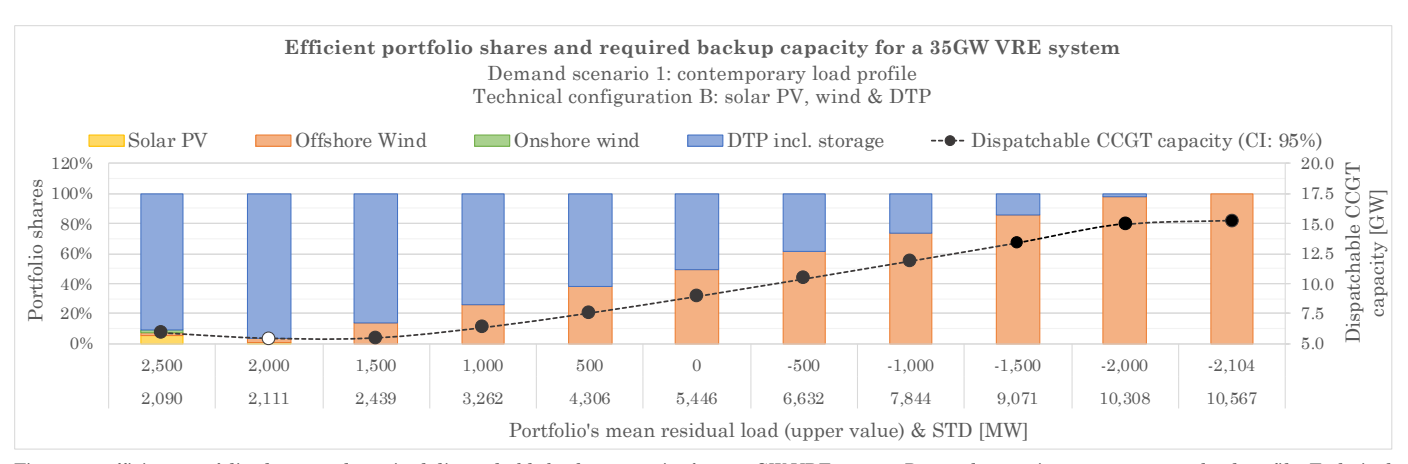


Figure 51: efficient portfolio shares and required dispatchable backup capacity for a 35GW VRE system. Demand scenario 1: contemporary load profile. Technical configuration D: solar PV, wind & DTP incl. storage. Note; the white dot marks the portfolio that requires the least backup capacity (most efficient).

## Appendix C2: Demand scenario 2 - increased peak loads

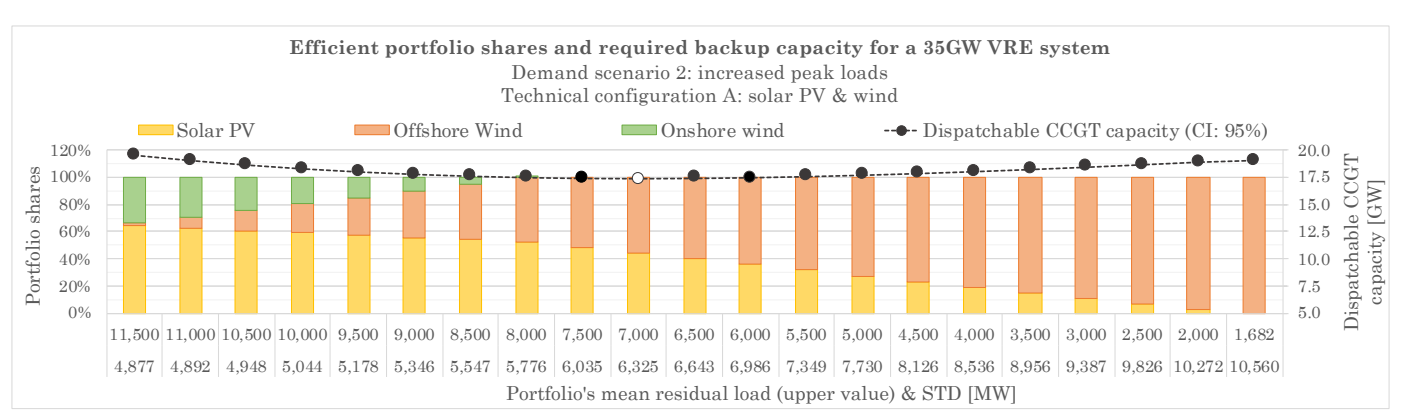


Figure 52: efficient portfolio shares and required dispatchable backup capacity for a 35GW VRE system. Demand scenario 2: increased peak loads. Technical configuration A: solar PV & wind. Note; the white dot marks the portfolio that requires the least backup capacity (most efficient).

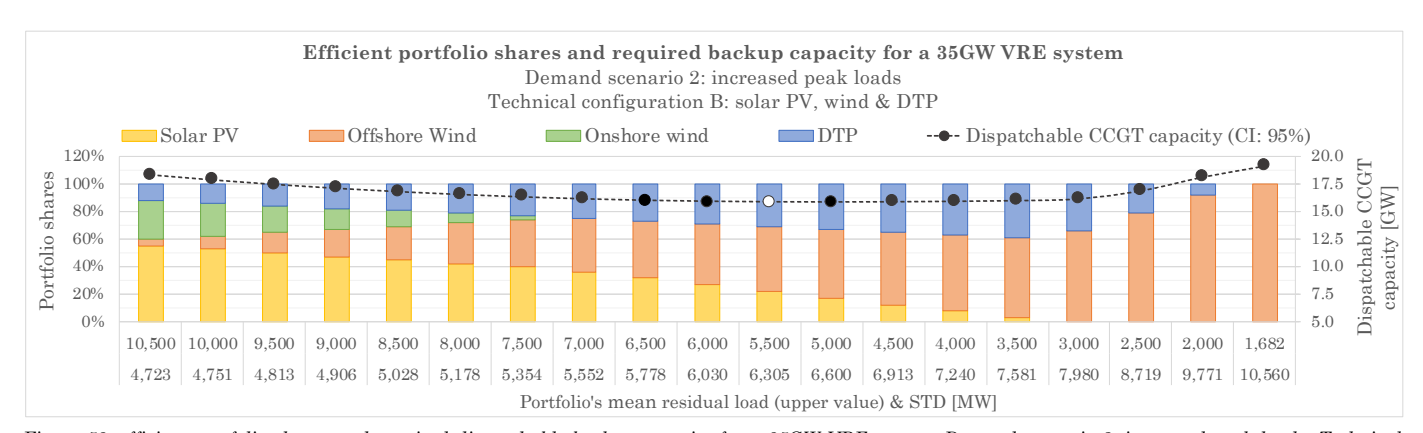


Figure 53: efficient portfolio shares and required dispatchable backup capacity for a 35GW VRE system. Demand scenario 2: increased peak loads. Technical configuration B: solar PV, wind & DTP. Note; the white dot marks the portfolio that requires the least backup capacity (most efficient).



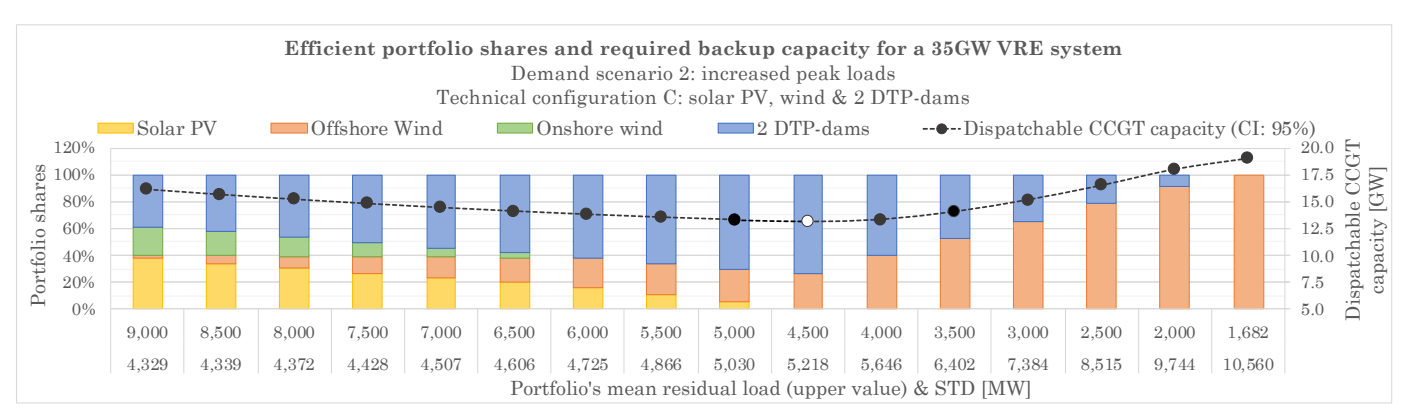


Figure 54: efficient portfolio shares and required dispatchable backup capacity for a 35GW VRE system. Demand scenario 2: increased peak loads. Technical configuration C: solar PV, wind & 2 DTP-dams. Note; the white dot marks the portfolio that requires the least backup capacity (most efficient).

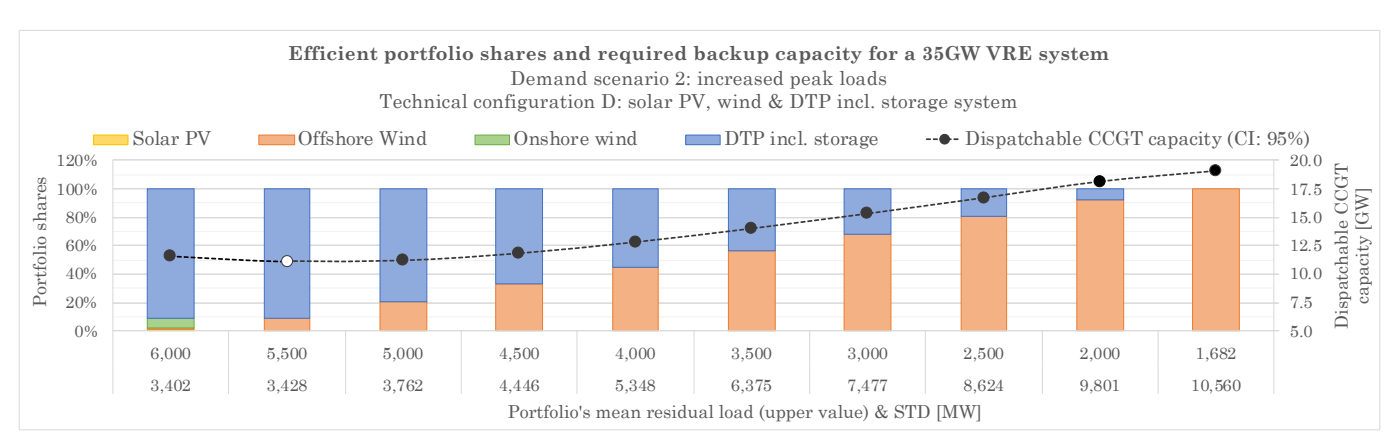
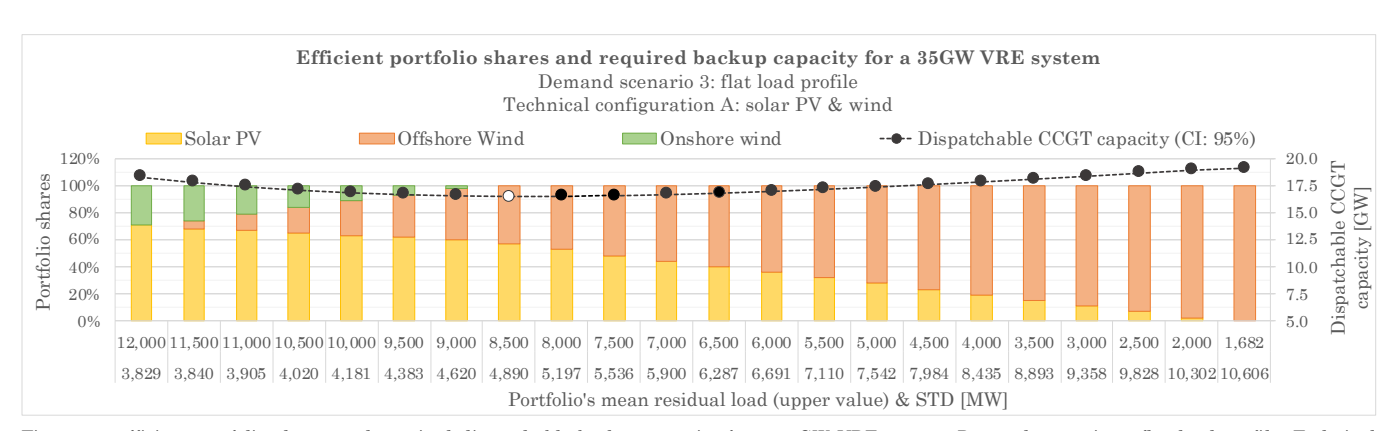


Figure 55: efficient portfolio shares and required dispatchable backup capacity for a 35GW VRE system. Demand scenario 2: increased peak loads. Technical configuration D: solar PV, wind & DTP incl. storage. Note; the white dot marks the portfolio that requires the least backup capacity (most efficient).

## Appendix C3: Demand scenario 3 - flat load profile



Figure~56: efficient~portfolio~shares~and~required~dispatchable~backup~capacity~for~a~35GW~VRE~system.~Demand~scenario~3:~flat~load~profile.~Technical~configuration~A:~solar~PV~&~wind.~Note;~the~white~dot~marks~the~portfolio~that~requires~the~least~backup~capacity~(most~efficient).



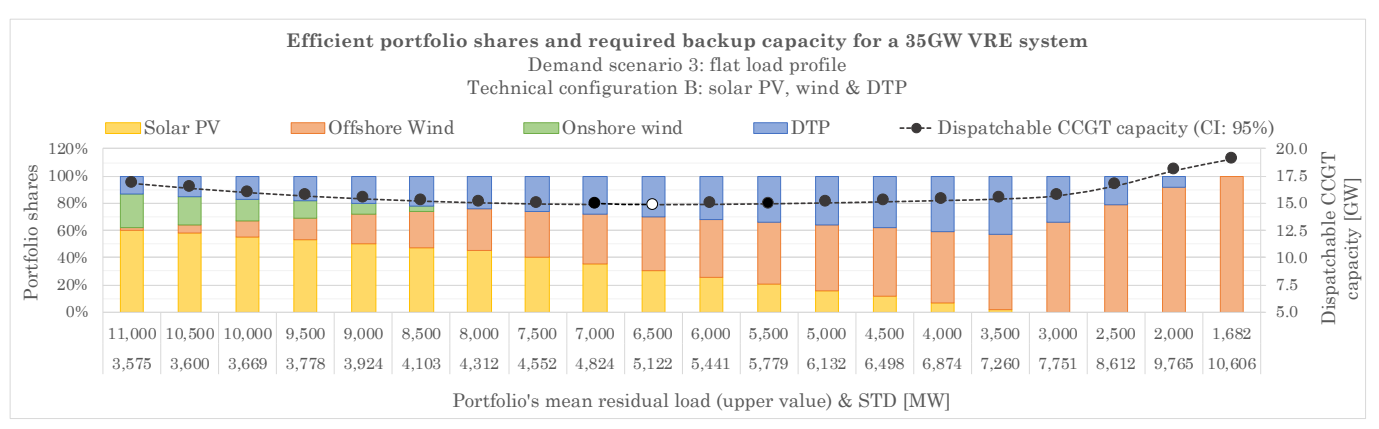


Figure 57: efficient portfolio shares and required dispatchable backup capacity for a 35GW VRE system. Demand scenario 3: flat load profile. Technical configuration B: solar PV, wind & DTP. Note; the white dot marks the portfolio that requires the least backup capacity (most efficient).

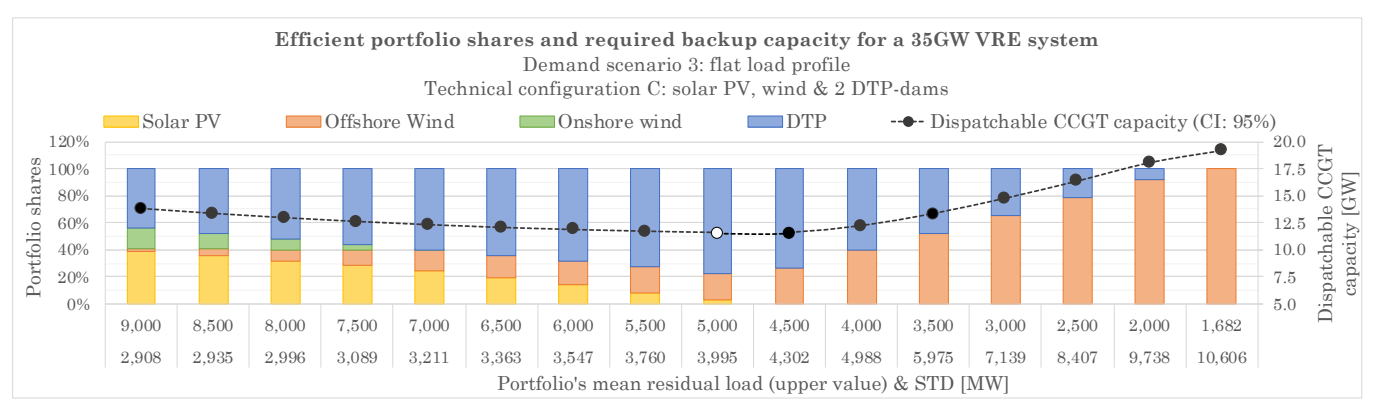


Figure 58: efficient portfolio shares and required dispatchable backup capacity for a 35GW VRE system. Demand scenario 3: flat load profile. Technical configuration C: solar PV, wind & 2 DTP-dams. Note; the white dot marks the portfolio that requires the least backup capacity (most efficient).

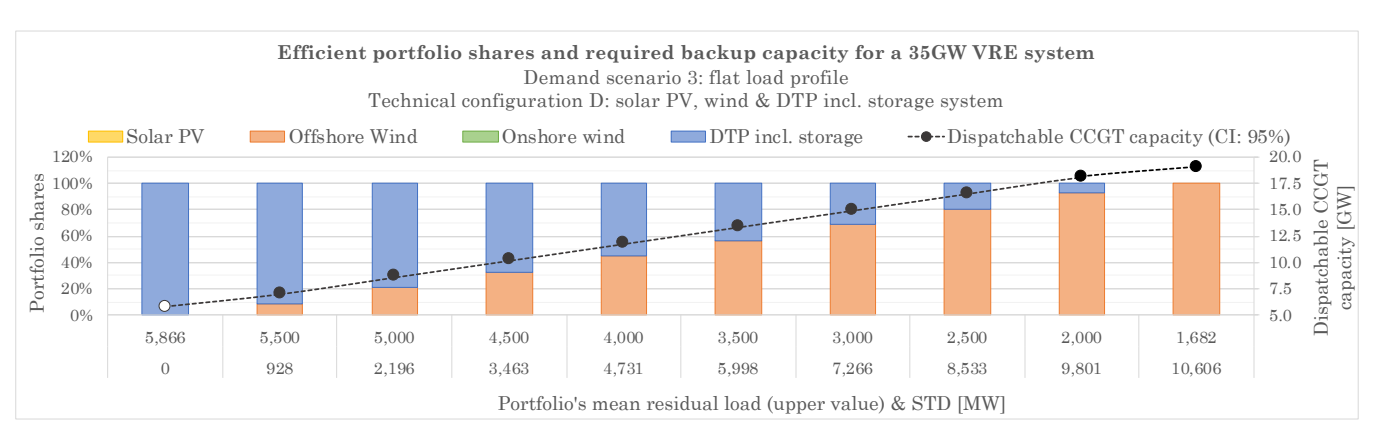


Figure 59: efficient portfolio shares and required dispatchable backup capacity for a 35GW VRE system. Demand scenario 3: flat load profile. Technical configuration B: solar PV, wind & DTP incl. storage. Note; the white dot marks the portfolio that requires the least backup capacity (most efficient).



# Appendix D: Efficient portfolio shares, backup capacity and system's LCOE

### Appendix D1: Demand scenario 1 – contemporary load profile

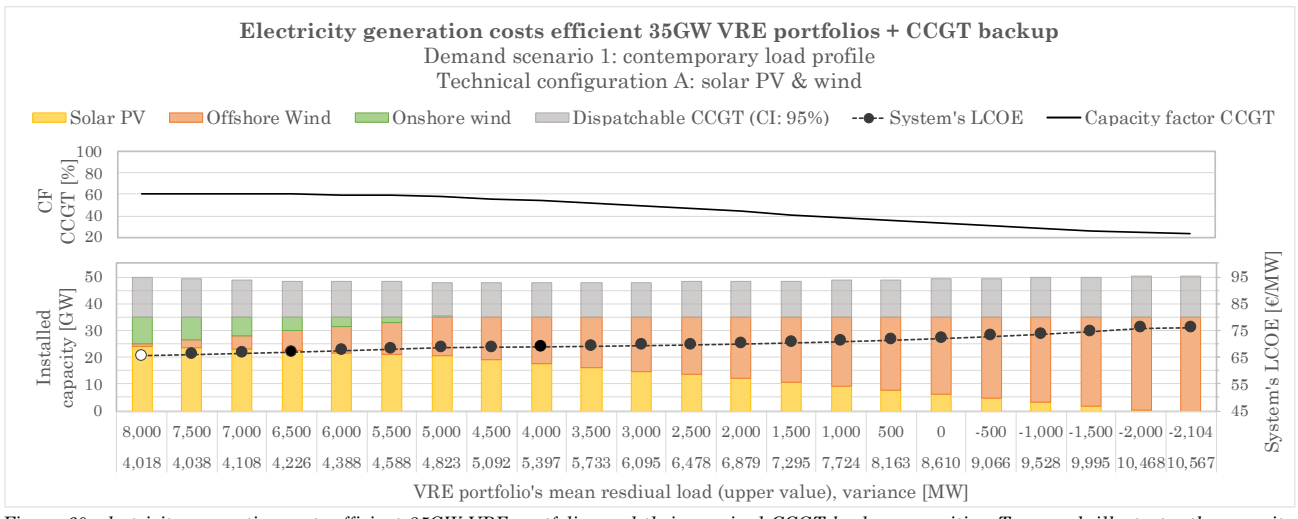


Figure 60: electricity generation costs efficient 35GW VRE portfolios and their required CCGT backup capacities. Top graph illustrates the capacity factor (CF) of the CCGT. Demand scenario 1: contemporary load profile. Technical configuration A: solar PV & wind. Note; the white dot marks the most cost-efficient system.

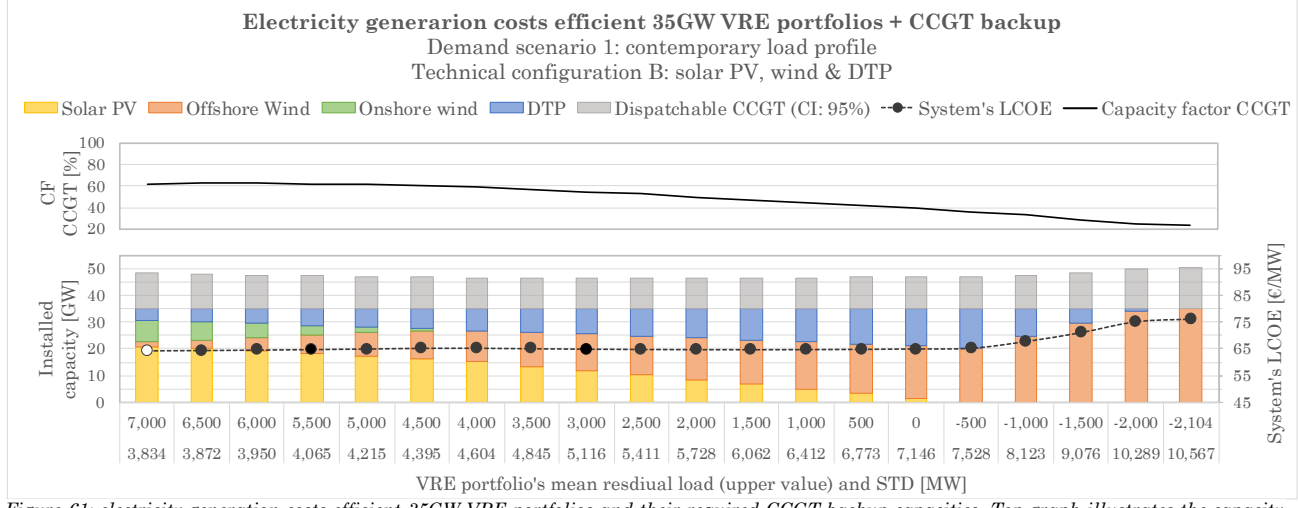


Figure 61: electricity generation costs efficient 35GW VRE portfolios and their required CCGT backup capacities. Top graph illustrates the capacity factor (CF) of the CCGT. Demand scenario 1: contemporary load profile. Technical configuration B: solar PV, wind & DTP. Note; the white dot marks the most cost-efficient system.



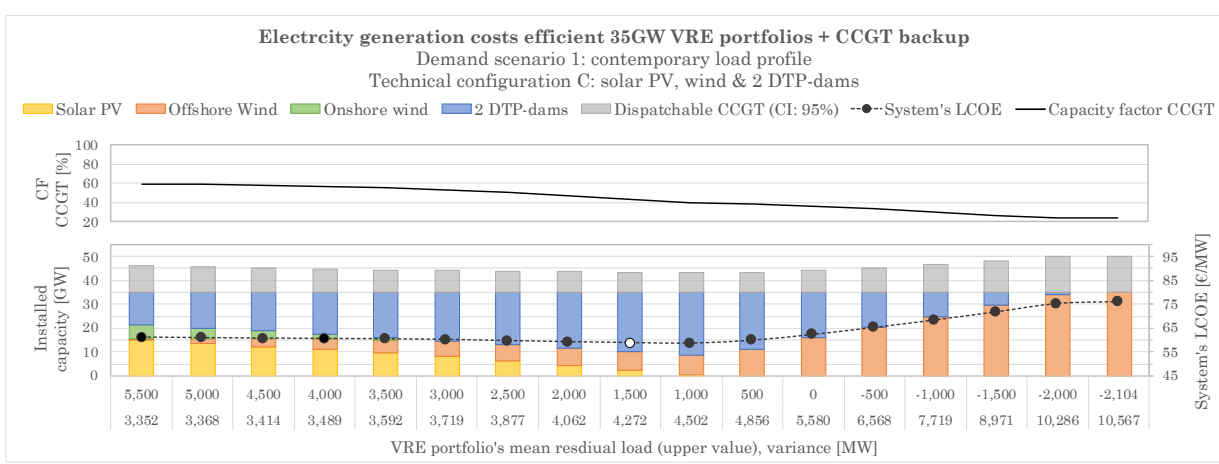


Figure 62: electricity generation costs efficient 35GW VRE portfolios and their required CCGT backup capacities. Top graph illustrates the capacity factor (CF) of the CCGT. Demand scenario 1: contemporary load profile. Technical configuration C: solar PV, wind & 2 DTP-dams. Note; the white dot marks the most cost-efficient system.

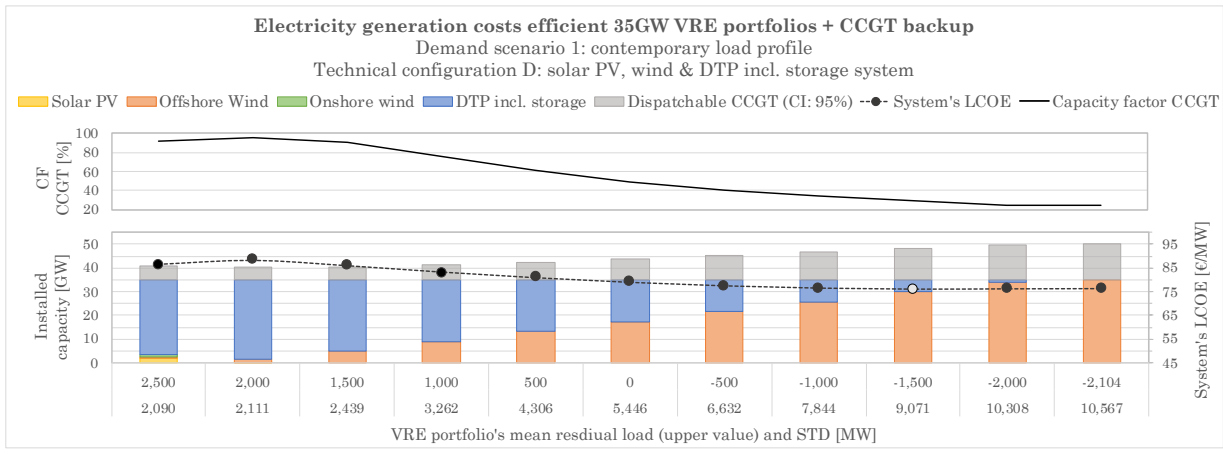


Figure 63: electricity generation costs efficient 35GW VRE portfolios and their required CCGT backup capacities. Top graph illustrates the capacity factor (CF) of the CCGT. Demand scenario 1: contemporary load profile. Technical configuration D: solar PV, wind & DTP incl. storage. Note; the white dot marks the most cost-efficient system.

## Appendix D2: Demand scenario 2 - increased peak loads

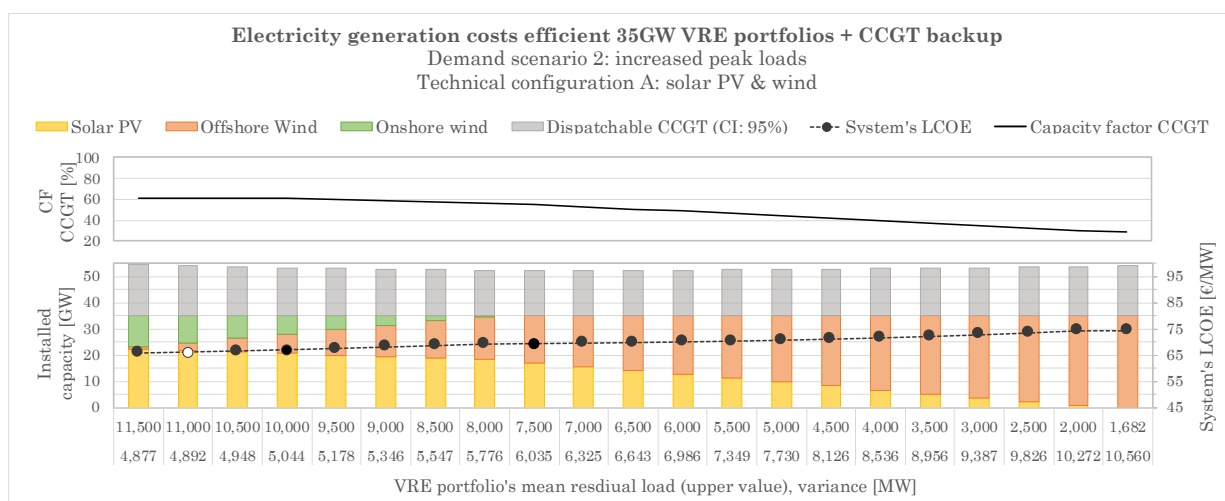


Figure 64: electricity generation costs efficient 35GW VRE portfolios and their required CCGT backup capacities. Top graph illustrates the capacity factor (CF) of the CCGT. Demand scenario 2: increased peak loads. Technical configuration A: solar PV & wind. Note; the white dot marks the most cost-efficient system.



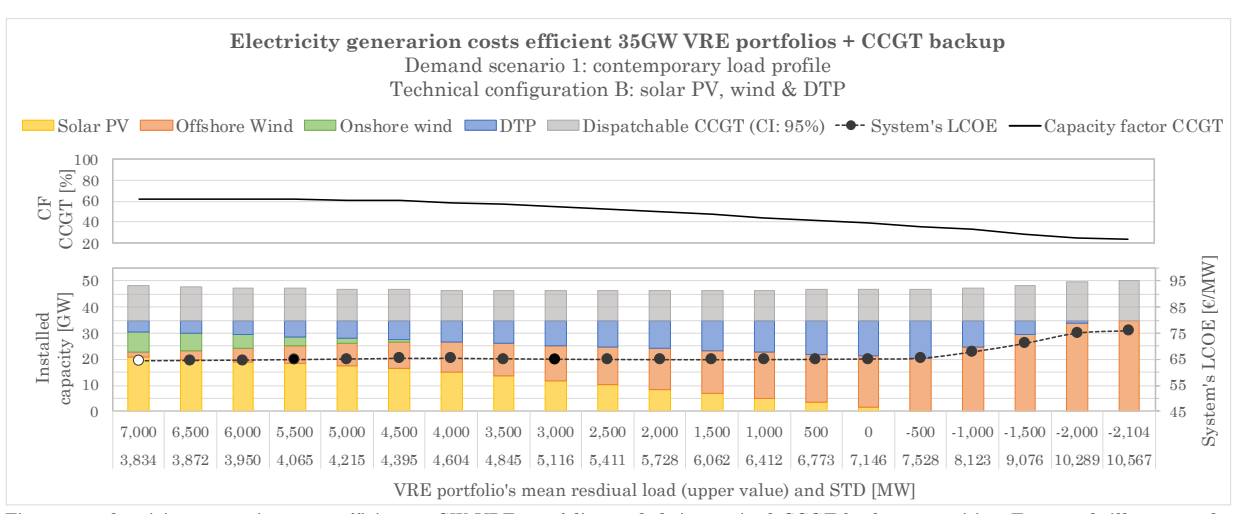


Figure 65: electricity generation costs efficient 35GW VRE portfolios and their required CCGT backup capacities. Top graph illustrates the capacity factor (CF) of the CCGT. Demand scenario 2: increased peak loads. Technical configuration B: solar PV, wind & DTP. Note; the white dot marks the most cost-efficient system.

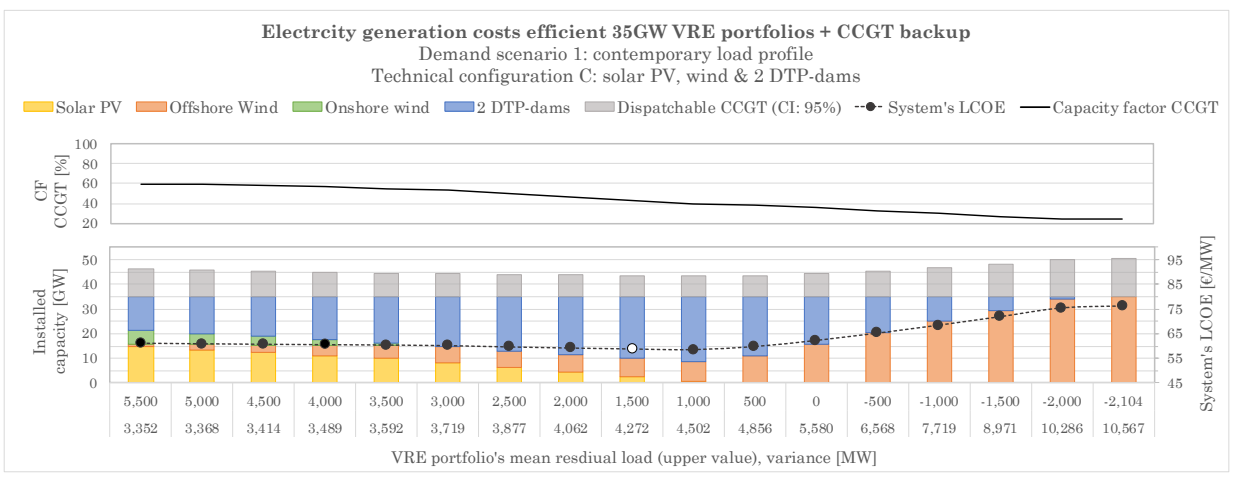


Figure 66: electricity generation costs efficient 35GW VRE portfolios and their required CCGT backup capacities. Top graph illustrates the capacity factor (CF) of the CCGT. Demand scenario 2: increased peak loads. Technical configuration C: solar PV, wind & 2 DTP-dams. Note; the white dot marks the most cost-efficient system.

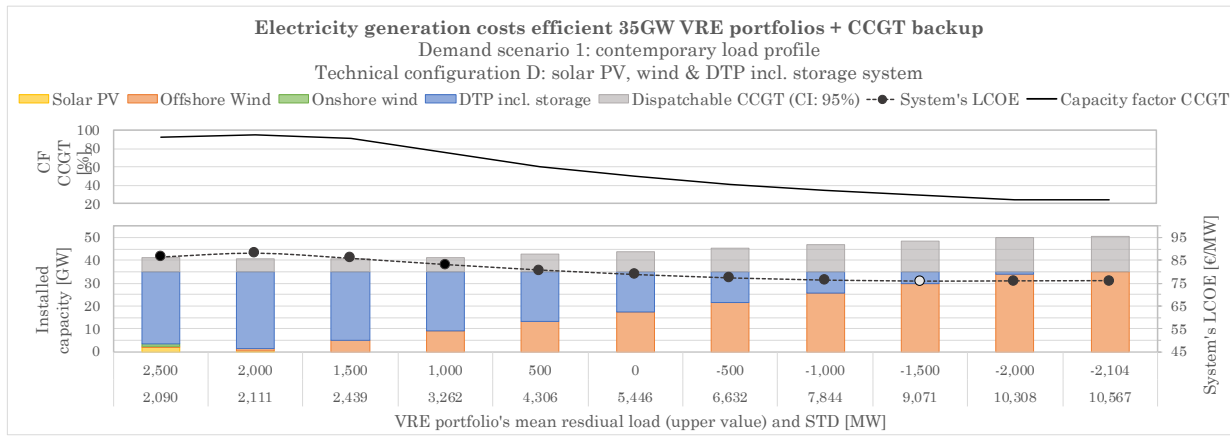


Figure 67: electricity generation costs efficient 35GW VRE portfolios and their required CCGT backup capacities. Top graph illustrates the capacity factor (CF) of the CCGT. Demand scenario 2: increased peak loads. Technical configuration D: solar PV, wind & DTP incl. storage. Note; the white dot marks the most cost-efficient system.



## Appendix D3: Demand scenario 3 - flat load profile

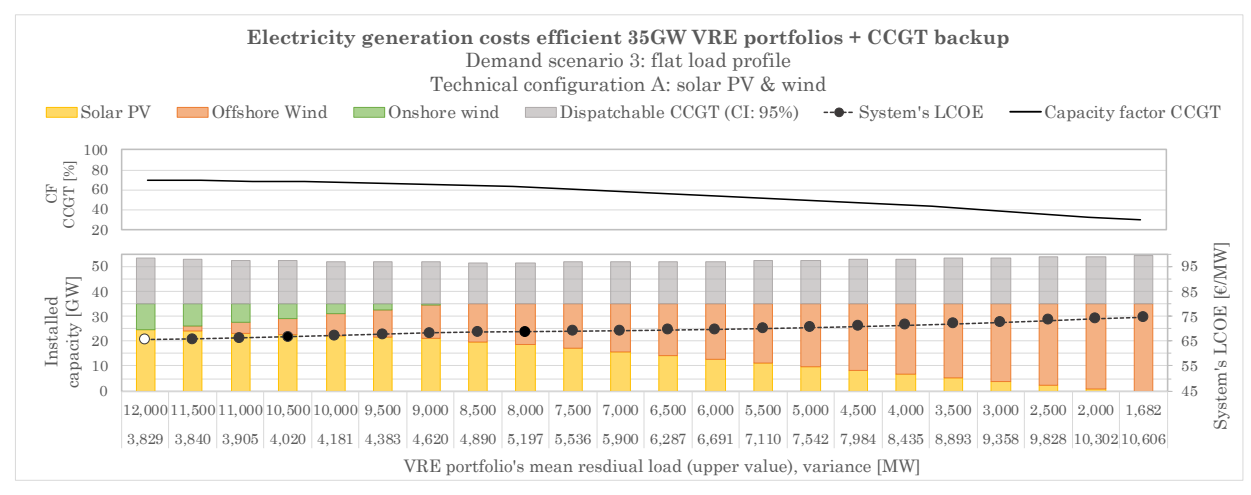


Figure 68: electricity generation costs efficient 35GW VRE portfolios and their required CCGT backup capacities. Top graph illustrates the capacity factor (CF) of the CCGT. Demand scenario 3: flat load profile. Technical configuration A: solar PV & wind. Note; the white dot marks the most cost-efficient system.

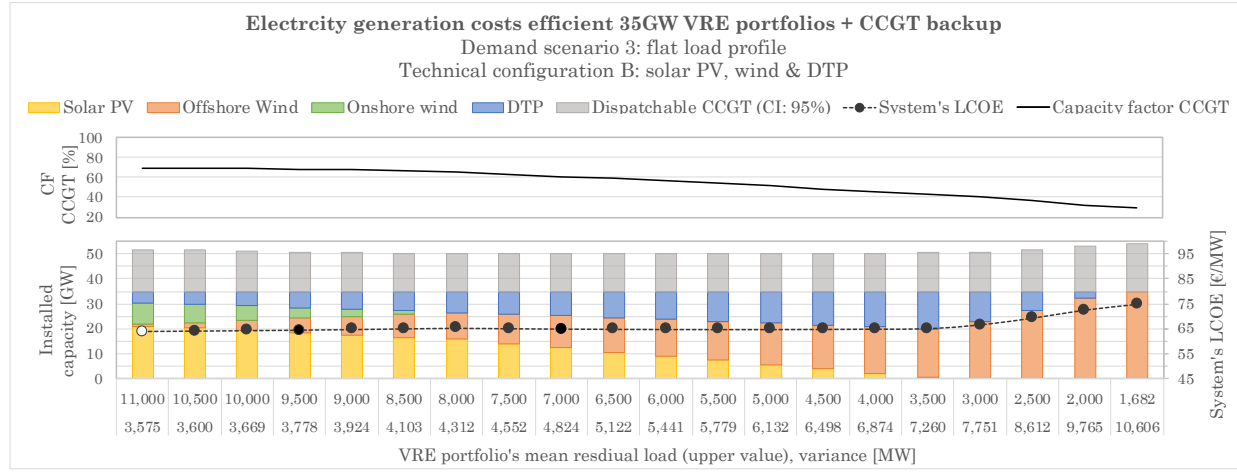


Figure 69: electricity generation costs efficient 35GW VRE portfolios and their required CCGT backup capacities. Top graph illustrates the capacity factor (CF) of the CCGT. Demand scenario 3: flat load profile. Technical configuration B: solar PV, wind & DTP. Note; the white dot marks the most cost-efficient system.

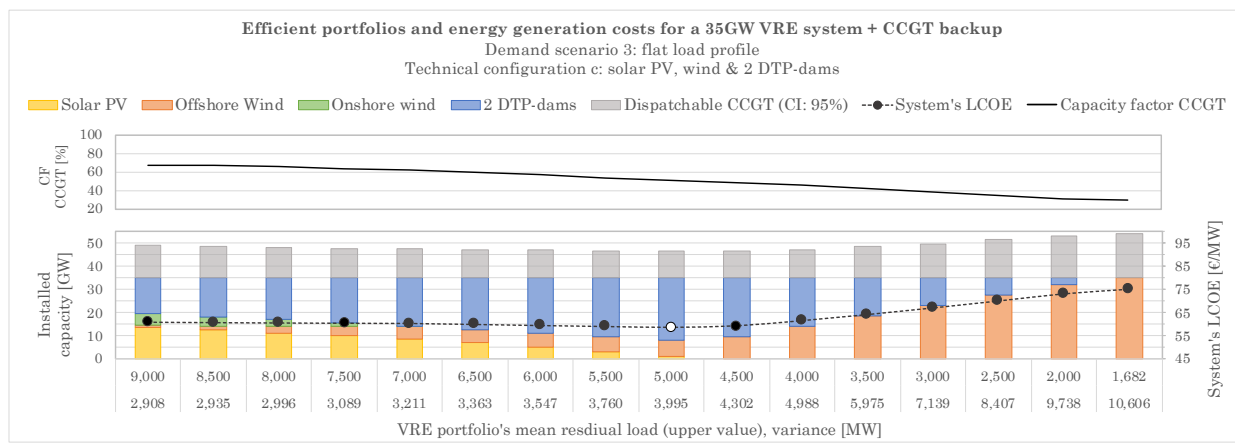


Figure 70: electricity generation costs efficient 35GW VRE portfolios and their required CCGT backup capacities. Top graph illustrates the capacity factor (CF) of the CCGT. Demand scenario 3: flat load profile. Technical configuration C: solar PV, wind & 2 DTP-dams. Note; the white dot marks the most cost-efficient system.



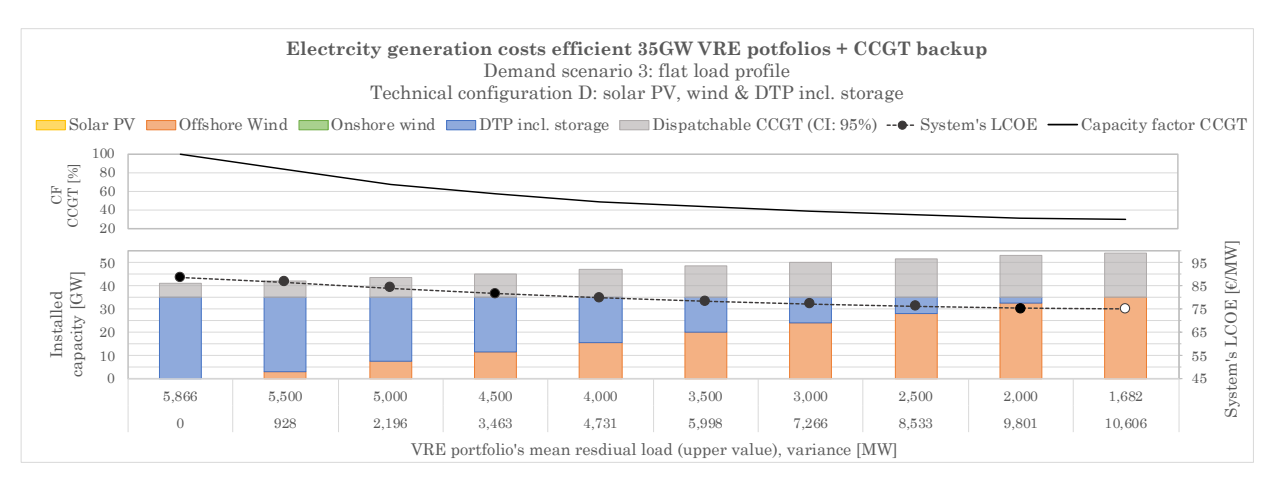
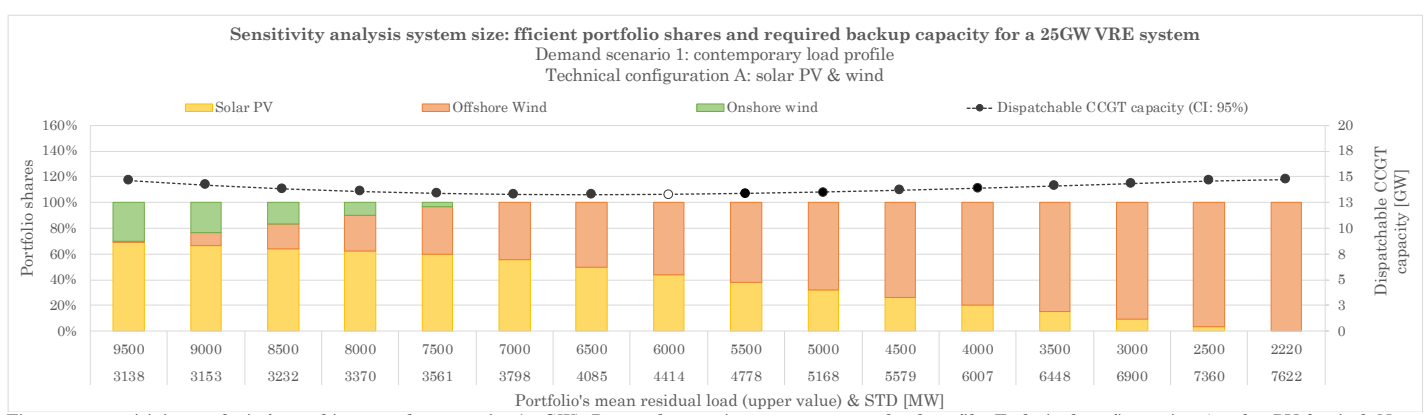


Figure 71: electricity generation costs efficient 35GW VRE portfolios and their required CCGT backup capacities. Top graph illustrates the capacity factor (CF) of the CCGT. Demand scenario 3: flat load profile. Technical configuration D: solar PV, wind & DTP incl. storage. Note; the white dot marks the most cost-efficient system.



## Appendix E: Sensitivity analysis - system size

## Appendix E1: Efficient portfolio shares and backup capacity - 25GW VRE



 $Figure~72: sensitivity~analysis~for~and~increased~system~size~(25GW).~Demand~scenario~1:~contemporary~load~profile.~Technical~configuration~A:~solar~PV~\&~wind.~Note;\\the~white~dot~marks~the~most~efficient~system.$ 

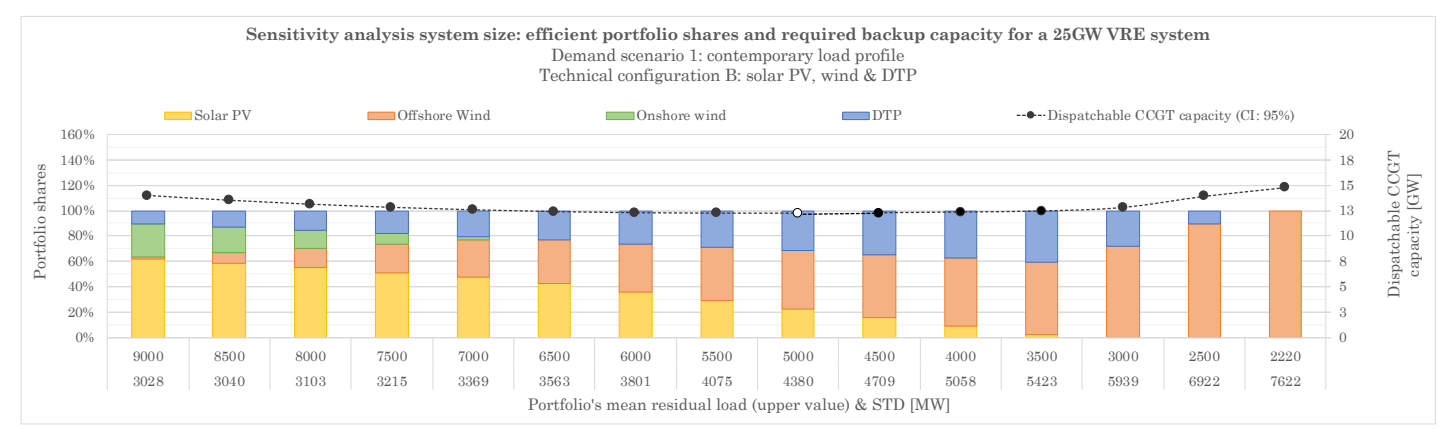


Figure 73: sensitivity analysis for and increased system size (25GW). Demand scenario 1: contemporary load profile. Technical configuration B: solar PV, wind & DTP. Note; the white dot marks the most efficient system.

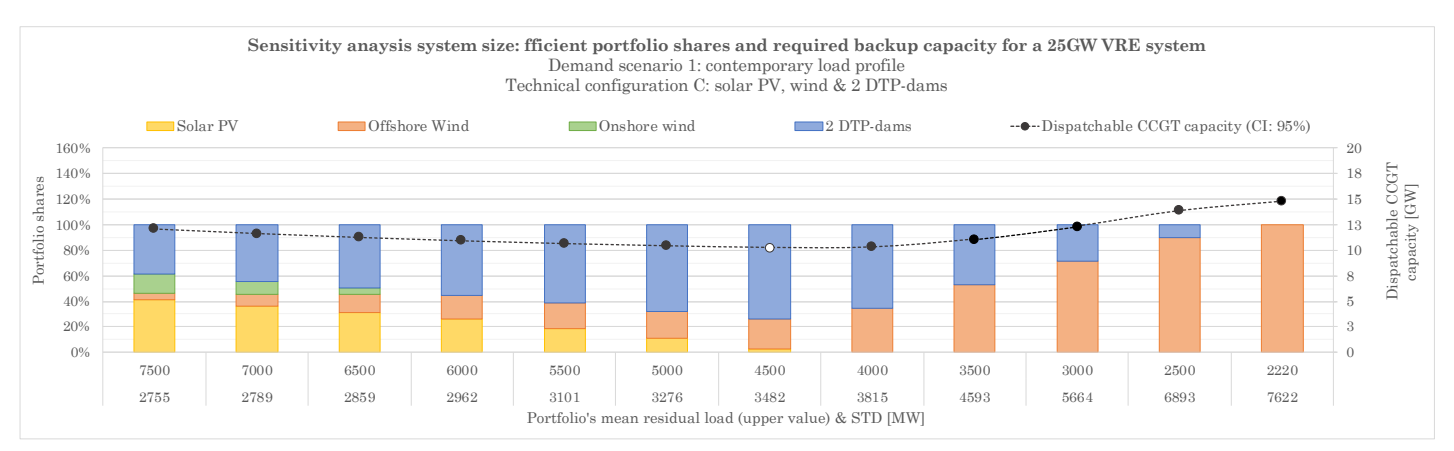


Figure 74: sensitivity analysis for and increased system size (25GW). Demand scenario 1: contemporary load profile. Technical configuration C: solar PV, wind & 2 DTP-dams. Note; the white dot marks the most efficient system.



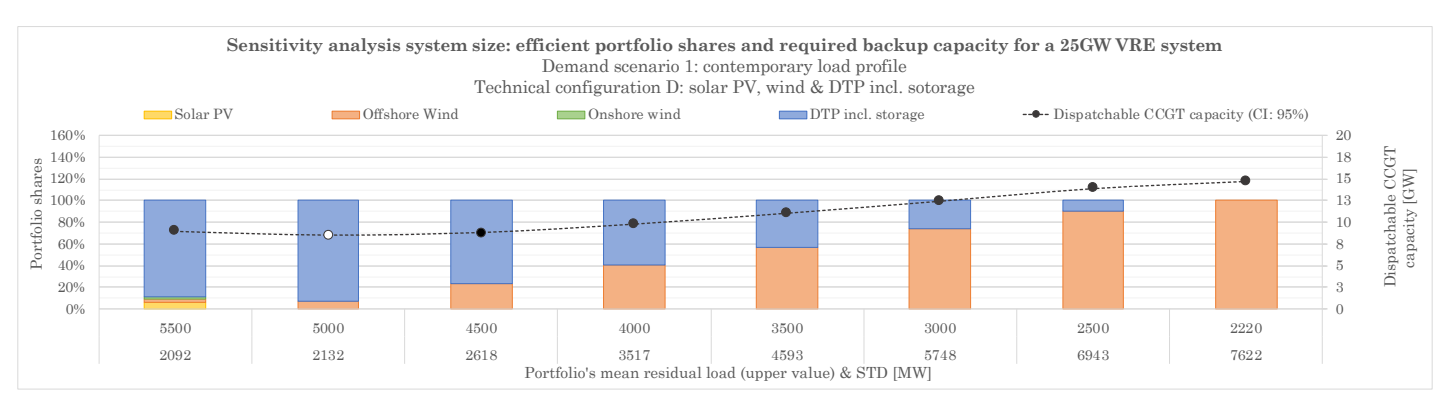


Figure 75: sensitivity analysis for and increased system size (25GW). Demand scenario 1: contemporary load profile. Technical configuration C: solar PV, wind & DTP incl. storage. Note; the white dot marks the most efficient system.

## Appendix E2: Efficient portfolio shares and backup capacity - 45GW VRE

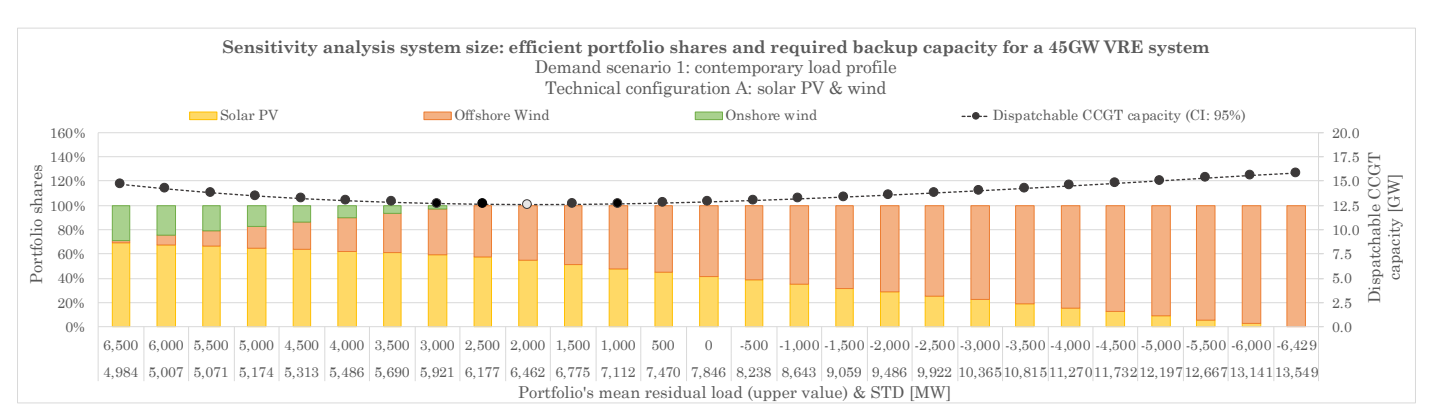


Figure 76: sensitivity analysis for and increased system size (45GW). Demand scenario 1: contemporary load profile. Technical configuration A: solar PV & wind. Note; the white dot marks the most efficient system.

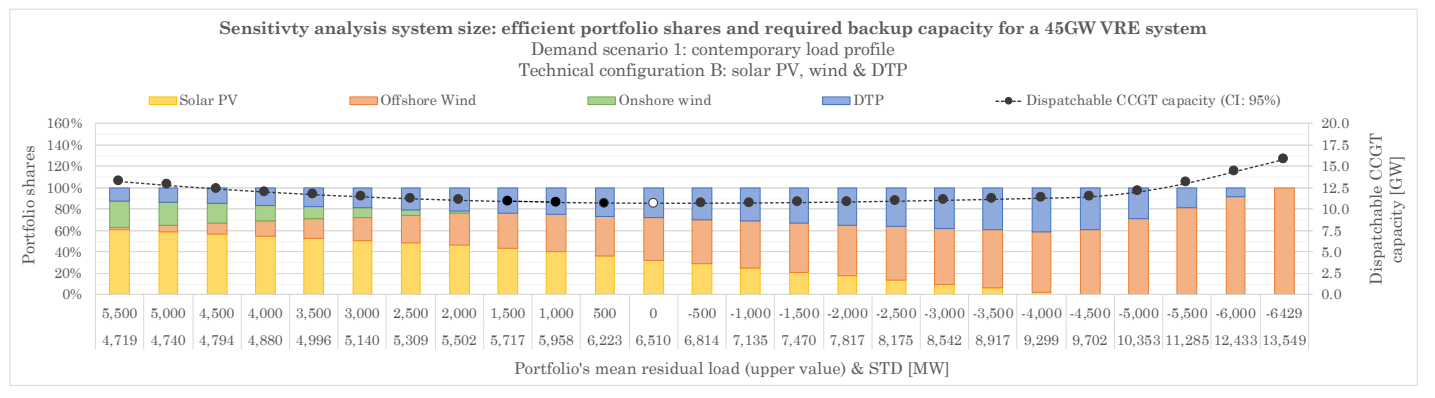


Figure 77: sensitivity analysis for and increased system size (45GW). Demand scenario 1: contemporary load profile. Technical configuration B: solar PV, wind & DTP. Note; the white dot marks the most efficient system.



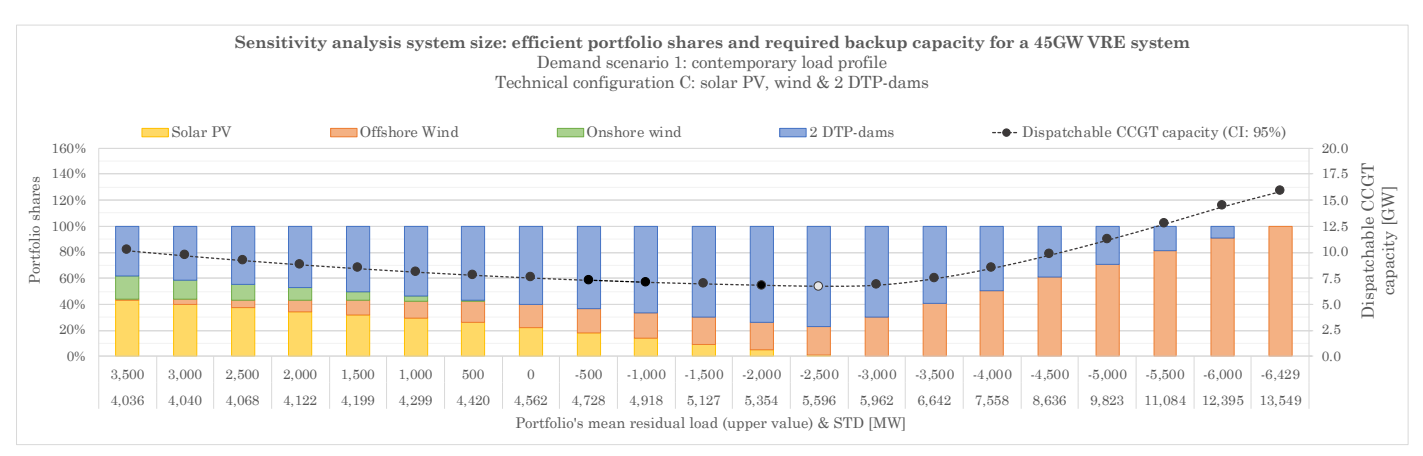


Figure 78: sensitivity analysis for and increased system size (45GW). Demand scenario 1: contemporary load profile. Technical configuration C: solar PV, wind & 2 DTP-dams. Note; the white dot marks the most efficient system.

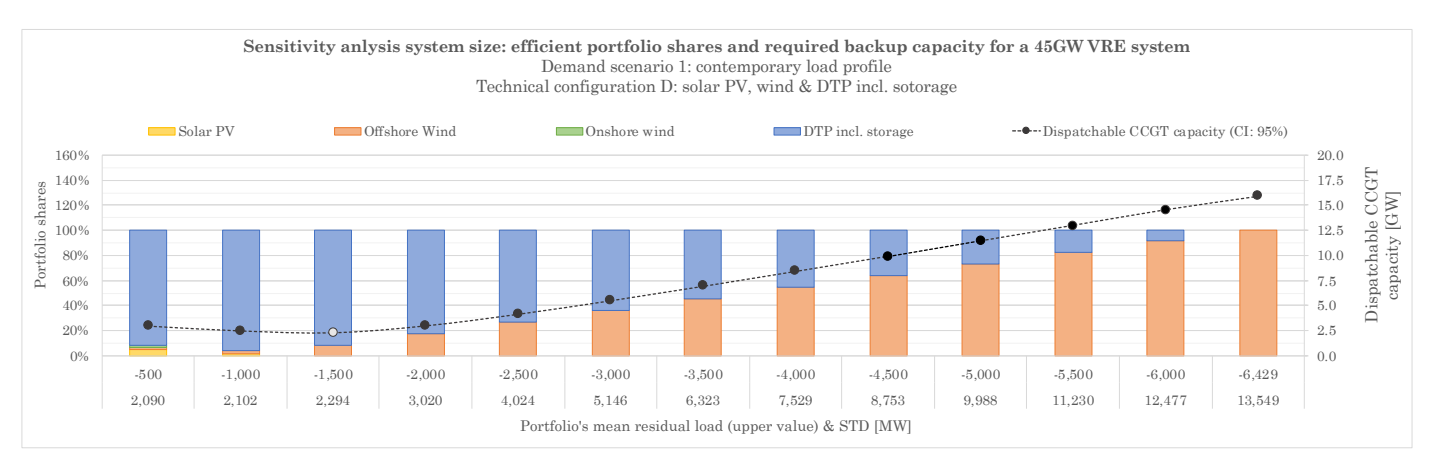


Figure 79: sensitivity analysis for and increased system size (45GW). Demand scenario 1: contemporary load profile. Technical configuration C: solar PV, wind & DTP incl. storage. Note; the white dot marks the most efficient system.



# Appendix F: Sensitivity analysis - increased confidence interval

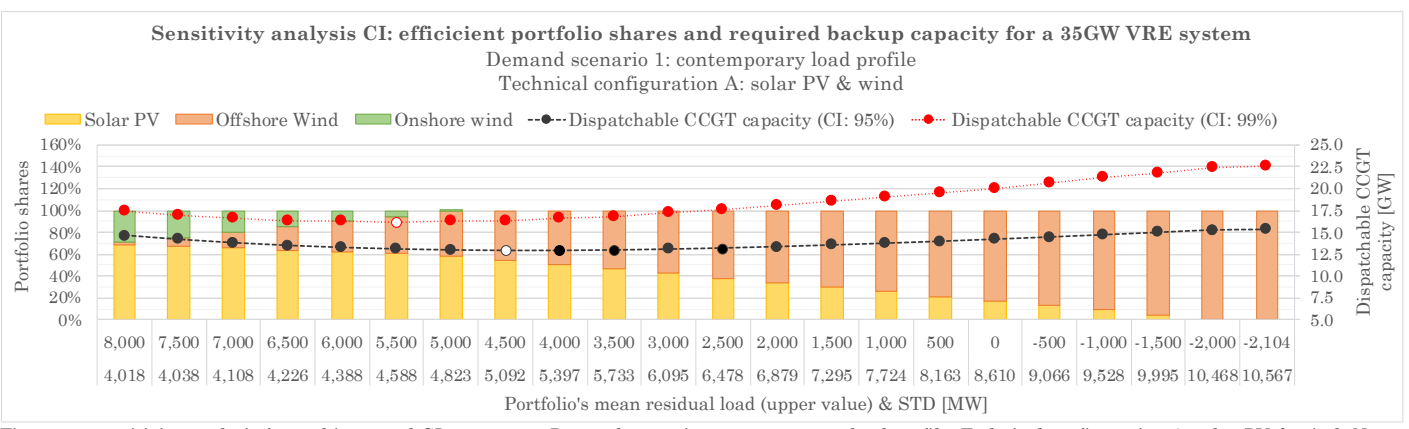


Figure 80: sensitivity analysis for and increased CI 95% - 99%. Demand scenario 1: contemporary load profile. Technical configuration A: solar PV & wind. Note; the white dot marks the most cost-efficient system.

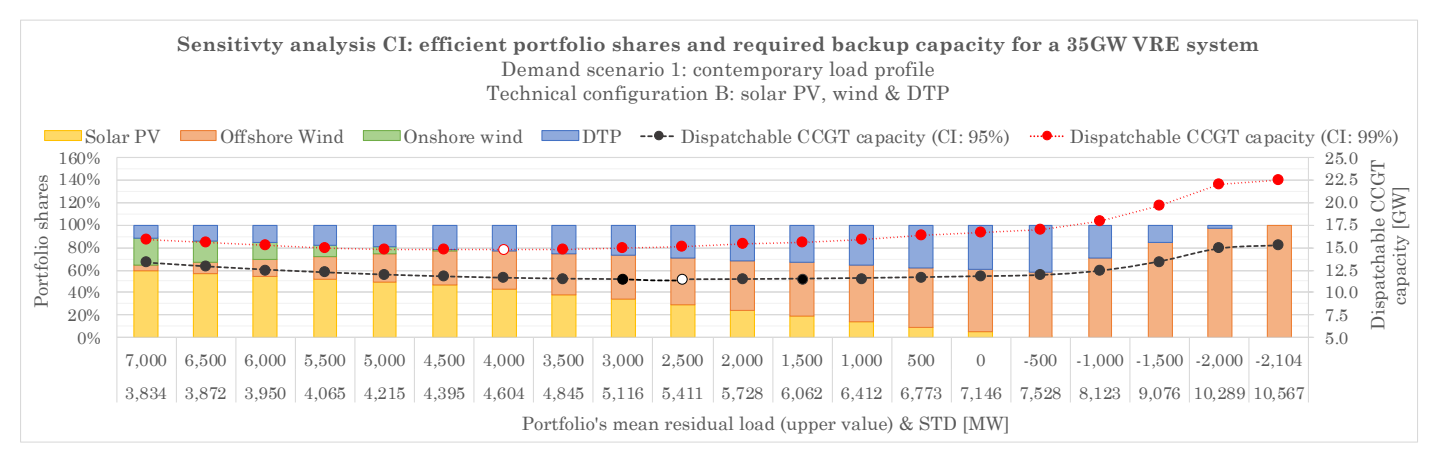


Figure 81: sensitivity analysis for and increased CI 95% - 99%.. Demand scenario 1: contemporary load profile. Technical configuration B: solar PV, wind & DTP. Note; the white dot marks the most cost-efficient system.

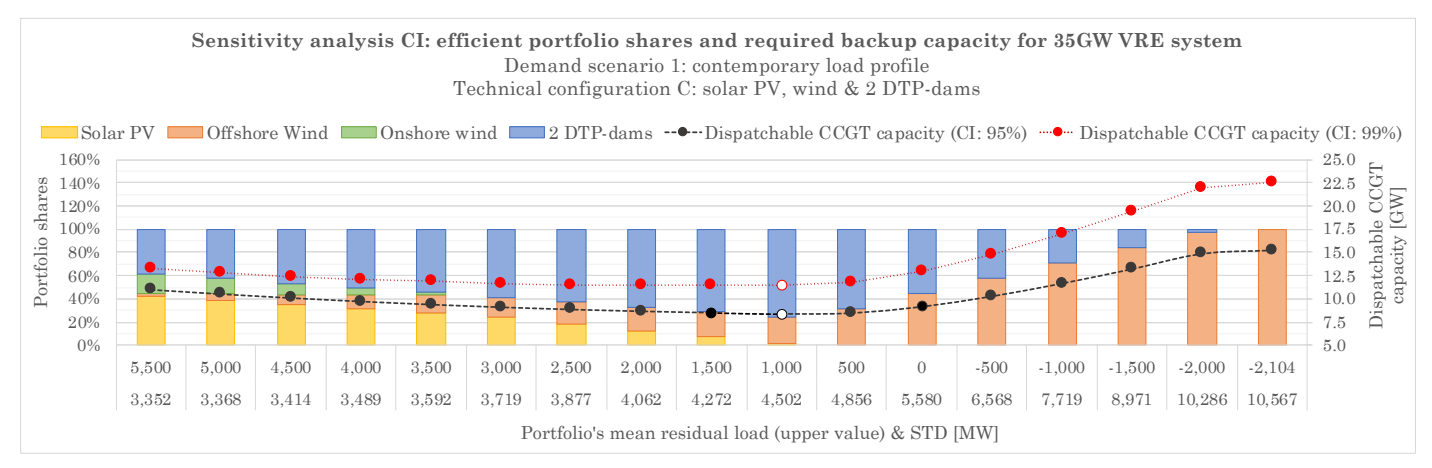


Figure 82: sensitivity analysis for and increased CI 95% - 99%. Demand scenario 1: contemporary load profile. Technical configuration C: solar PV, wind & 2 DTP-dams. Note; the white dot marks the most cost-efficient system.



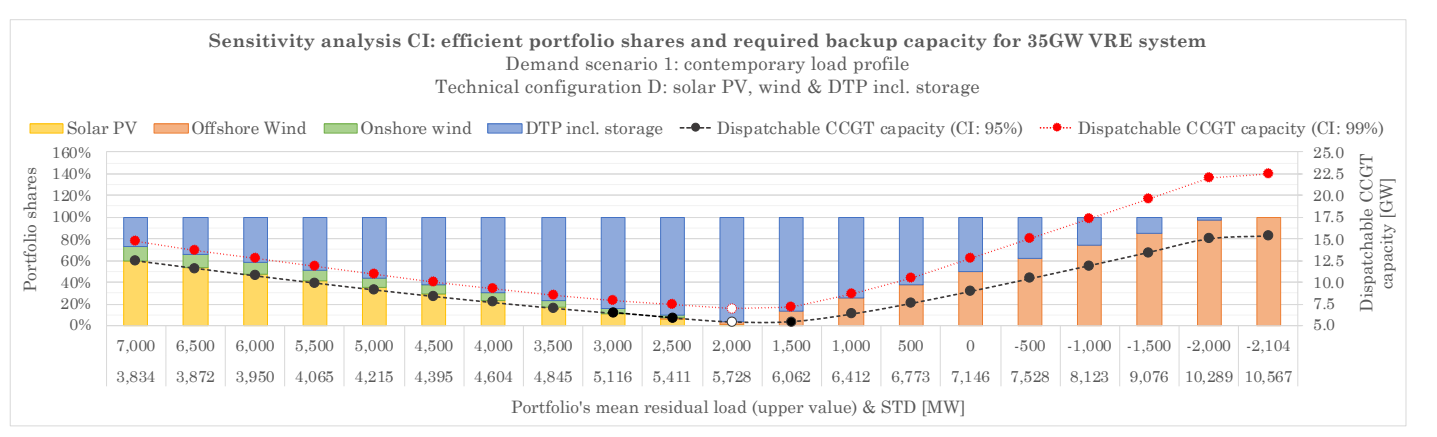


Figure 83: sensitivity analysis for and increased CI 95% - 99%. Demand scenario 1: contemporary load profile. Technical configuration D: solar PV, wind & DTP incl. storage. Note; the white dot marks the most cost-efficient system.



## Appendix G: Sensitivity analysis - increased CO2 price

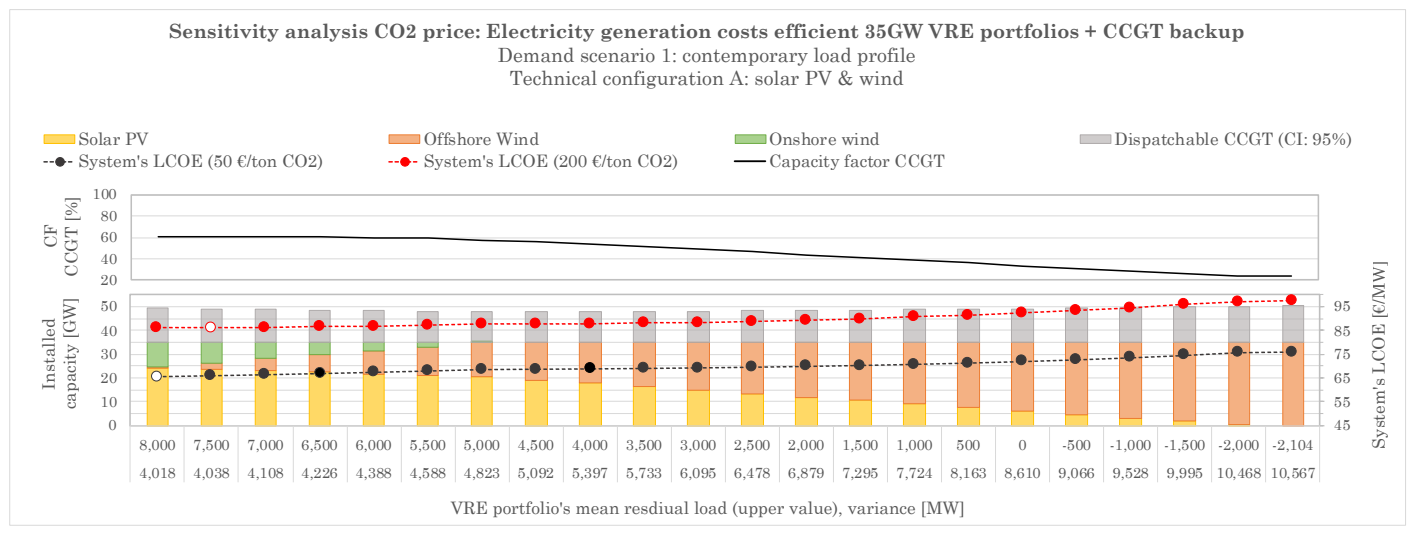


Figure 84: sensitivity analysis for and increased CO<sub>2</sub> price from 25 to 200  $\epsilon$ /ton CO<sub>2</sub>. Demand scenario 1: contemporary load profile. Technical configuration A: solar PV & wind. Note; the white dot marks the most cost-efficient system.

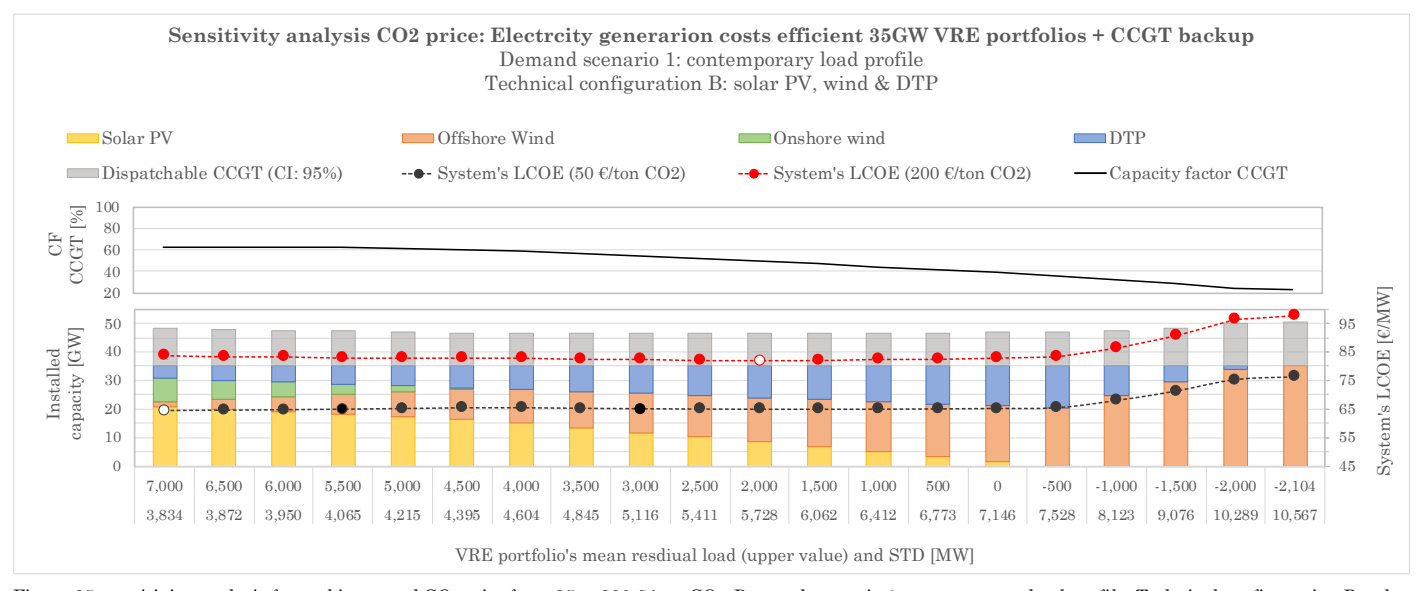


Figure 85: sensitivity analysis for and increased CO<sub>2</sub> price from 25 to  $200 \, \epsilon$ /ton CO<sub>2</sub>. Demand scenario 1: contemporary load profile. Technical configuration B: solar PV, wind & DTP. Note; the white dot marks the most cost-efficient system.



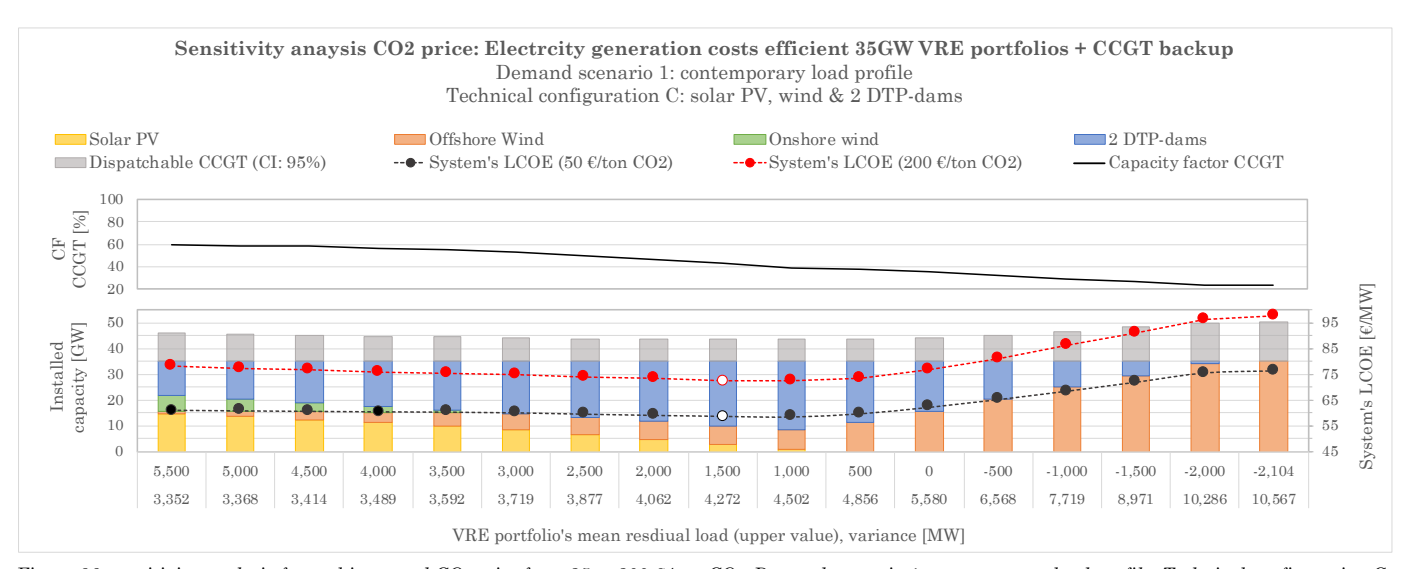


Figure 86: sensitivity analysis for and increased  $CO_2$  price from 25 to 200  $\epsilon$ /ton  $CO_2$ . Demand scenario 1: contemporary load profile. Technical configuration C: solar PV, wind & 2 DTP-dams. Note; the white dot marks the most cost-efficient system.

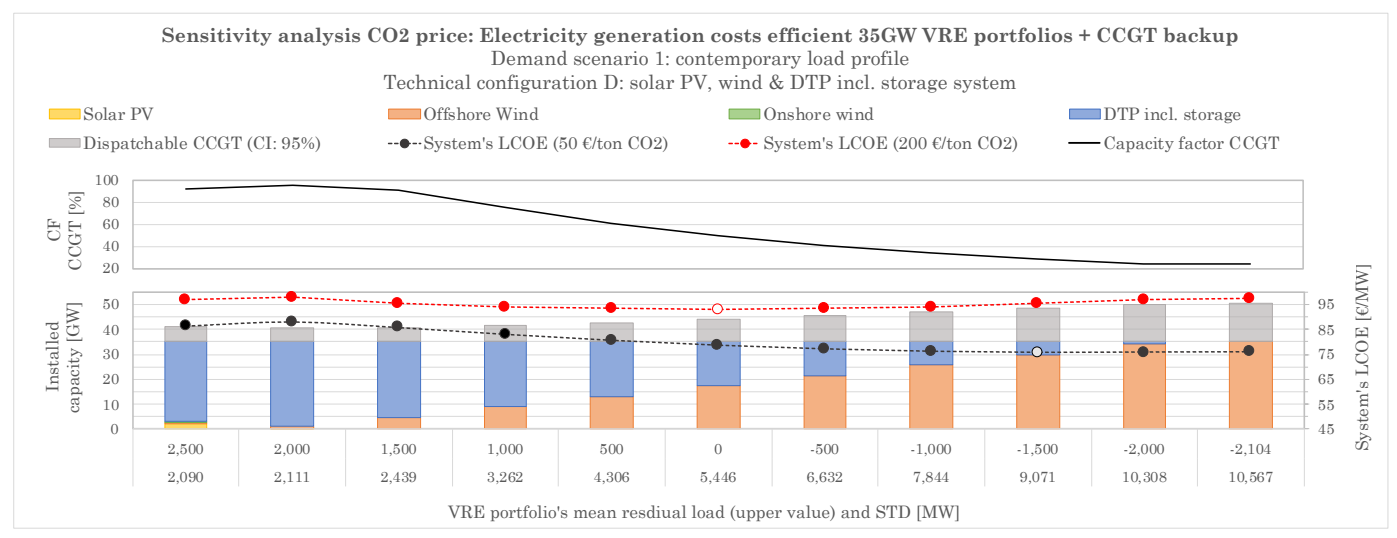


Figure 89: sensitivity analysis for and increased  $CO_2$  price from 25 to 200  $\epsilon$ /ton  $CO_2$ . Demand scenario 1: contemporary load profile. Technical configuration D: solar PV, wind & DTP incl. storage. Note; the white dot marks the most cost-efficient system.



## Appendix H: Distribution residual loads

Table 14: normal distribution parameters

Normal distribution parameters										
Off 1 O 1 O DWD DWD:										
	Solar PV	wind	wind	DTP	dams	storage				
Kurtosis <sup>1</sup>	1.79	-1.29	-1.29	-0.53	-0.99	-0.85				
$Skewness^1$	-1.39	-0.15	-0.15	-0.65	0.03	0.27				

 $<sup>^{1}</sup>$ For the data to be considered normally distributed kurtosis and skewness should be within -2 and +2 [43].

